UNCLASSIFIED
SECURITY CLASSIFICATION OF THIS PAGE

DTIC COPY

(2)

REPORT I

1a. REPORT SECURITY CLASSIFICATION
UNCLASSIFIED

AD-A224 091

2a. SECURITY CLASSIFICATION AUTHORITY

DTIC ELECTE S D

2b. DECLASSIFICATION / DOWNGRADING SCHEDULE

AUG 2 6 1990

Approved for public release; distribution unlimited.

4. PERFORMING ORGANIZATION REPORT NUMBER(S)

5. MONITORING ORGANIZATION REPORT NUMBER(S)
AFOSR-TR- 90 0674

6a. NAME OF PERFORMING ORGANIZATION
Hampton University

6b. OFFICE SYMBOL (If applicable)

7a. NAME OF MONITORING ORGANIZATION
AFOSR/NP

6c. ADDRESS (City, State, and ZIP Code)
Hampton, Virginia 23668

7b. ADDRESS (City, State, and ZIP Code)
BN 410
Bolling AFB DC 20332-6448

8a. NAME OF FUNDING / SPONSORING ORGANIZATION
AFOSR

8b. OFFICE SYMBOL (If applicable)
NP

9. PROCUREMENT INSTRUMENT IDENTIFICATION NUMBER
AFOSR-86-0345

8c. ADDRESS (City, State, and ZIP Code)
BN 410
Bolling AFB, DC 20332-6448

10. SOURCE OF FUNDING NUMBERS

PROGRAM ELEMENT NO.	PROJECT NO.	TASK NO.	WORK UNIT ACCESSION NO.
61103D	3484	A6	

11. TITLE (Include Security Classification)
Center for Electro Optics & Plasma Research - Final Technical Report

12. PERSONAL AUTHOR(S)
D. D. Venable, K. S. Han, J. H. Lee, J. K. Kim, S. M. Lee, M. B. Workman

13a. TYPE OF REPORT	13b. TIME COVERED	14. DATE OF REPORT (Year, Month, Day)	15. PAGE COUNT
FINAL	FROM 10/86 TO 12/89	April 1, 1990	180

16. SUPPLEMENTARY NOTATION

17. COSATI CODES			18. SUBJECT TERMS (Continue on reverse if necessary and identify by block number)
FIELD	GROUP	SUB-GROUP	1-Hz hypocycloidal pinch (HCP) pumped laser uv laser

19. ABSTRACT (Continue on reverse if necessary and identify by block number)

A 1-Hz hypocycloidal pinch (HCP) pumped laser was operated at 1 kJ input energy. The time integrated continuum spectrum of the pump light approximated that of a 15,000 K blackbody for the wavelength range above 250 nm. The pump emission was found to be stable at 1 Hz operation. The overall efficiency of the system was found to be 0.01% for single shot operation of pumping blue-green and near ultraviolet (uv) dye lasers 2 MW, but the laser output saturated with the input energy 4 kJ due to thermal lensing effects in the dye. Thermal effects introduced by nonuniform heating of the dye solution resulted in a reduction of the uv laser output as repetition rates increased. The thermal effects were significantly reduced by using a double walled dye cuvette. A theoretical model was developed to describe the electromagnetic acceleration of the plasma produced in the hypocycloidal pinch device. The computer model described the operation of the device in the snow-plow mode and took into account the unique geometry and electrical parameters of the HCP devices used in our laboratory. Numerical solutions were presented for plasma velocity

20. DISTRIBUTION / AVAILABILITY OF ABSTRACT	21. ABSTRACT SECURITY CLASSIFICATION
☒ UNCLASSIFIED/UNLIMITED ☒ SAME AS RPT. ☐ DTIC USERS	UNCLASSIFIED

22a. NAME OF RESPONSIBLE INDIVIDUAL	22b. TELEPHONE (Include Area Code)	22c. OFFICE SYMBOL
Howard R. Schlossberg	202-767-4906	NP

DD FORM 1473, 84 MAR 83 APR edition may be used until exhausted. All other editions are obsolete.

SECURITY CLASSIFICATION OF THIS PAGE
UNCLASSIFIED

Keywords: ultraviolet ... electrooptic
Equations of ... state

19. and appropriate trends were predicted for the experimentally determined risetime of the pump light and total irradiance as a function of pressure of the working gas. The device was found to be superior to other broadband pump sources for production of uv lasers.

Center for Electro Optics and Plasma Research

AFOSR-TR- 90 0674

Final Technical Report
AFOSR Grant Number-86-0345

April 1990

D. D. Venable, Co-Principal Investigator
K. S. Han, Co-Principal Investigator
J. H. Lee, Adjunct Research Professor
J. K. Kim, Visiting Research Professor
S. M. Lee, Graduate Student
M. B. Workman, Graduate Student

Hampton University
Department of Physics

Hampton, VA 23668

TABLE OF CONTENTS

LIST OF TABLES

LIST OF FIGURES

CHAPTER I: INTRODUCTION

Laser dyes are organic compounds which have a very short lifetime in the excited metastable state, and particularly, ultraviolet (uv) dyes have a large molar extinction coefficient for short-wavelength absorption bands. Therefore, an intense uv light source having a fast risetime is needed to make high power, high energy uv dye lasers. Until now, uv region dye lasers were mainly pumped by rare gas halides lasers,[1-3] nitrogen lasers,[4] YAG lasers,[5,6] and special types of coaxial flashlamps.[4,7-9] But these laser pumping sources require high cost, and flashlamps have poor output reproducibility and limitations on the input energy and output spectral efficiency for pumping uv dyes. In addition, the arc discharge of a flashlamp expands to only a portion of the bore diameter and its lifetime is typically less than 10^6 shots.[10-12]

In the late 1970's plasma focus devices, which were developed originally for fusion plasma studies and X-ray emission[13-15] were introduced as laser excitation sources.[16] The emission characteristics of the device strongly depended on geometry, input energy, and type and pressure of filling gas. When the device was operated at 27-kJ input energy with 3-Torr deuterium pressure, X-ray emitting dense plasma production was observed. Intense uv and vacuum uv emission were also observed for different working gases at the same input energy. For excitation of an atomic iodine laser, 3 units of the hypocycloidal pinch (HCP) array were employed. An iodine laser (λ=1.315 μm) and a xenon recombination laser (λ=2.027 μm) were pumped with this array at a high pressure mode of operation.[17]

Recently, multi-stage HCP arrays were introduced for pumping rhodamine 6G, blue-green and uv dye lasers beyond the explosion limit of the input power of coaxial flashlamps.[18,19] To pump the blue-green dye laser, the HCP apparatus was operated in a high pressure heavy-

gas filling mode. Laser output of 230 kW was achieved with 20 torr argon fill and 1.9 kJ electrical input energy.[20] The initial uv dye laser system showed successful excitation of BBQ, p-terphenyl and POPOP uv dyes.[21]

Comparison of various dye laser pump sources in the uv portion of the spectrum indicates that the HCP array has distinct advantages over the other sources in the lifetime and the input capability.[22] (*See Table I.*) Therefore the HCP array has been extensively utilized in our laboratories as a pump source for uv and blue-green dye lasers. When a 1-Hz HCP pumped laser was operated at 1 kJ input energy, the time integrated continuum spectrum of the pump light approximated that of a 15,000 K blackbody for the wavelength range above 250 nm. The pump emission was found to be stable at 1 Hz operation. However, thermal effects introduced by nonuniformly heating of the dye solution resulted in a reduction of the uv laser output as repetition rates increased. The overall efficiency of the system was found to be 0.01% for single shot operation of pumping blue-green dye laser >2 MW, but the laser output saturated with the input energy >4 kJ due to the thermal lensing effects in the dye.

Chapter 2 of this report describes a theoretical model that predicts the electrical behavior of the HCP device. This work is the basis for the thesis by Workman[23]. Chapter 3 describes the experimental device used for this research and presents data for utilization of this device as a uv laser pump source. This work served as the basis of the thesis by S. M. Lee[24]. In Chapter 4 the problems of thermal lensing in the device is discussed in detail. The project is summarized in Chapter 5.

TABLE I. COMPARISON OF VARIOUS PUMP SOURCES

PUMP SOURCE	Pulse width (μs)	Brightness uv (J/cm^2)	Fluores-ence Eff (%)	Life time (# Shot)	Tech Dev-elopment
Linear Xenon Flashlamp	>1	0.5	4-5	<10	Advanced
Metal-Doped	>1	1	8-15		Prototype
Coaxial-Xenon Flashlamp	>1	1	4-5	10	Advanced
Surface Discharge	>1	1	9-13		Prototype
Exploding Wire	1 0	1	4-5		Advanced
Hg Lamp	1 0	0.035	32	10	Advanced
Hypocycloidal Pinch	1	1	9-13	long	Prototype

CHAPTER 2: THEORETICAL MODEL

A computer model has been developed to describe the electromagnetic acceleration of the plasma produced in the hypocycloidal pinch device. The computer model describes the operation of the device in the snow-plow mode and takes into account the unique geometry and electrical parameters of the HCP devices used in our laboratory. Numerical solutions have been obtained for plasma velocity and appropriate trends have been predicted for the risetime of the pump light and total irradiance as a function of pressure of the working gas.

The Snow Plow Model for the HCP Device

For our application, we assume that the current sheet is in the form of a thin collapsing cylinder as shown in Figure 1. The height of the current sheet, h, is a constant and fixed by the electrode separation of the HCP device. The time varying current is designated by I(t). Originally, the cylindrical shell has a radius of r_o, and at a later time, t, the shell has collapsed to a smaller cylinder of radius r(t). We apply the model only to the case where $r_o > r(t) > r_{edge}$ where r_{edge} is the radius of the inner hole within the HCP device. For the dye laser pumping system, a quartz tube is placed at r_{edge} for the dye handling system.[24] This tube prevents the plasma from progressing pass this point. Thus, values of $r < r_{edge}$ are not of interest.

Equation of Motion

The magnetic pressure, P_B, on the current sheet is obtainable from Poyntings vector, S, by the equation

$$P_B = \frac{(S)}{c} = \frac{B^2}{2\mu_o}$$

where B is the magnetic field intensity, μ_o is the permeability of free space, and c is the speed of light. Further, the magnetic force F_B can be defined as the product of the magnetic pressure and the surface area, A, of the cylindrical current sheet, or

$$F_B = P_B A = \frac{\pi r(t) h B^2}{\mu_o} .$$

Then from Ampere's law the magnetic field intensity is given as

$$B = \frac{\mu_o i(t)}{2\pi r(t)} .$$

The working gas within the current sheet is snowplowed toward the center with momentum, p, given by

$$p = m(r) \frac{dr(t)}{dt} .$$

The mass m(r) swept by the collapsing cylinder is

$$m(r) = \rho \pi (r_o^2 - r^2(t)) h .$$

These results are combined to give the equation of motion for the system

$$- \frac{\mu_o i^2(t)}{4\pi r(t)} = \rho \pi \frac{d}{dt} \left\{ (r_o^2 - r^2(t)) \frac{dr(t)}{dt} \right\}$$

or

$$-\left(\frac{\mu_o}{4\pi^2\rho}\right) i^2(t) = (r_o^2 - r^2(t))\, r(t) \frac{d^2r(t)}{dt^2} - 2\, r^2(t) \left(\frac{dr(t)}{dt}\right)^2 .$$

The Equivalent Electrical Circuit

The electrical circuit of the HCP system is assumed to be an LRC circuit consisting of the charging capacitor, the inductance, L_{HCP}, and resistance, R_{HCP}, of the HCP device, and all other inductances, L_{ext}, and resistances, R_{ext}. The circuit schematic is shown in Figure 2.

The inductance and resistance of the HCP device are in general assumed to be variable and are dependent on the current sheet position and/or the working gas pressure, P. The total inductance of the circuit is given by

$$L_{total} = L_{ext} + L_{HCP}(P,t)$$

and the total resistance of the circuit is given by

$$R_{total} = R_{ext} + R_{HCP}(P,t).$$

The circuit is then governed by the equation

$$-R_{total}\, i - \frac{d}{dt}\left(L_{total} i\right) - \frac{q}{C} = 0$$

or

$$\left[\frac{1}{C}\right] q + \left[R_{ext} + R_{HCP} + \frac{dL_{HCP}}{dt}\right] \dot{q} + \left[L_{ext} + L_{HCP}\right] \ddot{q} = 0.$$

The inductance of the HCP device is defined to be the inductance of that section of the device behind the current sheet. Since the device is coaxial in geometry, see Figure 1, it is assumed that L_{HCP} is given by the product of a logarithmic term involving the ratio of the radius of the current sheet and the radius of the HCP device (path and return path of the current) and a constant L' to be determined from experimental data. Thus

$$L_{HCP} = L' \ln\left(\frac{r_o}{r(t)}\right).$$

The circuit equation therefore becomes

$$\left[\frac{1}{C}\right] q + \left[R_{ext} + R_{HCP} - \frac{\dot{r}(t)}{r(t)} L'\right] \dot{q} + \left[L_{ext} + L' \ln\left(\frac{r_o}{r(t)}\right)\right] \ddot{q} = 0 .$$

A series of four coupled differential equations can now be written by introducing the current, i, and velocity, v. Therefore,

$$\frac{dq(t)}{dt} = i ,$$

$$\frac{dr(t)}{dt} = v ,$$

$$\frac{di(t)}{dt} = \frac{-1}{L_{ext} + L' \ln\left(\frac{r_o}{r(t)}\right)} \left\{\left(R_{ext} + R_{HCP} - \frac{L' v}{r(t)}\right) i(t) + \frac{q}{C}\right\}$$

and

$$\frac{dv(t)}{dt} = \frac{-\delta i^2 + 2 r^2(t) v^2}{(r_o^2 - r^2(t)) r(t)}; \qquad \delta = \frac{\mu_o}{4 \pi^2 \rho} .$$

The boundary conditions for these equations are

$$q(0) = CV_o,$$

$$r(0) = r_o - \varepsilon ; \qquad 0 < \varepsilon << r_o,$$

$$i(0) = 0,$$

and

$$v(0) = 0.$$

Variable L and R

The HCP inductance and resistance were estimated from values measured when the HCP was connected in the circuit and compared to measured values when the HCP device was removed and the circuit was shortened. Then L' was approximated as

$$L' \approx \frac{2(L_1 - L_{ext})}{\ln\left(\frac{r_o}{r_{edge}}\right)}$$

where L_{ext} is the inductance of the circuit measured without the HCP device connected and L_1 is the average inductance of circuit measured with the HCP device connected. These quantities were determined as discussed earlier.[22]

We assume that the resistance of the HCP device depends only on the initial pressure of the working gas. Once this parameter is fixed, the HCP resistance is assumed constant and does not vary as the position of the current sheet changes. Further, a simple exponential dependence

is assumed, thus

$$R_{HCP} = R(p,t) \approx R_o e^{-\alpha p}.$$

In this report, we refer to the parameter α as the pressure constant for the device, and its value, as well as R_o, are treated as adjustable parameters in the model. We are currently in the process of relating these parameters to physical attributes of the device. These results will be discussed in a subsequent report.

Discussion

The differential equations were solved using the range of parameters appropriate for our HCP device. Figure 3 shows results of the model for speed of the collapsing current sheet as a function of HCP pressure. Pressure, P, was investigated in the range of 0.1 to 50 Torr. The adjustable parameters, R_o and α, ranged from 0.01 to 5 Ω and 0 to 0.5 $Torr^{-1}$, respectively.

The graphs in Figure 3 show that at low values of αP the velocity is related to the pressure through a simple power law

$$V \propto P^k$$

where k is approximately 0.5. This simple power relationship is consistent with the standard approximation made in the snow plow model where analysis is restricted to the first quarter cycle of the current signal and it is assumed that the current is linearly proportional to time during this period. However for such a case, k is found to be 0.25. Our value, which is dependent on the actual functional relation for the current, gives much better agreement with experimental observations. At large values of αP the velocity and pressure dependence deviates from the simple power rule and the velocity is seen to converge to that value obtained when the

resistance of the HCP device is negligibly small. For the data shown in Figure 3, R_{ext} is equal to 28 mΩ.

No plasma velocity data have been obtained for the current HCP system. Thus to test the validity of the model in predicting the plasma speed, calculations were made for the original HCP prototype[14] and for a second device used in our laboratories for a blue-green laser system.[25] The electrical and physical parameters of the systems tested are given in Table II. Figure 4 shows a graph of speed versus pressure for the system in Reference 14. The model results are calculated using the value of R_{ext} = 1.5 mΩ estimated from the circuit parameter given by the authors. The adjustable parameters α of 0.01 $Torr^{-1}$ and R_o of 1.4 mΩ give the best fit to the data. The model is observed to give reasonable agreement for the range of pressures tested. The value of k from the model (k=0.3) is somewhat smaller than the value for the experimental data (k=0.6).

Figure 5 shows similar data for the system described in Reference 25. The system parameters are given in Table II. These results are similar to those found for the system in Reference 14 in spite of the large difference in the physical and electrical parameters of the two systems. Thus indicating good agreement between the model and experimental results for a wide range of system parameters.

The spectral irradiance, I_s, of the HCP device can be shown[23] to be related to the peak current, I_p, produced in the HCP device by a relationship of the form

$$I_s = f\left(I_p^{\beta}\right)$$

where $\beta \cong 1$. For this report, a direct proportionality between I_s and I_p is assumed. We thus compare time integrated spectral irradiance to the peak current the model predicts for the

device.

Figure 6 shows the peak current as a function of pressure for the same parameters used in Figure 3. The model shows a wide range of results from nearly no dependence of I_p on pressure to a very strong dependence. For low values of α and R_o, I_p is only weakly dependent on pressure, with this dependence being dominated by the variable HCP inductance as observed when $\alpha = 0$ and R_o is small. A sharp rise is noted in I_p at low pressures and small values of R_o for all values of α. For large values of R_o, this strong dependence is only observed at high values of α. At high pressures, the peak current only weakly depends on pressure for all values of α and R_o.

These results were compared[26] to experimental data from References 24 and 25. Results in Figures 7 and 8 show good agreement between the model and experimental predictions. The trend of strong dependence of I_s on P at low values of pressure is clearly seen in the experimental data. The model correctly predicts this trend as well as the weak dependence exhibited at high pressures.

Finally, the risetime of the current signal is compared to the risetime of the measured spectral irradiance. Results are plotted in Figure 9 for the same conditions and range of parameters given in Figure 3. The trends in the results are observed to be similar in features to those in Figure 6. Experimental results for the devices in References 24 and 25 are compared to the model predictions as shown in Figures 10 and 11. The data in Figure 10 shows reasonable results in the absolute value of the risetime, but does not capture the trend in that the experimental data tend to show an increase in risetime with increase in pressure while the model predicts the system should begin to saturate within the pressure range shown. Also, in Figure 11 it is observed that the model fails to predict both the correct absolute value of the risetime (at low pressures) and the data trends at high pressure. This may be simply do to the

method used to define (and subsequently measure) the risetime for the experimental data. This is currently being investigated. On the other hand, the model does not take into account any of the physics involved in production of the emission during the plasma creation and run down stages. Thus total correlation is not expected. Since the results discussed in the previous paragraph in which I_s versus I_p were found to be in good agreement, it is believed that the model should predict the trend in the risetime without further enhancements. Therefore the measurement procedures are the prime suspect in the lack of agreement between model and experimental results.

The parameters utilized in the model for each of the three devices are given in Table III. The parameters α and R_o used were determine to be the values that gave good agreement between experimental results and model predictions for the situation in which I_s was compared to I_p for the devices in References 24 and 25. For the data in Reference 14, the values were chosen for the velocity measurements since these were the only results available for that experimental system.

TABLE II. SYSTEM PARAMETERS

Parameters	Ref 24	Ref 14	Ref 25
r_o (mm)	28.6	100	49
r_{edge} (mm)	6.3	50	13
h (mm)	3.2	50	12.8
# of electrodes	22	2	13
Capacitance (μF)	1.4	150	8.03
Voltage (kV)	30-38	19	20-40
Pressure (Torr)	.1-30	.5-15	1-30
Gas	Ar	D_2	Ar
R_{ext} (mΩ)	28	- -	34.9
R_{total}* (mΩ)	179 (@10 Torr)	2.9	34.9
L_{ext} (nH)	55	20	88.7
L_1 (nH)	135 (@ 10 Torr)	24	130.5

*The value of R_{total} and L_1 are measured as describe in Reference 22 for the data of References 24 and 25 and calculated from reported circuit parameters for Reference 14.

TABLE III. MODEL RESULTS

Parameters	Ref 24	Ref 14	Ref 25
k - Model	- - -	0.6	
R_o (mΩ)	200	1.4	100
R_{ext} (mΩ)	28	1.5	8.4
α ($Torr^{-1}$)	0.16	0.01	0.08

CHAPTER 3: THE LASER SYSTEM

HCP System Design

Based on the previous results for the HCP pumped dye laser, a new plasma focus device[27,28] array was designed for 1 Hz laser excitation. Figure 12 shows the detailed drawing of the HCP device. The device is made of a series of 23 thin molybdenum disk electrodes surrounded by 24 ceramic insulators. The small and large inner diameters of the electrodes are 0.5" and 1.5", respectively. The thickness of the electrodes is 1/8". When the device is operated in a heavy gas high pressure mode, the transfer efficiency, y_t, of the pumping light, which is the ratio of the intensity incident on the dye solution to the intensity of a ring shaped UV-plasma source, can be defined from simple geometric optics by the relation:

$$y_t = R_2/\pi R_1$$

where R1 and R_2 are the inner radius of the HCP device and the radius of the dye cuvette, respectively. The above relation is derived on the basis that the incident light intensity on the dye cuvette from a point source of ring type plasma has the ratio of $2R_2/2\pi R_1$ for the total irradiance of the point source. Therefore, small diameter electrodes are desirable for a high transfer efficiency. The thin thickness of the electrode and insulator contribute to a homogeneous axial distribution of the pumping light which reduces the thermal lensing effects due to axial inhomogeneities of the pump beam. Ceramic insulators, molybdenum electrodes and two stainless steel end electrodes minimize the vaporization of the active materials, and this leads to an expected long lifetime for the device and reduces the decrease in the laser output due to material sputtering for repetitive operation. In addition, the dead (dark) length of the cuvette was minimized by appropriate geometrical design of the end electrodes. Copper sulfide ($CuSO_4$), with conductivity of approximately 3×10^{-3} mhos, was used to provide equal potential

differences to each electrode. This solution also acted as a coolant in repetitive operation. The device was 17 cm long, about two times longer than the prototype used earlier. Since the resistance of the device was directly proportional to the length of the plasma distribution and inversely proportional to the diameter of the plasma ring, the device had a large resistance and thus a large portion of the stored energy dissipated within the device. The cylindrical ground transmission line and the close gap configuration between the inside plasma and the outside current return path minimized the inductance of the device. The estimated maximum inductance based on the geometry of the system was 80 nH. This was important to obtain a fast risetime for the current and the pumping light pulse. A uniform distribution of the pumping light inside the dye solution was desirable for making a large mode volume. If the radiant intensity, I_0, is incident into the dye solution at a particular wavelength, then the intensity, I, transmitted by the dye solution is given by Beer's Law, $I/I_0=10^{-\varepsilon Md}$, where ε is the molar extinction coefficient, M is the concentration of the solution in moles per liter, and d is the diameter of the dye cuvette. The extinction coefficient for a BBQ dye solution is 54000 (liter/mole cm) at 305 nm.[29] For a 10^{-4} mole/liter dye concentration and 3 mm inner diameter of the dye cuvette, the intensity ratio, I/I_0, is 0.024. At the center of the dye cuvette the intensity ratio is 0.16. The pumping light intensity of the core section of the dye cuvette is expected to be twice this intensity due to illumination from the opposite side. The system for this research used a suprasil tube with an inner diameter of 3 mm as the dye cuvette. The laser dye used was BBQ in a p-dioxane solution which had the peak absorption and fluorescence wavelengths of 305 and 382 nm, respectively. Therefore suprasil grade quartz was necessary. The vacuum of the HCP chamber was maintained with 48 large O-rings between the electrodes and the ceramic insulators and 2 small O-rings made of ethylene-propylene, which are resistive to the p-dioxane, between outside electrode and dye cuvette.

Experimental Configuration

The 1 Hz UV dye laser system consisted of 4 subsystems; 1) electrical system, 2) gas flow, dye circulation and cooling systems, 3) laser cavity, and 4) measurement system. Figure 13 shows the electric circuit diagram for the HCP system. The high voltage-capacitor charging power supply (Candela Laser Corp. Model HVD-2000 A) provided a charge rate of 2000 J/s and was operated up to a maximum of 40 kV with two 0.7 μF capacitors (Maxwell Labs.), which were connected in parallel. Since this power supply was connected with a load dependent oscillator, a 0.3 mH induction coil and a 16 kΩ resistor in series were used as a charging network for 1 Hz, 40 kV operation. The capacitor had a 50 kV maximum charging voltage. When the capacitor was operated at 40 kV, it provided 1.1 kJ of stored electrical energy. A rail-gap type switch was introduced for a low inductance discharge network. This rail-gap switch was specially designed for a parallel-plate transmission line with electrodes whose widths were equal to that of the transmission line. The switch will have low inductance if the current is distributed along the length of the rail electrodes. This will be achieved with a trigger pulse voltage having a fast risetime. The cross section of the switch is shown in Figure 14. The switch was surrounded by a cylindrical plexiglass housing which reduced the shock wave sound during the discharge. The electrode gap of the switch was adjustable so that the desired hold-off voltage could be obtained. Multiple trigger pins, which were operated with the trigger pulse having 0.7 risetime, were used to achieve reliable firing in repetitive operation. The switch was initiated by a trigger pulse generator (EG&G Electro-Optics, Model TM-12A) which produced up to 30 kV. The repetition of the trigger output pulse was set by an external oscillator (BK precision, 3010 Function Generator). To prevent reverse voltage through the trigger pulse system, four resistors, which had 50 kΩ each, connected in parallel were used in series with the switch. In addition, a small spark gap was inserted between the

12.5 kΩ resistor and the secondary coil of the trigger pulse generator to make a fast trigger pulse. A 500 pF capacitor was also used to isolate the trigger pulse generator from the main discharge circuit. To reduce the inductance of the discharge circuit, the capacitor bank and the HCP device were connected by a parallel transmission plate. The edge of this plate was rounded to reduce unwanted breakdowns. Soft copper pieces were used to prevent electrical arcs at contact surfaces of the conductors. The gas needle valve, vacuum gauge and leak detector system were installed to control the filling gas pressure of the HCP device. The HCP device and vacuum gauge were placed the same distance from the vacuum source to insure correct pressure measurements of the HCP device. The pressure monitoring system was attached at the ground side of the HCP device, while a gas tank and regulator system was attached at the high voltage side of the device and isolated from the ground.

Figure 15 shows the schematic diagram of the dye and $CuSO_4$ solution circulation systems. The dye circulation system consisted of a micropump, a mesh filter, a dye reservoir, and stainless steel and teflon tubes. For 1 Hz UV dye laser operation, the micropump, having 40 psi pressure, was chosen to provide fast dye solution circulation. A 0.2 μm mesh filter was inserted in the dye flow system to maintain the dye solution free from contamination. All materials contacting the p-dioxane solution was made of stainless steel and teflon which are chemically resistive to the solution. The 5 liter dye reservoir, made of stainless steel, was sufficient for cooling the heat generated when the dye solution was circulated at high speed. The stainless steel tube and the micropump were grounded to eliminate induced electrostatic charge from the dye solution and teflon tubes. Another micropump was used to circulate the 5 liter $CuSO_4$ solution to cool the HCP device.

The resonator system was constructed by using a flat total reflection mirror (R>99%) and concave mirrors having different reflectances. If R_1 and R_2 are the mirror radii and d is

the separation of the resonator mirrors, the stability condition of a spherical resonator is as follows:[30]

$$0<g_1g_2<1$$

where $g_1=1-d/R_1$ and $g_2=1-d/R_2$. For $R_1=2$ m, $R_2=\infty$ and $d=27$ cm, $g_1g_2=0.86$. Therefore, g_1g_2 satisfies the stable resonator condition.

Figure 16 shows a block diagram for the measurement system. The system was composed of 4 blocks; 1) electrical system analysis block, 2) time dependent spectroscopic analysis block, 3) time integrated spectroscopic analysis block, and 4) laser energy, beam profile, and beam divergence measurement block. The voltage waveform of the main discharge circuit was analyzed with a series resistance voltage divider, an oscilloscope (CRO), and an IBM personal computer (PC) system. Time dependent HCP emission properties were measured by a photomultiplier (PM) tube and CRO system through a bandpass filter. Absolute irradiance was calibrated with deuterium and tungsten standard sources. A short pulse standard source (50 μs), which is comparable to the HCP light emission, was made by inserting a mechanical chopper in front of the PM tube. The thermal effect on the dye solution was monitored by passing a He-Ne laser through the dye cuvette when the HCP system was operating repetitively. The repetitive characteristics of the BBQ dye laser were measured with a PM tube and CRO (Tektronix, Model 7104) and digital camera system (DCS). The data acquisition of 1 Hz operation was possible by the DCS and PC computer system. The output energy of the laser was measured with an energy meter. Its beam characteristics were measured by a linear photodiode array obtained from an optical multichannel analyzer (OMA).

Time Dependent Spectroscopic Analysis

To evaluate the new HCP plasma array as a UV laser excitation source, optical pulse

shape, absolute irradiance, and angular and axial distributions of the source were determined at the surface of the laser active material. For excitation of laser active materials which have a short lifetime (0.9 ns for a BBQ dye solution) for the upper laser level, a light pulse with a fast risetime is needed as discussed in Chapter 1. It is known that the optical pulse of an electrical discharge has different emission spectra at the initial breakdown phase and at the after-glow state. In order to pump BBQ dye, the optical pulse from the source was evaluated in the absorption wavelength band (λ=310 nm, $\Delta\lambda$=20 nm) of the dye. The temporal behavior of the light for 30 kV charging voltage and 10 Torr filling gas pressure is shown in Figure 17. The pulse shown in the figure is seen to be composed of an initial breakdown phase and an after glow state as expected. Risetime, which is defined as a time interval corresponding to 10% and 90% of the signal intensity, and FWHM of the pulse are 0.37 and 0.8 μs, respectively. This risetime is sufficient for pulse operation of the BBQ dye laser. The time at which the intensity of the pulse reaches a maximum, 0.7 μs, is consistent with that of the current waveform. Figure 18 shows risetime of the optical pulse as a function of the charging voltage. The risetime decreased as charging voltage increased. The risetime dependence on pressure is shown in Figure 19. The risetimes of optical pulses increased as the pressure increased. For these data the charging voltage was kept constant at 30 kV. These results can be explained by Paschen's law. For a given gap distance between electrodes, the spark development of argon gas into an arc (here the argon was used as the filling gas of the HCP chamber) was affected by the applied voltage and the gas pressure. In the high gas pressure and low applied voltage region, the spark development is retarded by the collision among electrons, moleculars and impurity atoms. Therefore, the risetime of the optical pulses in this region was slow compared to that of the low pressure and high applied voltage region. Since the optical pulse contains stronger UV emission in the initial surface discharge stage of the breakdown, the FWHM of the optical pulse in the absorption band of BBQ does not increase with increasing gas pressure as shown in Figure 20.

From these results, one could predict the optimum lasing conditions for a BBQ dye laser to be the highest capacitor charging voltage and pressures in the range of 10 to 15 Torr.

To measure the peak absolute irradiance of the pumping light at the surface of the laser active material, a UV enhanced PM tube (Amplex 150 UVP) system having a narrow bandpass filter and neutral density filters was used in combination with a chopper system and a standard deuterium source which had a smooth spectral output in the UV region. Figure 21 shows the arrangement for the irradiance measurement system. To measure irradiance incident on the BBQ dye solution, the absolute irradiance measurement was made after the light signal transmitted through the walls of the suprasil dye tube. In this measurement arrangement, the light signal arriving on the surface of the dye solution came from a semicircle of the UV emitting area of HCP device. On the other hand, the standard deuterium source, which was used to calibrate the light signal, was treated as a point source. Therefore, the ratio of HCP irradiance to the standard source irradiance measured after reflection from the aluminum reflector was corrected for this geometric difference between the two light sources. To overcome this difference, the surface of the suprasil tube was sanded so that it would diffuse the incident light. This diffused window made it possible to determine the correct ratio of the irradiances by the standard source and the HCP light emission. All of the optical components used were UV enhanced. The optical fibers (Fiberguide Industries), the neutral density filters (Oriel), and the suprasil quartz tube (Heraeus Quartz, T21), all of which transmit down to 200 nm; and an aluminum reflector, were used for measuring UV light emission from the HCP system. Linearity tests for the PM tube were performed in the voltage range used for this experiment. The result of a PM tube linearity test is shown in Figure 22. All measurements were performed in the range having linear response. Also the output voltage signals, one from the deuterium standard source and another from the HCP light signals, were measured in the same voltage range by using neutral density filters to attenuate the HCP light intensity. A

PM tube does not have constant response to different pulse widths due to variations of its effective capacitance between the anode and the final dynode. To calibrate this difference, a mechanical chopper utilizing a 30,000 RPM series wound motor was used with the standard source, which had a continuous emission. The chopper was located in front of the detecting point of the light. From this mechanical chopper system, a 50 μs pulse width was obtained. This FWHM was comparable with that of the HCP light pulse. A secondary 30 W UV light source (Oriel Corporation Model 6313), was calibrated with a UV-40 Standard Deuterium Light Source (Optronics Laboratory). This calibration was performed with an OMA system based on the absolute irradiance value of the UV-40 supplied with the lamp. The wavelength band received by the PM tube was selected by a bandpass filter (λ=310 nm, $\Delta\lambda$=20 nm) which corresponded to the optimum absorption wavelength of BBQ dye solution. The voltage signal of the standard source detected by the PM tube should be large enough to minimize the error which comes from the dark current noise of the PM tube. The voltage signal were measured in the range which satisfies the signal to noise ratio condition. This was made possible by selecting a detecting point close to the standard source. Figure 23 shows the variations of irradiance depending on the distance between the light source and the detecting points. From the figure, a best fit curve was found with a function of the form r^{-b}, where b=1.8±0.3. From these calibrations, 1 kW/cm^{2}nm spectral irradiance was determined as peak emission irradiance of the HCP emission at 310 nm, with 30 kV capacitor charging voltage and 10 Torr filling gas pressure. Figure 24 shows variations of the peak absolute spectral irradiance at 310 nm measured as a function of filling gas pressure. This result shows a slight increase in the peak spectral irradiance up to 20 Torr. Figure 25 shows the applied voltage dependence of the spectral irradiance. The increasing trend of spectral irradiance was slowed in the high applied voltage region. These results will be further analyzed when time integrated spectral irradiance is discussed in the next section.

Azimuthal and axial distributions of the spectral irradiance of the HCP device were also taken into consideration. Figure 26 exhibits the homogeneous azimuthal distribution of the HCP emission for 10-Torr working gas pressure and 30-kV capacitor charging voltage. This homogeneity is a consequence of the uniform plasma formation in the HCP device initiated by the uniform initial surface discharge. However, Figure 27 shows an irregular axial distribution that depends on the working gas pressure and the position from the insulator or the electrode. The irregularity at 1-Torr working gas pressure is more dependent on the measurement position from the insulator or the electrode than that of 10 Torr filling gas pressure. This difference by gas pressures may be explained as follows. In the high pressure mode, the ring type plasmas having a large volume were formed along the surface of the ceramic insulators. On the other hand, more focused plasmas having small volume were formed along the dye cuvette in the low pressure mode, and this plasma gives an irregular pumping light distribution on the dye cuvette. Since this type of irregularities could possibly lead to non-uniform heating of the laser active material, and consequently refractive index gradients which work as a thermal lens, they will adversely affect the laser output. To avoid this kind of problem, a diffused quartz tube was used for the system. The detailed analysis of the thermal effect based upon this irregularity will be discussed later in the section on stabilities of the pumping light and the dye solution up to 1 Hz operation.

Time Integrated Spectroscopic Analysis

The time integrated spectral irradiance from 250 to 700 nm was measured by using an Optical Multichannel Analyzer (OMA, EG&G Model 1450) which consisted of a grating spectrometer and a diode array detector. Three wavelength bandwidths of 75, 150, and 600 nm covered by the OMA system could be chosen by selecting one of 3 different gratings. The diode array detector active area was 2.5 mm H x 25 mm W and contained 1024 elements. Each

element was 25 μm wide. The spectral response of the detector ranged from 200 to 1100 nm. The same optical transfer geometry as that of the time dependent spectroscopic analysis was employed in these measurements.

Wavelength calibration of the OMA system was done by using the mercury arc spectrum. In this calibration, at least five different mercury spectrum lines were chosen for accuracy. All optical components were fixed during the data acquisition. Software was developed to perform the calculations for the irradiance calibration. The calibration was performed as follows. The ratio of the NBS-traceable spectral irradiance of the standard source to the corresponding OMA counts for 1 second was made, and this ratio was used as an optical transfer calibration factor for a given optical transfer system, such as dye cuvette, aluminum reflector, optical cable, neutral density filter, and OMA system. The OMA counts for the HCP emission divided by the temporal FWHM of the light pulse and multiplied by this calibration factor gave the spectral irradiance of the HCP emission. Figure 28 shows the quantitative spectral irradiance of the HCP emission with operating conditions of 30 kV, 10 Torr. The spectral irradiance below 400 nm was calibrated by the deuterium standard source enriched in the UV region, and the spectral irradiance above 400 nm was calibrated by the tungsten standard lamp which had a smooth emission spectrum in the visible region. The calibrated spectral irradiance from both calibrations at a match-up wavelength, 400 nm, coincided within 8% error. The spectrum below 250 nm was cutout due to weak sensitivity of the instruments in the UV region below 250 nm. The OMA trace shows considerable line spectra which were attributed to the argon transitions and the excited Si species from the ionized substrate. The continuum emission of the spectrum could be interpreted by an ideal blackbody. Comparison of blackdody curves with the spectrum shows that T_b (effective brightness temperature) is about 15000 K. Since the maximum in the blackbody spectrum could be calculated by the Wien's displacement law i.e.

$$\lambda_{max}T = 2.898 \times 10^{-3} Km \ .$$

For BBQ dye, the maximum of the absorption band exists at 310 nm. From the above equation, the calculated corresponding temperature is 9348 K at 310 nm. Since the maximum wavelength of the HCP device exists at 183 nm for the 15000 K, a spectrum converting into the laser absorption band is necessary to increase the spectral efficiency. Figure 29 shows the spectral irradiance of the HCP emission at 1 Torr. The other parameters were kept the same as that of 10 Torr gas pressure operation. The figure shows a reduced visible emission relative to the UV emission (visible/UV) compared to that of 10 Torr. The reduction in UV emission is also observed for the case of less stored energy as shown in Figure 30, which was obtained with 0.7 μF capacitance, 30 kV capacitor charging voltage, and 10 Torr filling gas pressure. These results are consistent with a model which relates the radiated energy to the plasma current density. In a low pressure region, the velocity of plasma current sheet is high, but optical density is low, and the UV emission is dominant compared to the visible emission. For a low input energy with the high filling gas pressure, the current density is low, but optical density is high, and the visible emission is dominant.

The spectral efficiency for the BBQ dye laser could be determined from the OMA spectrum. The irradiance, E, in the range λ_1 to λ_2 is

$$E = \int_{\lambda_1}^{\lambda_2} E_\lambda d\lambda$$

where E is the spectral irradiance of the HCP emission. The shaded area in Figure 28 represents the absorption band (280-330 nm) of the BBQ dye. Integration of this shaded area yielded an irradiance of 45 kW/cm^2. For a known temperature, T, the ratio of radiance in the

given wavelength band to the total radiance could be determined by the blackbody radiation functions.[31] For the measured temperature, 15000 K, of plasma source and the wavelength of 250 nm, which was the wavelength cut out due to weak sensitivity of the OMA device, the value of λT was 0.38 (cm deg). For this value, the ratio of radiance in the region from 0 to 250 nm to the total radiance was 0.4438. Since the integrated irradiance in the range 250 to 700 nm was 190 kW/cm^2, the total irradiance became 341.6 kW/cm^2. Therefore, the determined spectral efficiency of the HCP spectrum was 13% as a pumping source of the BBQ dye laser. The temporal FWHM of the HCP emission in this wavelength region was 0.8 μs. Therefore the irradiance of 45 kW/cm^2 corresponds to 36-mJ/cm^2 energy density which is incident on the laser active material within the BBQ dye laser pump band. The incident total energy was 1.2 J for the 32 cm^2 surface area of the laser active material.

Figure 31 shows the capacitor charging voltage dependence of the time integrated irradiance for HCP emission within the BBQ dye laser pump band. The dependence is slightly faster than a linear relation. The figure shows a continuous increase with increasing charging voltage while the peak irradiance value showed a saturation in the time dependent measurement as also seen in Figure 25. This is due to the fact that there is an increasing trend in the FWHM of the optical pulse without increasing the peak irradiance value as the capacitor voltage increased.

The pressure dependence of the time integrated irradiance in the same pump band is shown in Figure 32. The integrated radiance increases rapidly in the lower pressure region below 15 Torr and then saturates above 15 Torr. This trend was similar to that observed for time dependent spectroscopic analysis shown in Figure 24. But in the low pressure region, the temporal FWHM of the pump light in the absorption band of BBQ dye increases up to 10 Torr, and the irradiance increases rapidly. The FWHM shows a slight decrease in the high pressure

region. This could explain the saturation trend of the irradiance above 15 Torr.

Stabilities of Pumping Light and Dye Solution up to 1 Hz Operation Mode

Pumping light stability and thermal stability of dye solution were studied to obtain basic data for a stable output of the UV laser. The newly designed HCP system was repetitively operated up to 1 Hz with different filling gas pressures in the region of 1 to 50 Torr and 37-kV capacitor charging voltage. During the repetitive operation, the working gas pressure was maintained constant by flowing the filling gas. Also the charging capacitor voltage was set at a constant value. The fast charging of the capacitor bank was possible by use of a resonant high voltage charger. The charging time for a 1.4 μF capacitor was approximately 0.023 with 16 kΩ charging resistor at 30 kV applied voltage. This charging time was sufficient for 1 Hz operation at a constant charging voltage. The 16 kΩ resistor was immersed in distilled water to prevent heating and breakdown over the surface of the resistor. Since the HCP device was surrounded by $CuSO_4$ solution which works as a coolant as well as a voltage divider to the HCP electrodes, the temperature of the device could be maintained at a constant value (<30°C) by circulating the coolant. The schematic diagram of the circulation system was shown earlier in Figure 16.

Figure 33 shows a strip chart recording of repetitive operation of the HCP device. The data acquisition system was not calibrated. This figure shows good reliability of the high voltage switching system and the HCP system. This reliable switching was possible by adopting a rail gap switch with multiple trigger pins in the ground rail side. Figure 34 shows the quantitative HCP emission intensity as a function of firing number of the device at 1 Hz operation. The data were obtained with a UV enhanced PM tube (Amplex 150 UVP), a narrowband pass filter (λ_0=310 nm, $\Delta\lambda$=20 nm) and UV optical light transfer systems. For repetitive data

acquisition, a digital camera system was used along with a properly designed software system. The peak intensity was measured for every fifth shot. The observed signal fluctuated by less than 8% for the 130 shots evaluated. This decreasing effect could be interpreted by the erosion of the dye cuvette surface and in part by the evaporation of the electrode and the insulator. Even though the pumping light intensity fluctuated less than 8% for the 130 shots, the stability of the UV dye laser output intensity was influenced more by the thermal gradient of the p-dioxane dye solution inside the laser resonator. When the HCP system was fired, the inhomogeneous pumping light distribution on the dye cuvette along the axial direction introduced irregular heating of the dye solution in that direction. This inhomogeniety in the axial direction lead the dye solution to act like a lens due to a nonhomogeneous refractive index. Figure 35 shows the devised method used to study the thermal effect by monitoring the divergence of a He-Ne laser beam passing through the dye solution while the HCP device was operating repetitively. The intensity of the He-Ne laser beam after passing through the dye solution was detected by the photodiode detector system. The output He-Ne laser beam was observed to defocus by the thermal effect of pumping and the detector signal dropped to some value V_2, where $V_2<V_1$. After a brief time delay, the detector signal was recovered to the its original value, V_1. The value V_2/V_1 indicates the degree of the thermal effect. To reduce this thermal effect on the dye solution during repetitive operations up to 1 Hz, the effect was studied with factors such as the dye temperature, dye refresh rate, discharge repetition rate, and diffused transmission.

Figure 36 shows a typical signal detected by the photodiode detector system at 30 kV, 10 Torr, and 0.7 Hz operating conditions. The maximum signal for the output He-Ne laser beam was 0.6 V and the restoring rate was established to be 0.7 Hz at a 15 s^{-1} refresh rate and at room temperature for the dye solution. The dye solution was maintained free from contaminations by inserting a 0.2 μm mesh filter, which was made of teflon, in the dye flowing

tube as shown in Figure 16. Figure 37 shows the restoring time as a function of the refresh rate for different dye temperatures of 24, 18, and 14 °C. The freezing temperature of the p-dioxane was 11.8 °C below which flowing can not be made. Here the restoring time was defined as the time required for the output He-Ne laser beam to recover 68% of its original value, V_0. Since the thermal gradient of the dye solution was caused by an inhomogeneous pumping light distribution and by the a dye cuvette being heated from hot plasma, a fast refresh rate was more efficient than lowering the temperature of the dye solution in this temperature range. Figure 38 shows the variation of output of the He-Ne laser beam intensity for numbers of firing at 1 Hz, 10 Torr, and 30 kV operation mode. The refresh rate was 15 s^{-1}. At the above operating conditions, the decrease of output intensity was 75%. This result shows that the cooling of the dye cuvette was insufficient to account for the accumulated heat of the dye cuvette transfered from the hot plasma during the 1 Hz repetitive operation. A diffused superasil tubing was inserted around the dye cuvette to reduce the inhomogeneous distribution of the pump light on the dye solution and to isolate the dye solution from the hot plasma. For single shot operation at 30 kV as shown in Figure 39, 0.3 s of the restoring time was monitored by a He-Ne laser at 18 s^{-1} refresh rate. From this result it is expected that the repetitive operation of the dye laser up to 3 Hz operation is possible by using a properly designed diffuser. A secondary converting dye solution, which was employed in Candela dye laser system, could also be used to insulate the heat conducting from the hot plasma to the dye cuvette. Another heat insulation method, which is possible by making vacuum space between the inner dye cuvette and the outer diffused quartz tubing, could be used for the UV laser.

Laser Characteristics in a Single Pulse Operation

The emission of the newly designed HCP device which produced intense UV radiation with

a fast risetime permitted the excitation of a BBQ dye laser. Experiments were performed in single pulse operation with parameters of argon filling gas pressure, capacitor charging voltage, and transmittance of output coupler. Also, the laser energy, beam profile, and divergence of the laser beam were measured.

The output laser energy was measured with a pyroelectric energy meter (Molectron, Model No. J3-05). For the experimental parameters of 10 Torr filling gas pressure, 630 J capacitor charging energy, 50% output mirror transmittance, and 5 x 10^{-4} M BBQ concentration in p-dioxane solution, 60 mJ of laser energy was obtained in the single pulse operation. To prevent detector saturation a neutral density filter and 5% transmittance output mirror were calibrated at that laser wavelength and inserted between the energy meter and the laser output mirror to attenuate the output laser energy. The output laser energy (60 mJ) corresponded to a overall efficiency, the ratio of the laser output energy to the stored capacitor energy, of 0.0095%. The internal efficiency, which is defined as the ratio of laser energy to the pumping light energy in the absorption band of the dye, of the laser is 5% for the 1.2 J of the total pumping enrgy incident in the dye solution. It is predicted that an elongated length of the HCP device is necessary to increase the load resistance and the laser gain inside the resonator.

Figure 40 shows an oscilloscope trace of the temporal behavior of the BBQ dye laser monitored with a PM tube. The leading signal before the cursor is due to electrical noise. The signal parameters were analyzed by a digital camera system. The laser pulse had a FWHM of 0.23 μs and a risetime of 40 ns. This short pulse width compared to 0.8 μs of the pumping light pulse at 310 nm could be interpreted by the quenching effect of the triplet state. This result is inconsistent with the assumptions about the absence of triplet effect in a short pulse BBQ dye laser (40 ns FWHM) pumped by XecL laser.[1]

The pressure dependence of the output laser energy is shown in Figure 41. Applied

capacitor energy of 630 J and 5 x 10^{-4} M BBQ dye concentration were used. This pressure dependence could be interpreted by the pump light distribution and optical properties of the pumping light. As mentioned earlier, the axial distribution of the pumping light at the surface of the dye solution is different depending on the working gas pressure and the positions of the insulator and the electrode. In the pressure region studied, the axial irregularity of pumping light in the low pressure region depends more on the positions of the electrode and the insulator compared to that of the high pressure region. The dye solution was subject to refractive index variation due to temperature gradients caused by this irregularity of the axial distribution of the pumping light. The thermal effect dramatically reduced the output intensity of the laser in the region below 5 Torr. Even though the output intensity of pumping light increases up to 20 Torr, the laser intensity does not increase due to the increase in risetime of the pumping light as the fill gas pressure increases. The slight increases in the risetime resulted in a gradual decrease in laser intensity above 10 Torr. As a result, the optimum filling gas pressure was at 10 Torr.

Figure 42 shows the applied voltage dependence of the output laser energy. The fill gas pressure was set at 10 Torr. The output laser energy increased proportional to the input energy up to 0.65 kJ. The increasing trend was slowed in the region above 0.65 kJ. This trend was well matched with the applied voltage dependence of the pumping light. Therefore more extraction energy is expected for the increased input energy. The slope efficiency, which is defined as the ratio of increased laser energy to the increased stored capacitor energy, was calculated as 0.01% in the linearity increasing region. Table IV summarizes the efficiencies of the BBQ dye laser.

The untuned laser wavelength was measured using an OMA system. The grating resolution of this device was 0.0076 nm/cell. Two modes was observed at the peak laser wavelength of 385.26 and 385.69 nm with a separation of 0.43 nm. The FWHM was 2.76 nm

as shown in Figure 43.

The beam profile and the beam divergence of the laser were measured with the OMA photodiode detector array. The array consists of 1024 elements of single photodiode cell, and the length of the array was 2.54 cm. To make this measurement the detector was removed from the OMA spectrometer. For a spherical resonator, the field distribution at any point inside the resonator can be obtained by the Kirchoff integral.[32] This field distribution can be given by

$$U(x,y,z,t)=\left(\frac{w_o}{W}\right)H_m\left(2^{1/2}\frac{x}{w}\right)H1\left(2^{1/2}\frac{y}{w}\right)\left(e^{-\frac{(x^2+y^2)}{w^2}}\right)\sin(x,y,z)\sin(wt),$$

where

$$w^2=w_0^2[1+(2z/d)^2].$$

The spot size at the center of the resonator is given by

$$w_0=(d\lambda/2\pi)^{1/2},$$

and the divergence of the laser beam is $\theta=(2\lambda/\pi w_0)$. For resonator parameters used in the laser HCP system, i.e., R_1=2 m, $R_2=\infty$, and d=27 cm, the calculated spot size at the center of the resonator was 0.129 mm and a 1.9 mrad was calculated as the beam divergence of the BBQ dye laser. Figure 44 shows the measured beam profiles in the x and y directions. This beam profile is close to the TEM_{02} mode. As expected from the calculation of the pump light distribution inside the dye solution, the pumping light was sufficient to reach laser threshold in the core section of the dye cuvette. Figure 45 shows the measured beam profiles at 60, 80, and 100 cm from the output mirror coupler. From these profiles, a 2 mrad beam divergence was measured. This value compared favorably with 1.9 mrad which was calculated from the theoretical field description for the spherical resonator.

The useful laser power output from the total power emitted by the stimulated emission is

related to atomic, optical, and pumping parameters which could be derived from the rate equations. If the triplet loss is included in the internal loss and the excited vibronic state is assumed as the lower laser level, the dye laser kinetics could be treated as a four-level laser. Figure 46 shows the laser output energy for the transmittance of the output coupler of resonator. The maximum laser output energy was obtained at 50% transmittance of the output coupler. As the transmittance increased up to 50%, the output laser energy increased due to the increased photon loss through the output coupler. But for increased transmittance above 50%, the available laser energy goes into the internal laser cavity loss due to the increased laser threshold energy. This increased internal loss resulted in a decreased laser output energy.

Laser Characteristics in Repetitive Operation

The characteristics of the BBQ dye laser under repetitive operation were studied with parameters of the repetition rate and the refresh rate of the dye circulation. During the experiment, 2 liter p-dioxane dye solution was circulated at the desired refresh rate. And the relative laser intensity was recorded by the digital camera system connected with a UV enhanced photodiode.

Figure 47 shows the stability of the output laser energy dependence on the number of firing of the laser system at the different repetition-rates. The refresh rate was maintained 15 s^{-1} during the data acquisition. The output laser energy fluctuated with the increasing number of firing. But the laser energy maintained constant for the number of firing with deviations less than 15% for 30 times firing. Figure 48 shows the laser energy variation vs the repetition rate of the system. The data points were obtained from the stabilized laser output after 5 shots. As anlyzed earlier in the section of stabilities of pumping light and dye solution up to 1 Hz opeartion, the restoring had an exponential function with respect to a time. The rate was established to be 0.7 Hz at 15 s^{-1}. Therefore, the decreased laser energy with the increased

repetition rate may be explained by the mainly thermal gradient of the dye solution. Laser energy of 8 mJ was measured for the 1-Hz repetition rate.

A FWHM of the laser pulse was measured at the varied refresh rate as shown in Figure 49. As expected, the FWHM of the laser was increased as the refresh rate increased. The quenching effect on the laser pulse may be attributed from the thermal of the dye solution.

The laser energy dependence on the number of firing at the different refresh-rates was shown in Figure 50. The repetition rate was 0.5 Hz. The laser energy for the low refresh rate decreased more rapid than that of the high refresh rate due to the accumulated heat of the dye cuvette during the repetitive operation. Figure 51 shows clearly the thermal effect on the output laser energy. The laser energy increased for increased refresh rate. The small laser energy at a low refresh rate may be the result of the heating of boundary layer of the dye solution from the hot UV irradiation. Although the refresh rate of the dye circulation was 15 s^{-1} at room temperature, 2 s restoring time was needed to get a half of the maximum energy obtained from single shot operation. Those results indicated that thermal insulation of the dye cuvette from the hot plasma source is necessary for the repetitive operation above 0.5 Hz. Table V shows the parameters of the BBQ dye laser. These thermal effect will be discussed in the next chapter.

TABLE IV. EFFICIENCIES OF BBQ DYE LASER

Electrical Efficiency (%)	: 68
Spectral Efficiency (%)	: 13
Internal Efficiency (%)	: 5
Slope Efficiency (%)	: 0.01
Overall Efficiency (%)	: 0.0095

TABLE V. PARAMETERS OF BBQ DYE LASER

Absorption Peak Wavelength (nm)	: 307
Untuned Laser Wavelength (nm)	: 386
Laser Energy of Single Shot (mJ)	: 60 (For V_0=30 kV)
Optimum Filling Gas Pressure (Torr)	: 10
Optimum Output Coupler (%)	: 50
Extracted Energy Density (mJ/cm^3)	: 50
Maximum Power (kW)	: 260
Pulse Width (FWHM, μm)	: 0.23
Divergence Angle (mrad)	: 2
Repetition Rate (Hz)	: 1
Laser Energy (mJ) at 1 Hz	: 8

CHAPTER 4: THERMAL EFFECTS

In order to study the thermal effect, which is caused by non-uniformity of the HCP plasma light source consisting of a series of electrode-insulator disk pairs, a LD490 dye laser system was set up as shown in Figure 52. The nature of the thermal effect was studied by the transmitted intensity variation of a He-Ne probe laser beam traversed through the dye cuvette placed on the axis of the HCP array as function of the input energy and the dye flow rate.

For the reduction of the thermal effect, a double-walled cuvette is introduced to replace the single cuvette. The transmitted intensity variation of the laser probe beam for the double-walled cuvette, which is filled with ethanol or LD490 dye instead of air, was compared with that of the single dye cuvette. Furthermore, the laser output of LD490 dye with double-walled cuvette was compared with single cuvette. Details of the experiment and discussions on the results follows.

Experimental Arrangement

Figure 52 shows a block diagram of the experimental arrangement used for the study of thermal effect caused by non-uniformity of the pump source. The experimental setup consists of a hypocycloidal pinch (HCP) array, a high voltage power source, a plasma switch with its triggering system, a vacuum pump and a dye circulation system. The power source consists of a 1.4μF capacitor and a power supply which has a maximum charging rate of 2 kJ/sec at 40 kV. An inverse-pinch switch which has a low inductance and a long life time is used. In order to trigger the switch, the combined mechanical and electrical methods are used. The mechanical method is to initiate triggering by adjusting the filling gas pressure of the chamber, and the electrical method is to initiate triggering through the multiple pins between electrodes by sending the electrical pulse with the short risetime about 30 kV. A vacuum system which

consists of vacuum pump, vacuum gauge, needle valve etc., controls the working gas pressure in the HCP array. Using a micropump, dye flow rate in the dye cuvette of the HCP array is controlled.

As shown in Figure 53, the HCP device generates the relatively uniform and radially pinching plasma. In order to minimize sputtering from the electrodes of the HCP and increase the purity of the generated plamsa, electrodes are made of molybdenum, the insulators are ceramic and end plates are stainless steel. Thickness of electrodes and ceramic insulators are 1/8" and the inner diameters of electrodes are 0.5" and 1.5" alternately. Electrodes with inner diameters of 0.5" and 1.5" are alternatively placed between the ceramic insulators in order to minimize the shadow created by the electrodes. The HCP array is made of 23 electrodes and 24 insulators, and the length of the HCP array is 6". Double tubes (outer tube has ID 8 mm and OD 10 mm and inner tube ID 4 mm and OD 6 mm) are located along the central axis of the HCP array. Dye solution is circulated in the inner tube and the space between the inner and outer tubes is filled with the cooling media. The space between electrodes and the outer tube is circulated with argon working gas whose pressure is varied. In order to provide the uniform potential difference between electrodes and cool the electrodes which are heated by hot plasmas, the HCP array itself is placed inside a container, and the space between electrodes and the container is filled with copper sulfide solution ($CuSO_4$), that had a conductivity of approximately 3×10^{-3} mhos.

In this experimental arrangement the homogeneity of the plasma light is increased by reducing the thickness of the electrodes of the HCP array. Furthermore, the resistance of the HCP is increased by reducing the inner diameter of the electrodes in order to maximize the electrical energy transfer to plasma. Finally, the risetime of plasma light from the HCP array is minimized by reducing the external-circuit inductance of the system.

Experiment and Results

In order to study the thermal effect of the plasma on the dye cuvette, the variation of the transmitted intensity of the reference laser (He-Ne) beam through the dye cuvette is measured with a PM tube as functions of input energy, dye flow rate etc. In order to reduce the thermal effects, the double-walled cuvetted is introduced and measured the effects of the media between the tubes.

Figure 53 shows the general characteristics of the thermal effect of the plasma of HCP on the reference laser beam. As soon as the plasma pulse arrives at the dye cuvette where the laser probe beam passes through, the cross section of the probe beam starts diffusing and its intensity becomes weakest. That is to say, the probe beam becomes defocussed and focussed by narrowing its cross section. Finally, the probe beam recovers the original beam intensity. Correspondingly, we define the time duration from the beginning of defocussing through the end of focussing to be called a recovery time. In case of the single cuvette, the defocussing phase is clearly distinguished from the focussing phase, but in the double-walled tube the defocussing phase is clear but the focussing phase is not clear.

Experimental conditions of the HCP device are follows: the range of input energy to HCP array is 180 - 473 J (the applied voltage 16 - 26 kV), the range of argon fill-gas pressure is 1 - 5 torr, the LD 490 dye concentration is 4×10^{-4} moler, and the range of dye flow rate is 10 - 40 cc/sec.

As shown in Figure 54, the recovery time is about 100 msec for the single cuvette without dye solution. The recovery time becomes longer as the input energy to the HCP device increases. When the LD490 dye solution is circulated in the dye cuvette, the thermal effect becomes stronger, and the recovery time becomes several seconds. Figure 54 shows the recovery time as a function of input energy to the HCP at a constant flow rate of LD490 dye solution in the cuvette. Figure 54 indicates that the recovery time becomes longer as the

plasma temperature increases. Figure 55 shows the recovery time as a function of the flow rate of dye solution in the cuvette for the constant input energy to the HCP. It is noted that as the flow rate increases, the recovery time is significantly reduced but is still longer than the time required for the dye solution, which is exposed to the HCP light, to be passed out from the cuvette.

When the double-walled cuvette filled with air, ethanol or LD490 dye are place in the HCP, thermal effect is significantly reduced as compared with the single cuvette. The recovery time for the double -walled cuvette in the HCP is several ten milliseconds, which is small by two orders of magnitude as compared with the single cuvette. Figure 56 shows the recovery time as a function of input energy to the HCP with LD490 dye solution in the cuvette. Similar to the case of the single cuvette in the HCP, the recovery time increases with the input energy but small with ethanol in the space (jacket) between two walls as compared with air in it. Furthermore, the recovery time with LD490 dye solution in the space is the order of 1 millisecond, and reduces as the input energy increase on the contrary to the single cuvette. Similar to the single tube in the HCP, the recovery time with the double tubes decreases as the flow rate of dye solution in the inner tube increases as expected.

Figure 57 shows the risetime of the defocussing phase for the laser probe beam when the HCP light advances toward the dye cuvette. The risetime of defocussing the probe beam is several microseconds with both single cuvette and double-walled one in the HCP. The risetime of defocussing with the double-walled cuvette in the HCP is considerably longer than that with the single one. Furthermore, the risetime of defocussing with a medium such as ethanol or LD490 dye solution, which fills the space between double-walled cuvettes, is longer than that with air medium. One interesting behavior is that the risetime of the defocussing probe beam due to thermal effect is longer than that of the plasma light and is shorter than the duration of the plasma light regardless of both the single and double-walled cuvette.

When a double-walled cuvette is used for pumping blue-green laser, the plasma light from the HCP must pass through the medium filled in the jacket space between double-walled cuvette before the light reaches to the lasing dye. Consequently, it is necessary to find the optical effect of the double-wall. Using an optical multichannel analyzer (OMA), the comparative study of the HCP light spectra is made with the different media such as ethanol, LD490 dye and air in the space between the dual cuvettes. Subsequently, the pumping efficiency of the blue-green laser is also compared for the different media such as ethanol and LD490 dye in the jacket of the double-wall cuvettes.

Figure 58 shows the spectrum of the plasma light under the conditions: 5 Torr argon working pressure and 473 J of input energy. The spectrum indicates that the distribution of light intensity with the medium of ethanol is very similar to that with air in the space between tubes but the intensity with ethanol is stronger than that with air. On the other hand, the irradiance spectrum in the region of 420 - 600 nm with LD490 dye solution in the jacket is significantly stronger than that with ethanol or air. This is due to the fluorescent light (near 500 nm) of LD 490 dye which is generated as the result of absorbing the portion of the HCP light near 400 nm. As expected, the uv spectrum become stronger as the input energy increases. When we compare only the spectral intensity near the absorption band of LD490 dye (λ = 396 nm)) for the different medium of air, ethanol or LD490 in the jacket space of the dual cuvettes, we find that the overall spectral intensity with ethanol is stronger than that with air. However, the spectral intensity with L490 dye is stronger than with air in case of lower input energies as shown in Figure 59.

Figure 60 shows the intensity of blue-green laser as a function of input energy for the different medium in the jacket space of the double-walled cuvette. As expected, the intensity of laser output increases as the input energy to HCP increases. It is especially noted that the intensity of laser output with ethanol is stronger than that with air as the input energy

increases. This shows that choosing the suitable medium in the jacket space is important for increasing the laser efficiency. In case of LD490 dye in the jacket space, the intensity of the laser output for the lower input energy range is weaker as compared with that with air, but the laser output sharply increases as the input energy increases until it exceeds that with air or water.

Discussion

Plasma light, which is generated by the electrical discharge between multi-electrodes in the HCP array, advances radially toward the central axis of the HCP device by the hypocycloidal-shape current distribution. Consequently, the index of refraction of dye solution in the cuvette is nonuniformly changed along the axis by the plasma light. Furthermore, the transmitted laser probe beam experiences scattering and variation of intensity, that is, thermal effect.

When the double-walled cuvettes are used in the HCP for the reduction of thermal effect, the general behavior of the physical characteristics for the HCP light is similar to that with a single cuvette but the variation of the light intensity along the axis of the HCP is reduced and consequently the thermal effect is alleviated significantly. Therefore, the following phenomena are expected with ethanol or LD490 dye in the jacket space of the laser tube: While the variation of the light intensity along the axis of the HCP becomes very small, the risetime of defocussing of the laser probe beam becomes longer due to the thermal insulation provided by the cooling medium such as ethanol or LD490 dye and partial absorption of the plasma light by the medium. Consequently, thermal effect on the laser is reduced and delayed.

Since the index of refraction of the medium filled in the jacket space is different from that of air, the amount of the light received by the dye cuvette is different. When the thickness of the tube is neglected, the amount of light directed to the inner dye cuvette is limited by the incident angle $\theta_1 = \sin^{-1}(a/b)$, where a is the diameter of the inner tube and b the diameter of

outer tube. On the other hand, if the index of refraction n' of the medium is different from that of air, the amount of light transmitted into the inner dye cuvette is increased to the incident angle $\theta_2 = \sin^{-1}(a/b)(n'/n)$ due to refraction. Figure 61 shows the schematic diagram of the geometrical ray tracing for determining the angle of beams directed into the inner dye cuvette. In our case, a = 6 mm and b = 8 mm, $\theta_1 = 40^0$ with air and $\theta_2 = 55^0$ with ethanol, in agreement with the observed results.

In the case of LD 490 dye solution which fills the jacket space, the light directed into the inner dye cuvette is not only increased as mentioned above but also the spectrum conversion of near 400 nm into the fluorescent light near 490 nm takes place. Consequently, the availability of the HCP light near 390 nm in the inner dye cuvette is expected to be reduced for laser pumping. Therefore, the efficiency of pumping the blue-green lasers which require 390 nm band will be decreased. On the other hand, if we use converter dye whose absorption band lies in a shorter wavelength region but its fluorescent band coincide with the absorption band (390 nm) of the blue-green laser dye, then the efficiency of blue-green laser pumping will be enhanced. For example, the absorption band of LD390 is 355 nm and its peak of fluorescence is 386 nm which is near the peak of LD 490 absorption band (see Figure 62). Hence, LD390 is used as a converter dye and LD490 as laser dye, then it is expected that the efficiency of pumping blue-green laser will be enhanced by optimizing the concentrations of LD390 and 490 dyes. Indeed our experimental results have verified this relation.

CHAPTER V: SUMMARY AND CONCLUSION

A new array of plasma focus device which is designed for the UV emission was operated up to 1 kJ at 1 Hz. The excitation source was used to pump a BBQ dye laser. The electrical system parameters were analyzed based upon the voltage signal of discharge circuit. The net HCP resistance was measured to be 178 mΩ at 30 kV for 10 Torr filling gas pressure. The resistance is 4.5 that of the prototype used earlier. The inductance of the system was 0.68 times that of the prototype, and measured as 135 nH. The reduction of the inductance was possible by the nail gap switch operating in multiple channels and by the plate transmission line and the proper geometry of the HCP device. And the peak current of the circuit was measured to be 64 kA. From these electric parameters, an electrical system efficiency of 68% was estimated.

The HCP light emission characteristics were studied by the time dependent and time integrated spectroscopic analyses. The risetime, t_r, and the FWHM of the pulse were 0.4 and 0.8 μs, respectively for the emission in the absorption band of the BBQ dye. Since the typical triplet lifetime, t_T, of the most dye solutions range from 10^{-3} to 10^{-7} sec, the above risetime of the optical pulse satisfies the condition, $t_r > 2t_T$, of the pulse operation of the dye laser. The irradiance of the HCP light emission was determined by detector systems calibrated by the deuterium and the tungsten standard sources. The irradiance of 45 kW/cm^2 was measured in the range 280 to 330 nm from the OMA data analysis for the 30-kV and 10-Torr operation. This corresponds to the spectral efficiency of 13% for the total irradiance of 341.6 kW/cm^2 in the range 280 to 330 nm. From the blackbody radiation spectrum, the color temperature of the HCP plasma was estimated as 15000 K. Since the maximum radiance for this temperature

exists at 183 nm, a spectrum conversion into the laser absorption is necessary to increse the spectral efficiency. The emission of HCP plasma shows good isotropic distribution in the axial direction, but inhomogeneous distribution in the axial direction at low fill gas pressures. This inhomogeneity was reduced at high (>10-Torr) fill gas pressures.

The use of the ceramic insulator and the molybdenum electrodes provided the minimized vaporization of these active materials under the repetitive operation. The fluctuation of the irradiance was observed less than 8% for the 130 shots evaluated. Since the thermal effect of the dye solution was monitored by a He-Ne reference laser for the repetitive operation mode. The restoring time was measured as 1.4 sec for the 15 s^{-1} refresh rate and the room temperature. But the restoring time was reduced as 0.33 sec by inserting the diffuser around a dye cuvette. Therefore, it is expected that 3 Hz repetitive operation is possible at these operating conditions by inserting the properly designed diffuser.

A BBQ dye laser was pumped with the UV plasma source. The peak wavelength of the laser was measured at 385.26 and 385.69 nm. The output laser energy of 60 mJ was obtained with the stored capacitor energy of 630 J. This corresponds to the overall efficiency of 0.0095% and the slope efficiency of 0.001%. The divergence of the laser was measured as 2 mrad. The optimum conditions of the UV laser were the working gas pressure of 10 Torr and the output-couplers of 50% transmission

The characteristics of the laser under repetitive operation were studied with the parameters of repetition rate, refresh rate of the dye circulation. The output laser energy decreased for the increased repetition rate due to the thermal gradient of the dye solution. The insulation of the dye cuvette from the hot plasma may be needed to prevent the decrease of the output laser energy for high repetition rates. The output laser energy shows almost linear increase with respect to the increasing refresh rate of the dye circulation. The laser energy of 8 mJ was measured for the 1 Hz repetitive operation and 15 s^{-1} refresh rate. The output laser

energy maintained constant with deviation less than 15% for the 30 shots evaluated at the variable repetitive operation up to 1 Hz. The photochemical decomposition or the contamination of the dye solution were not observed for the 30 shots.

A model has been developed to predict velocity, peak current and risetime for and HCP system operating in the snow plow mode. Numerical results have been presented for three different HCP devices. The snowplow model gives reasonable results for plasma velocity and spectral irradiance when the HCP resistance is assumed to be a function of working gas pressure and the HCP inductance is assumed to be a function of the position of the plasma sheet. The physical significance of the fitting parameters utilized in the analysis are discussed in the thesis by Workman[23]. The model shows excellent agreement with experimental data in most cases tested.

When a HeNe laser probe beam passes through the cuvette which placed in the axis of the HCP device and the plasma pulse advances radially toward the cuvette, the HCP pumping light in the dye cuvette experiences the following thermal effects are measured in terms of recovery time, risetime, laser output as functions of input energy, flow rate and cooling media etc: Recovery time of the transmitted probe beam is several seconds with a single dye cuvette. The recovery time increases as the input energy to HCP increases but decreases as the flow rate increases. Recovery time of the laser probe beam is several ten microseconds with the dual-walled cuvettes and is decreased to 1/100 as compared several seconds with single cuvette. Furthermore, the recovery time with the medium of ethanol or LD490 dye solution in the jacket of the cuvette is smaller than that with air The risetime of defocussing beam due to thermal effect is several microseconds. The risetime with double-walled cuvette is longer than that with a single cuvette. Furthermore, the risetime with double-walled cuvette which is filled with ethanol or LD490 dye solution becomes longer than that with air. In all cases, the risetime of defocussing beam due to the thermal effects is longer than the risetime of plasma light and

shorter than the duration of the plasma light.

The blue-green laser output using HCP pumping light is about same for the case of the single cuvette and the double-walled cuvette with air. However, the laser output increases with some media such as ethanol and water in the jacket space of the cuvette. Therefore, by using the double-walled cuvette and filling with proper medium, thermal effect caused by the HCP were significantly reduced and the laser efficiency increased.

REFERENCES

1. P. Cassard, P. B. Corcum, and A. L. Alcock, "Solvent Dependent Characteristics of XeCL Pumped UV Dye Lasers", Appl. Phys., 25, 17 (1981).
2. W. Zapka and U. Brackmann, "Shorter Dye Laser Wavelengths from Substituted P-terphenyls", Appl. Phys., 20, 283 (1979).
3. C. Rulliere, J. P. Morland, and O. de Witte, "KrF Pumps New Dyes in the 3500A Spectral Range", Opt. Commun., 20, 337 (1977).
4. Horace W. Furmoto and Harry L. Ceccon, "Ultraviolet Organic Liquid Lasers", IEEE J. Quantum Electronics, QE-6, 262 (1970).
5. B. B. MacFarland, "Laser Second-Harmonic Induced Stimulated Emission of Organic Dyes", Appl. Phys. Lett., 10, 208 (1967).
6. M. M. Maley and G. Mourou, "The Picosecond Time-Resolved Fluorescence Spectrum of Rhodamine 6G", Opt. Commun., 10, 323 (1974).
7. A Hirth, R. Meyer, and K. Schetter, "A Reliable High Power Repetitive Pulsed Dye Laser", Opts. Commun., 40, 63 (1981).
8. J. B. Marling, J. G. Hawley, E. M. Liston, and W. B. Grant, "Lasing Characteristics of Seventeen Visible-Wavelength Dyes Using a Coaxial Flashlamp Pumped Laser", Appl. Opts., 13, 2317 (1974).
9. Mitsuo Maeda and Yasushi Miyazoe, "Efficient Ultraviolet Organic Dye Laser Pumped by a High Power Nitrogen Laser", Japan J. Appl. Phys. 13, 827 (1974).
10. R. H. Dishington, W. R. Hook, and R. P. Hilberg, Flashlamp Discharge and Laser Efficiency", Appl. Opts., 13, 2300, (1974).
11. C. T. Fang and J. F. Lee, "Transient Self-Inductance and Simmer Effects in Linear Flashlamps for Laser Pumping", Appl. Opts., 25, 92 (1986).
12. R. G. Hohlfeld, W. Manning, and D. A. MacLennan, "Self-Inductance Effects in Linear

Flashtubes: An Extension to the Markiewicz and Emmett theory", Appl. Opts., 22, 1986 (1974).

13. N. W. Jalufka, M. D. Williams, and Ja H. Lee, "Current Sheet Collapse in a Plasma Focus", The Phys. Fluids., 15, 1954 (1972).

14. Ja H. Lee, Donald R. MacFarland, and Frank Hohl, "Production of Dence Plasmas in a Hypocycloidal Pinch Apparatus", The Phys. Fluids, 20, 313 (1977).

15. Ja H. Lee and Donald R. MacFarland, "A Dense Plasma Ultraviolet Source", Virginia J. Science, 29, 183 (1978).

16. Ja H. Lee, D. L. MacFarland, and F. Hohl, "Ultraviolet Laser Excitation Source", Appl. Opts., 19, 3343 (1980).

17. K. S. Han, D. K. Park, and J. H. Lee, "A High Pressure Plasma Source for Pumping Atomic Iodine Laser", Virginia J. Science, 35, 169 (1984).

18. Harry Rieger and Kyekyoon Kim, "Optical Pumping of Dye Laser with an Array of Dye Laser", J. Appl. Phys., 52, 5381 (1981).

19. K. S. Han, S. H. Nam, and Ja H. Lee, "High Power Blue Green Laser by Hypocycloidal-Pinch Plasmas", J. Appl. Phys., 55, 4113 (1984).

20. K. S. Han, C. H. Oh, and Ja H. Lee, "Spectrum Converter Dye for Enhancement of Blue-Green Laser Efficiency", J. Appl. Phys., 60, 10 (1986).

21. W. J. Yi, D. D. Venable, and Ja H. Lee, "Ultraviolet Dye Lasers by Hypocycloidal Pinch Plasmas", Proceedings of the International Conference on Lasers' 86, 411, STS Press, McLean, VA (1987).

22. D. D. Venable, J. H. Lee, and K. S. Han, "Center for Electro Optics and Plasma Research Annual Technical Report", AFOSR grant number-86-0345, March 1988.

23. M. B. Workman, M. S. Thesis, Hampton University, Hampton, VA 23668, in preparation.

24. S. M. Lee, One Hertz Ultraviolet Source for Laser Excitation, M. S. Thesis, Hampton

University, Hampton, VA 23668, 1988.

25. K. S. Nam, Megawatt Blue-Green Dye Laser Excitation by A Hypo-cycloidal Pinch Plasma, M. S. Thesis, Hampton University, Hampton, VA 23668, 1988.

26. D. D. Venable, M. B. Workman and J. H. Lee, "Numerical Simulation of the Plasma Motion in a Hypocycloidal Pinch Device", Bulletin of the American Physical Society, 34, 120, (1989).

27. D. D. Venable, S. M. Lee, J. H. Lee and K. S. Han, "A One-Hertz Hypo-cycloidal Pinch Plasma Pump-Source for Ultraviolet Dye Lasers", Proceedings of the International Laser Science Conference IV, Atlanta, GA, Oct. 2-6, 1988.

28. D. D. Venable, J. H. Lee, and K. S. Han, "Center for Electro Optics and Plasma Research Progress and Forecast Report", AFOSR grant number-86-0345, July 1988.

38. Oragio Svelto, Principles of Lasers (Plenum, New York, 1976), P. 231.

39. Isadore B. Berlman, Handbook of Fluorscence Spectra of Aromatic Molecules (Academic Press, New York and London, 1971), P. 244.

40. A. E. Siegman, An Introduction to Lasers and Masers (McGraw-Hill Book Company, New York, 1971), P. 322.

41. D. D. Venable, Center for Electro Optics and Plasma-Annual Report, Hampton U., Hampton, VA (1988).

42. Exciton, Laser Dyes Catalog, Exciton Chemical Company, INC, Dayton, Ohio (1983).

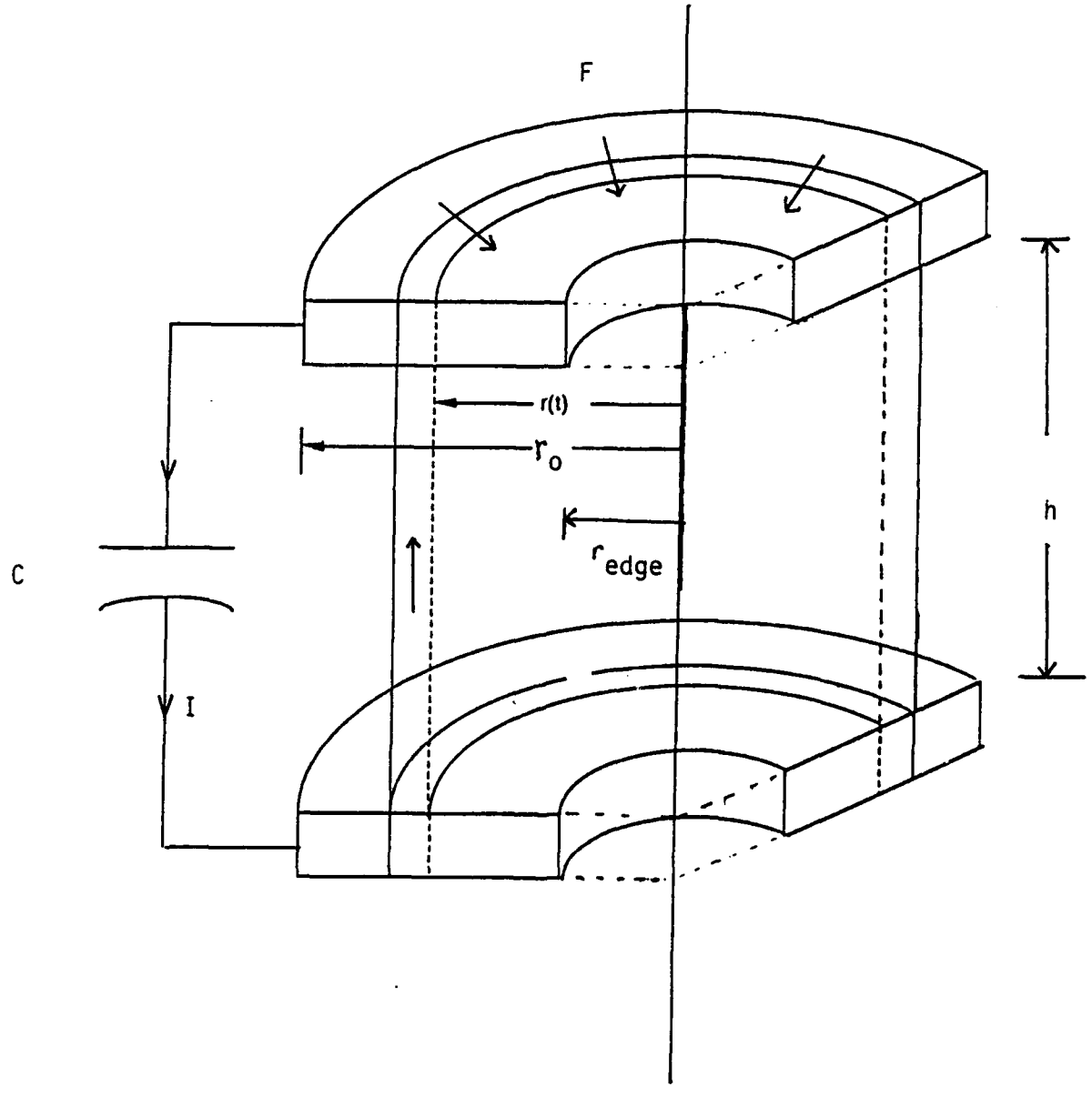

FIGURE 1. Model representation of HCP plasma sheet.

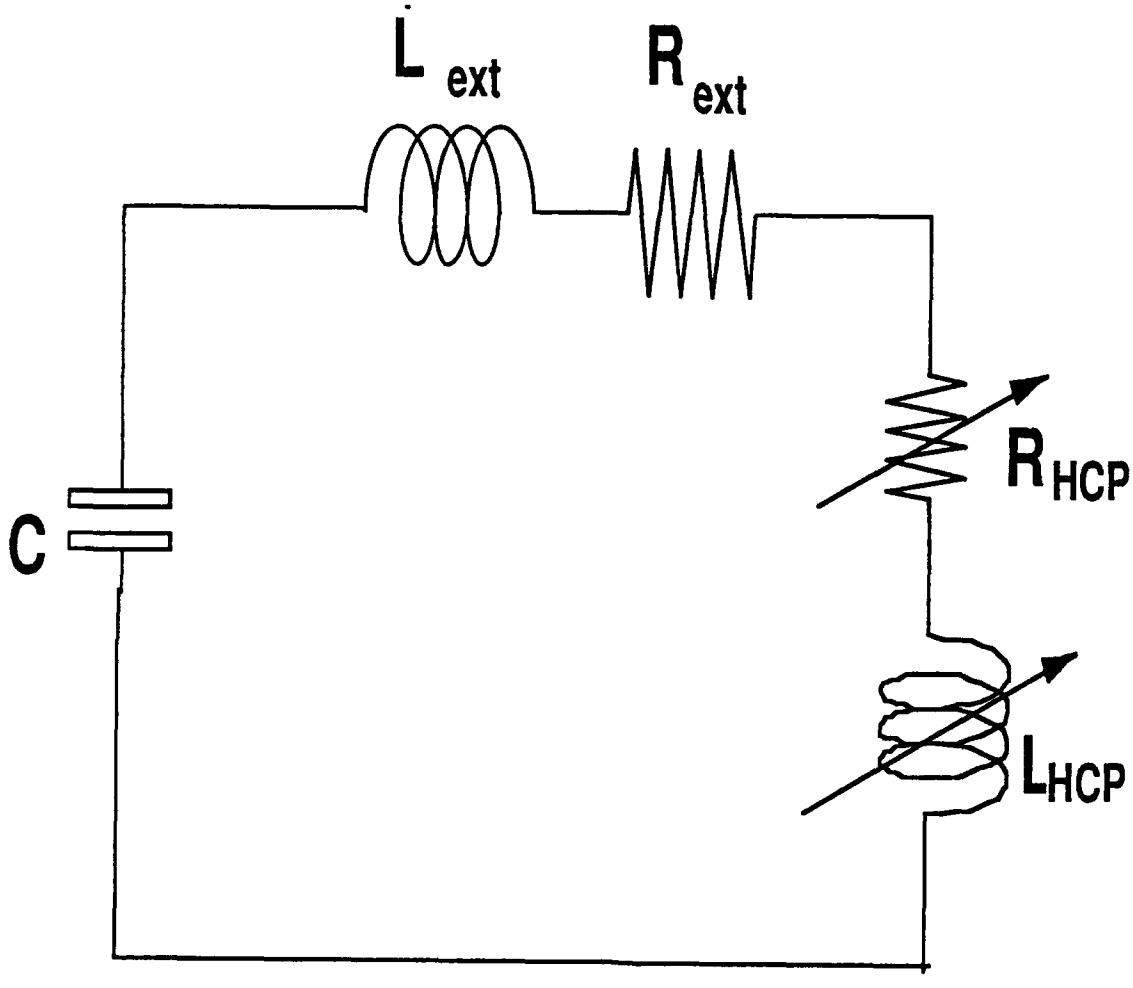

FIGURE 2. Equivalent electrical circuit for the HCP device.

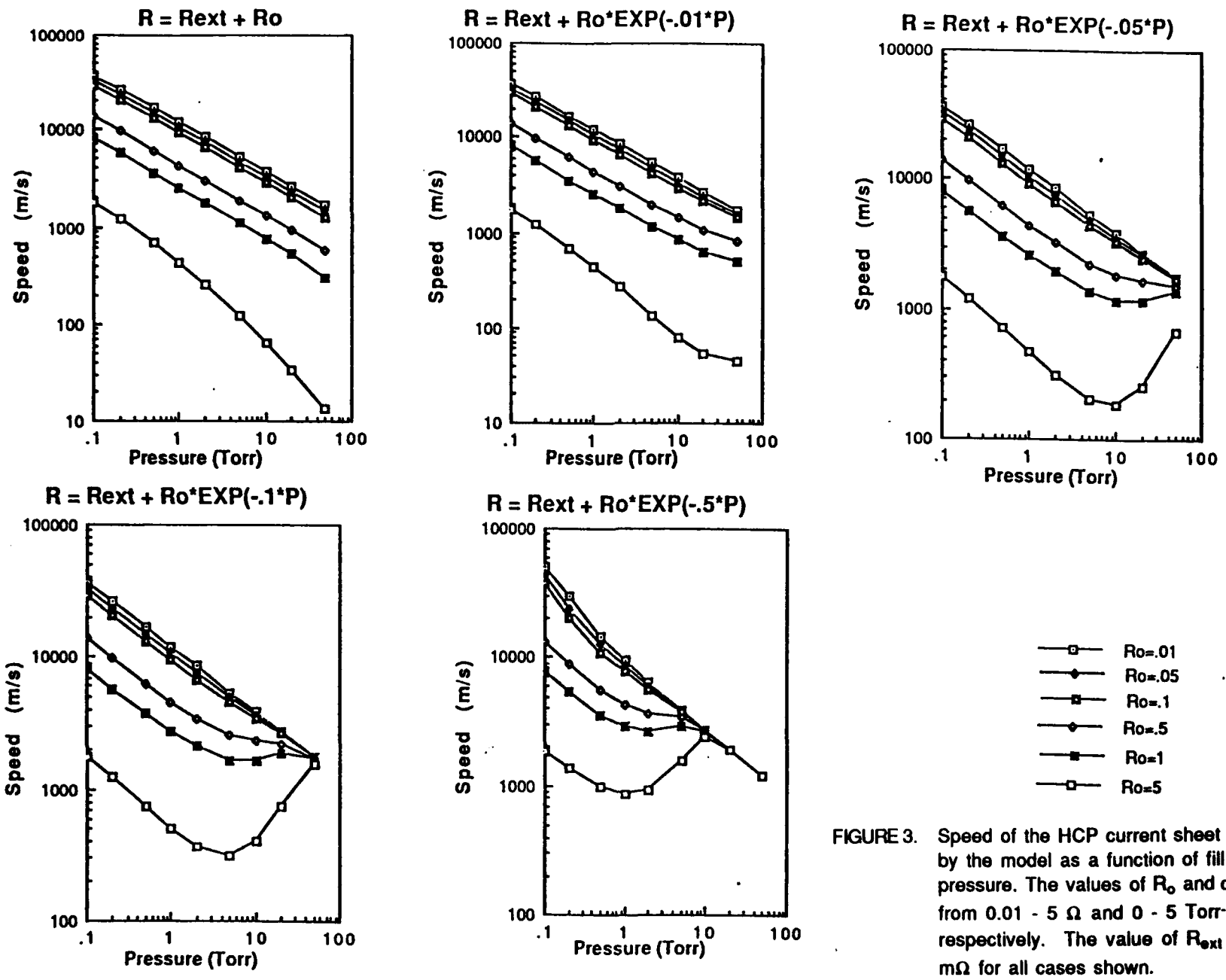

FIGURE 3. Speed of the HCP current sheet predicted by the model as a function of fill gas pressure. The values of R_o and α range from 0.01 - 5 Ω and 0 - 5 $Torr^{-1}$, respectively. The value of R_{ext} was 28 mΩ for all cases shown.

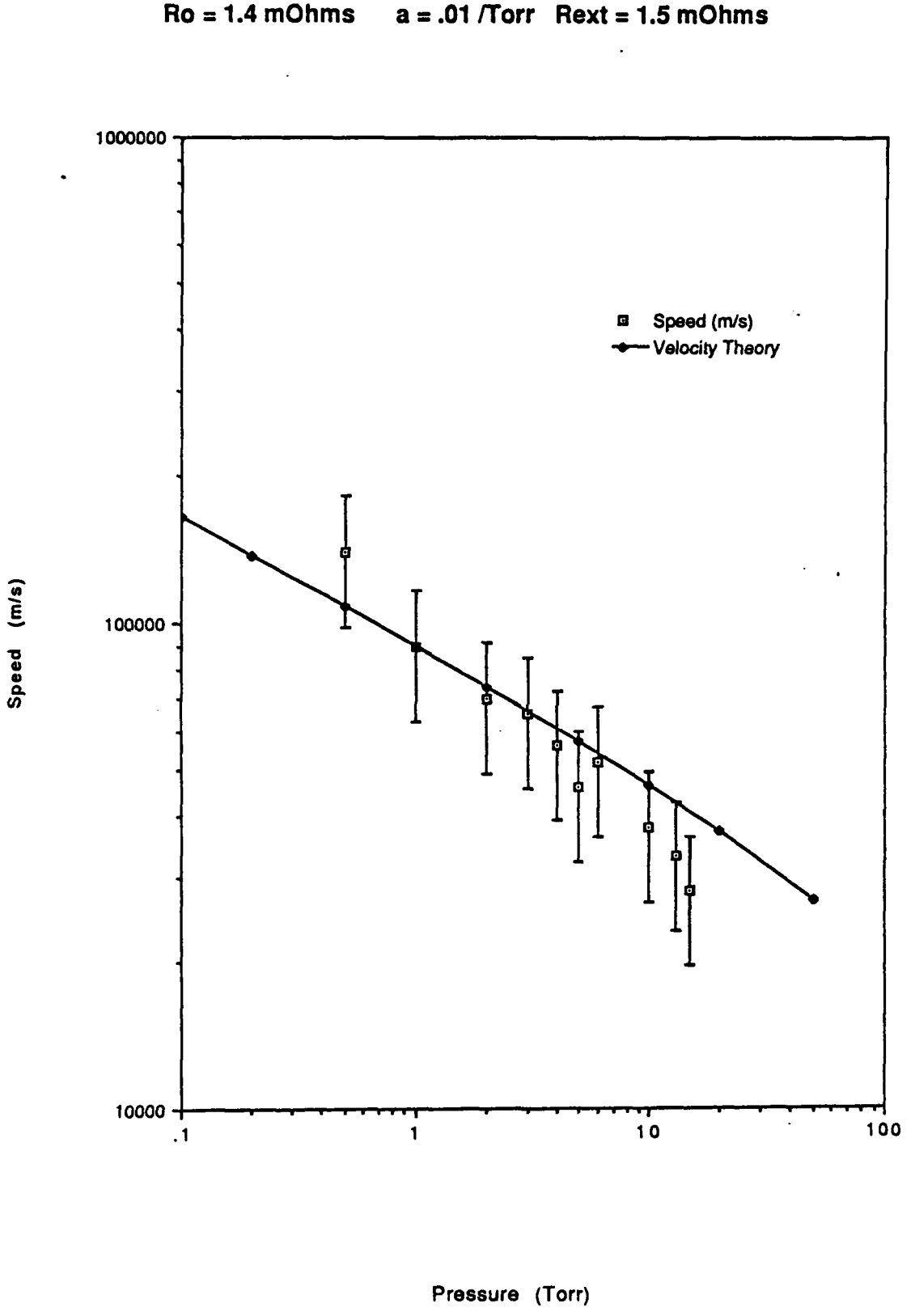

FIGURE 4. Speed versus pressure data for the system described in Reference 14. The system parameters are given in Table II and the fitting parameters in Table III.

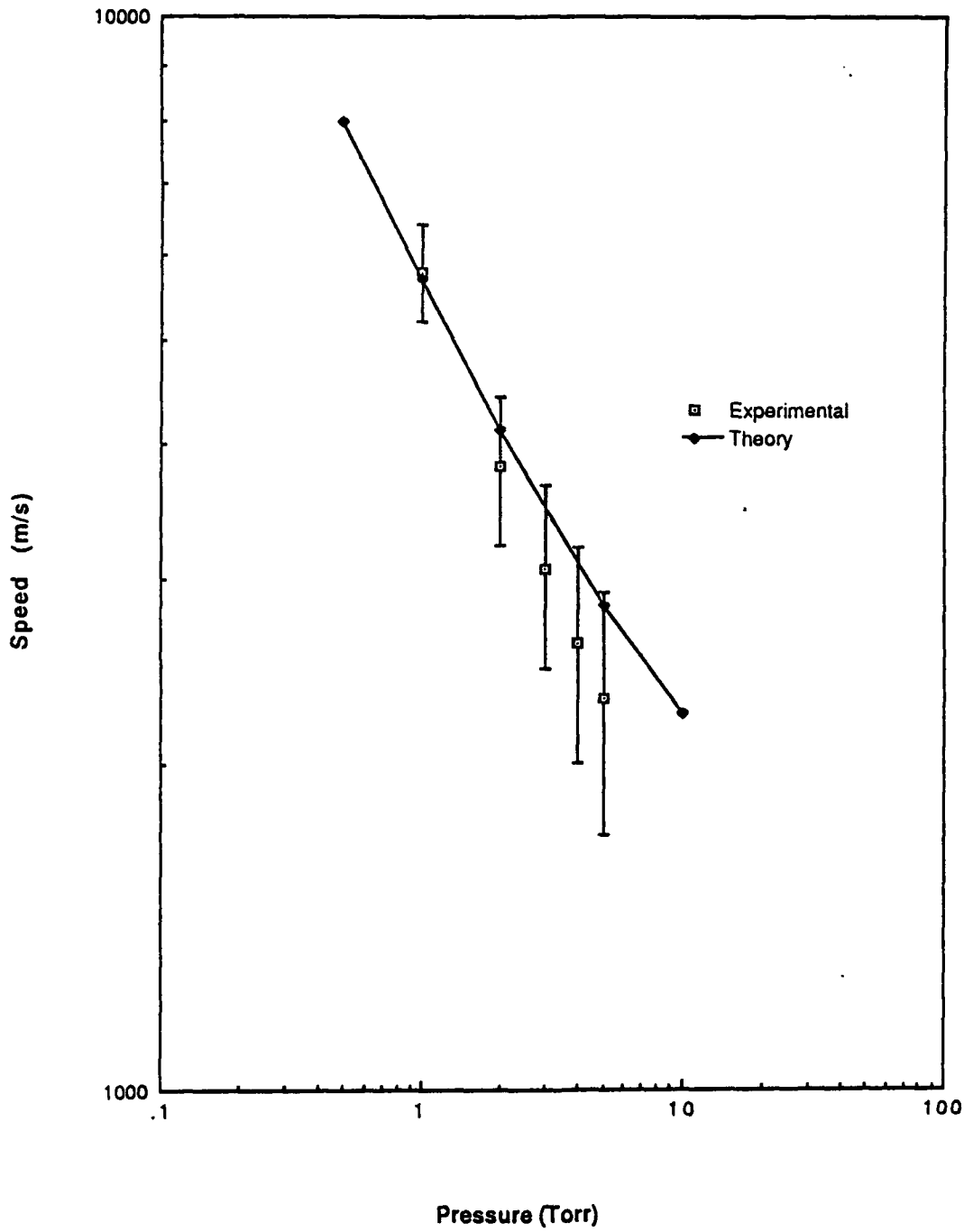

FIGURE 5. Speed versus pressure data for the system described in Reference 25. The system parameters are given in Table II and the fitting parameters in Table III.

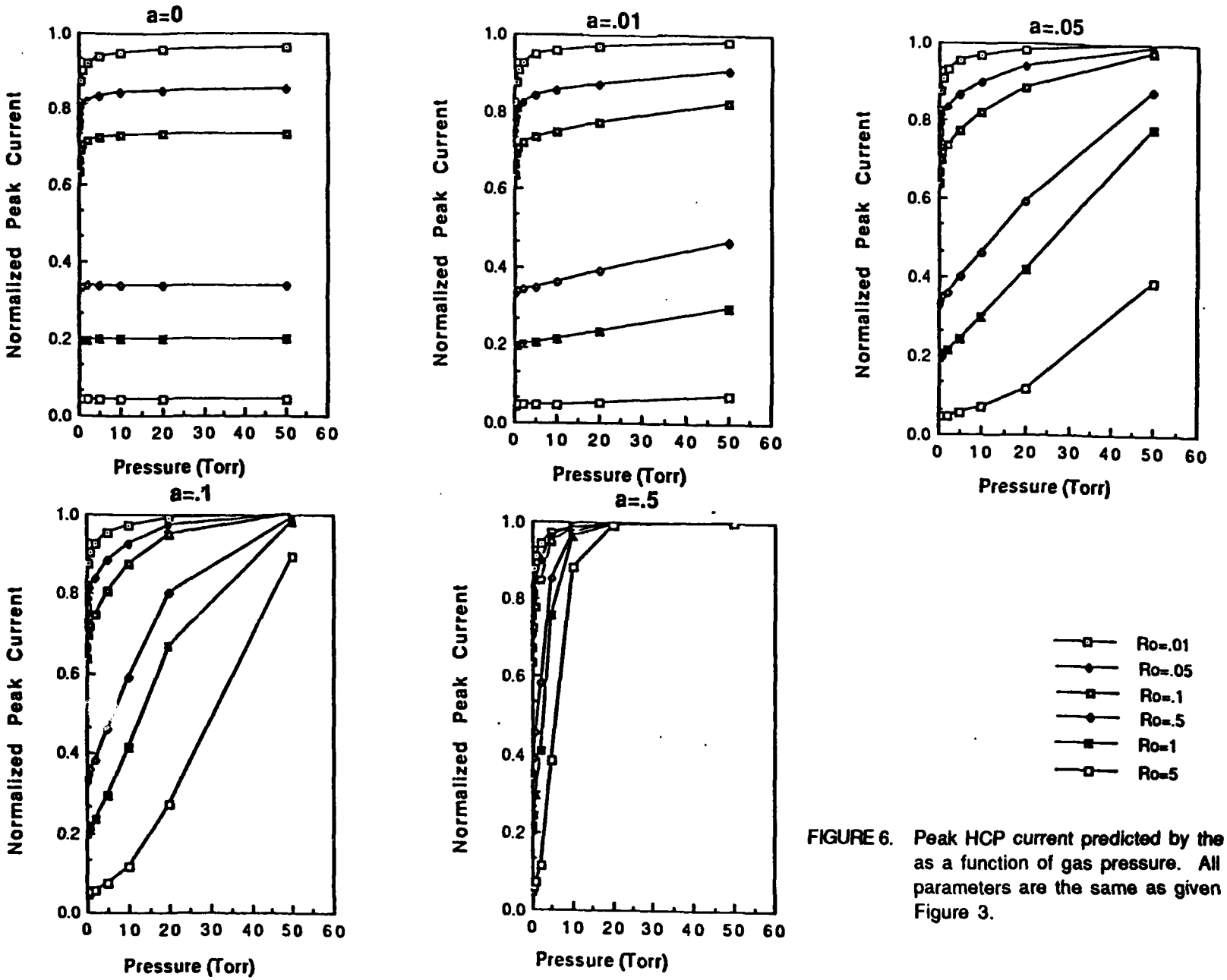

FIGURE 6. Peak HCP current predicted by the model as a function of gas pressure. All parameters are the same as given in Figure 3.

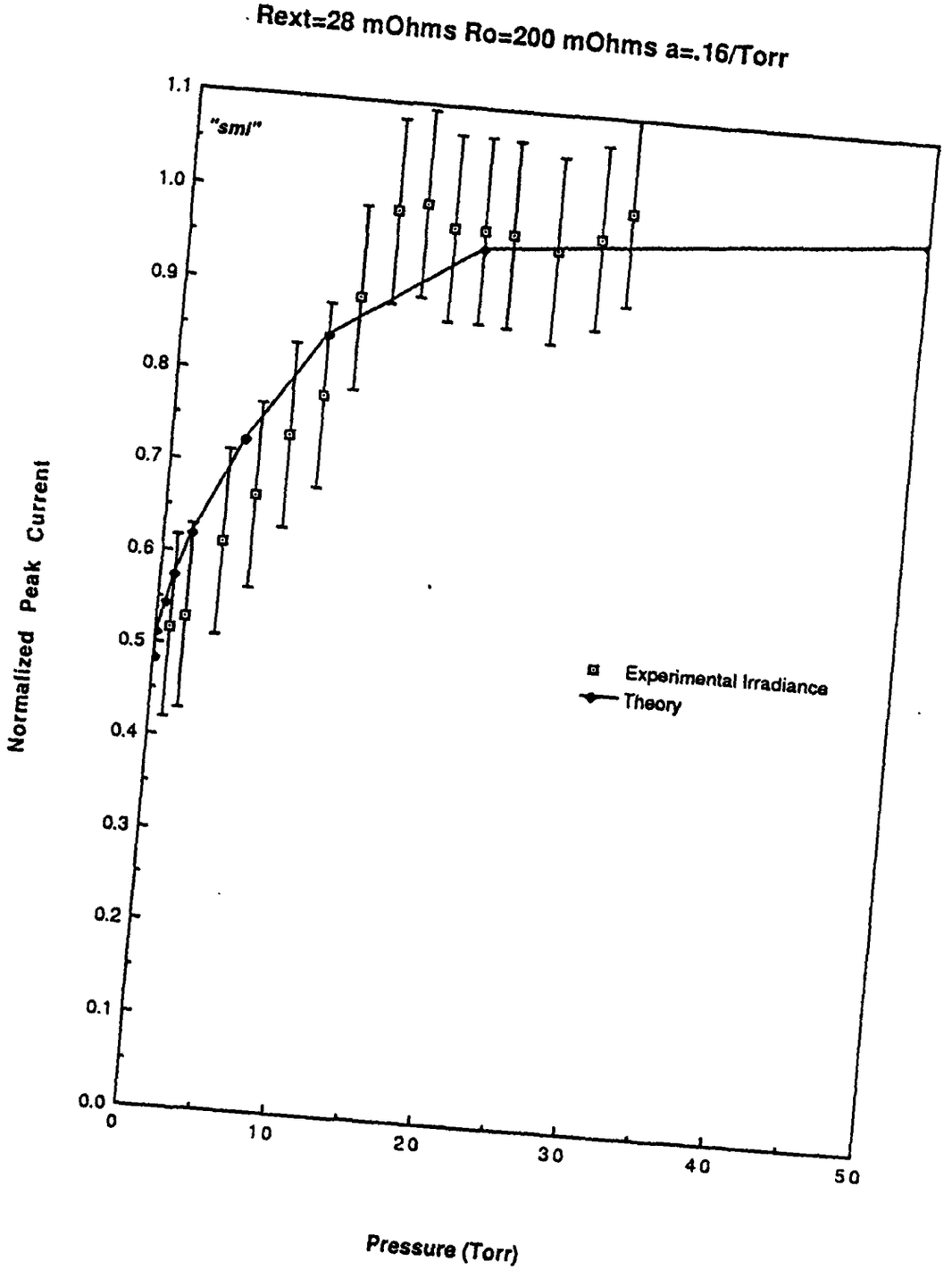

FIGURE 7. Spectra irradiance, I_s, (squares) for the device described in Reference 24 plotted as a function of gas pressure. The solid line is the peak current predicted from the model using the parameters given in Table III.

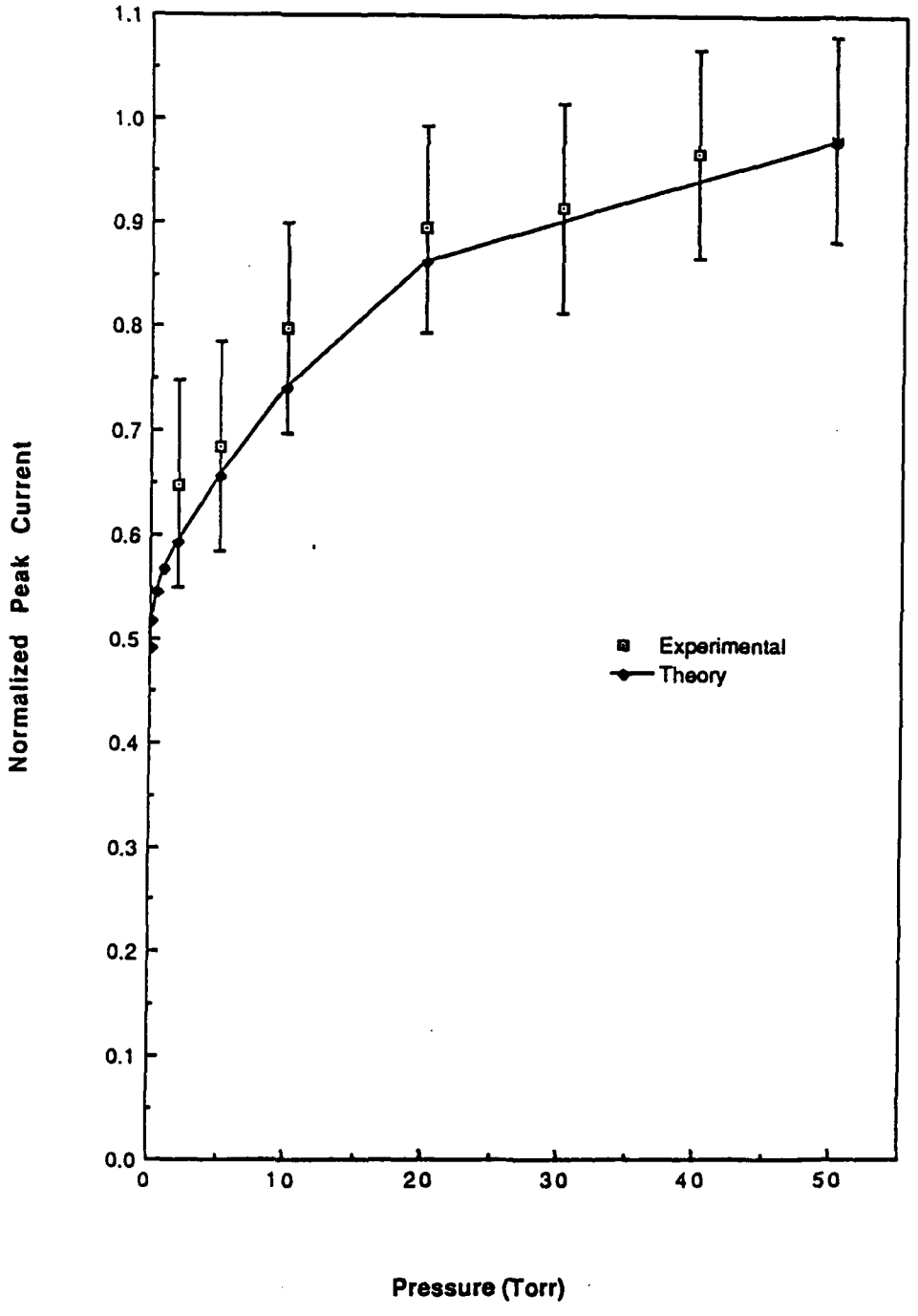

FIGURE 8. Same data as in Figure 7 but for the system described in Reference 25.

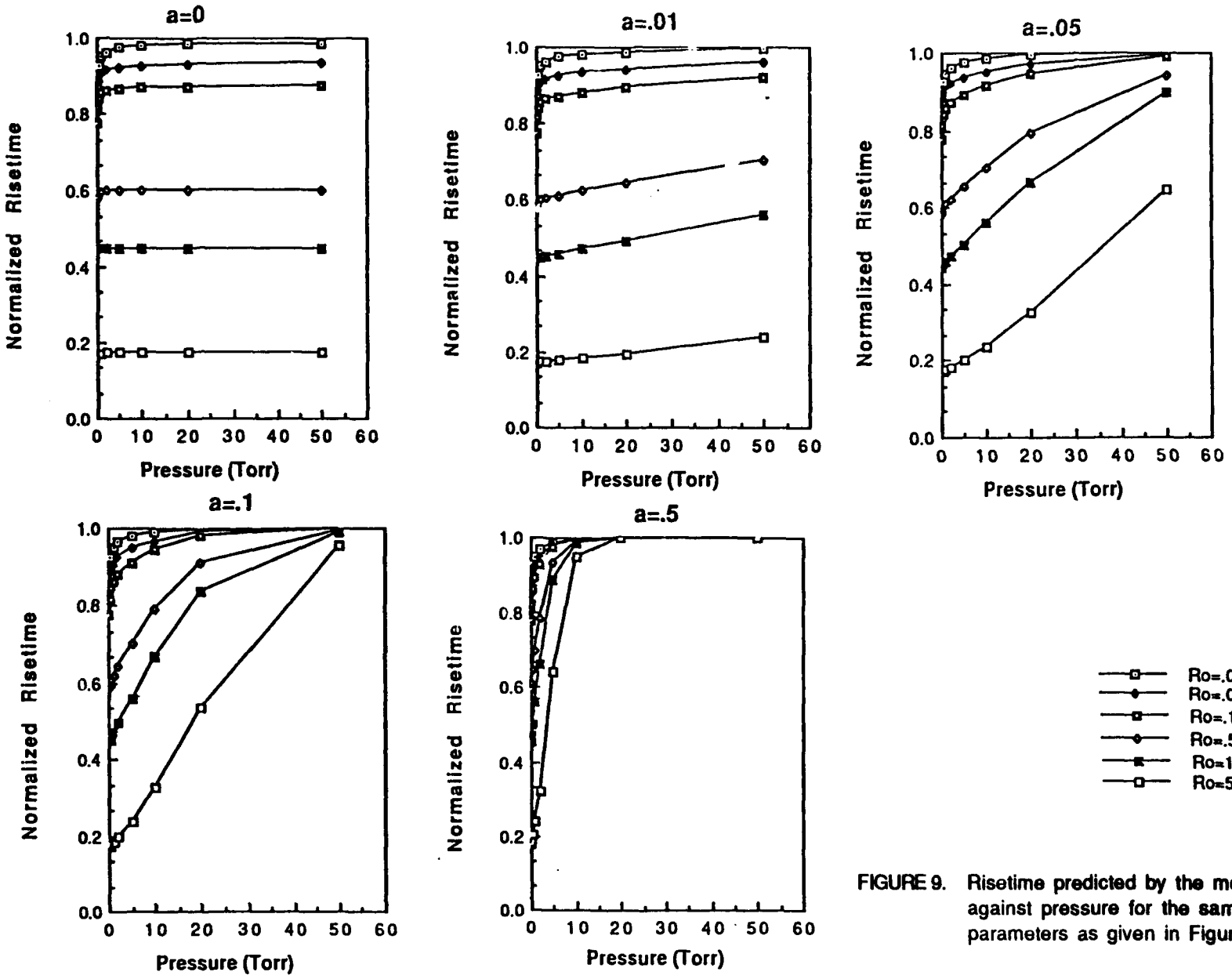

FIGURE 9. Risetime predicted by the model plotted against pressure for the same parameters as given in Figure 3.

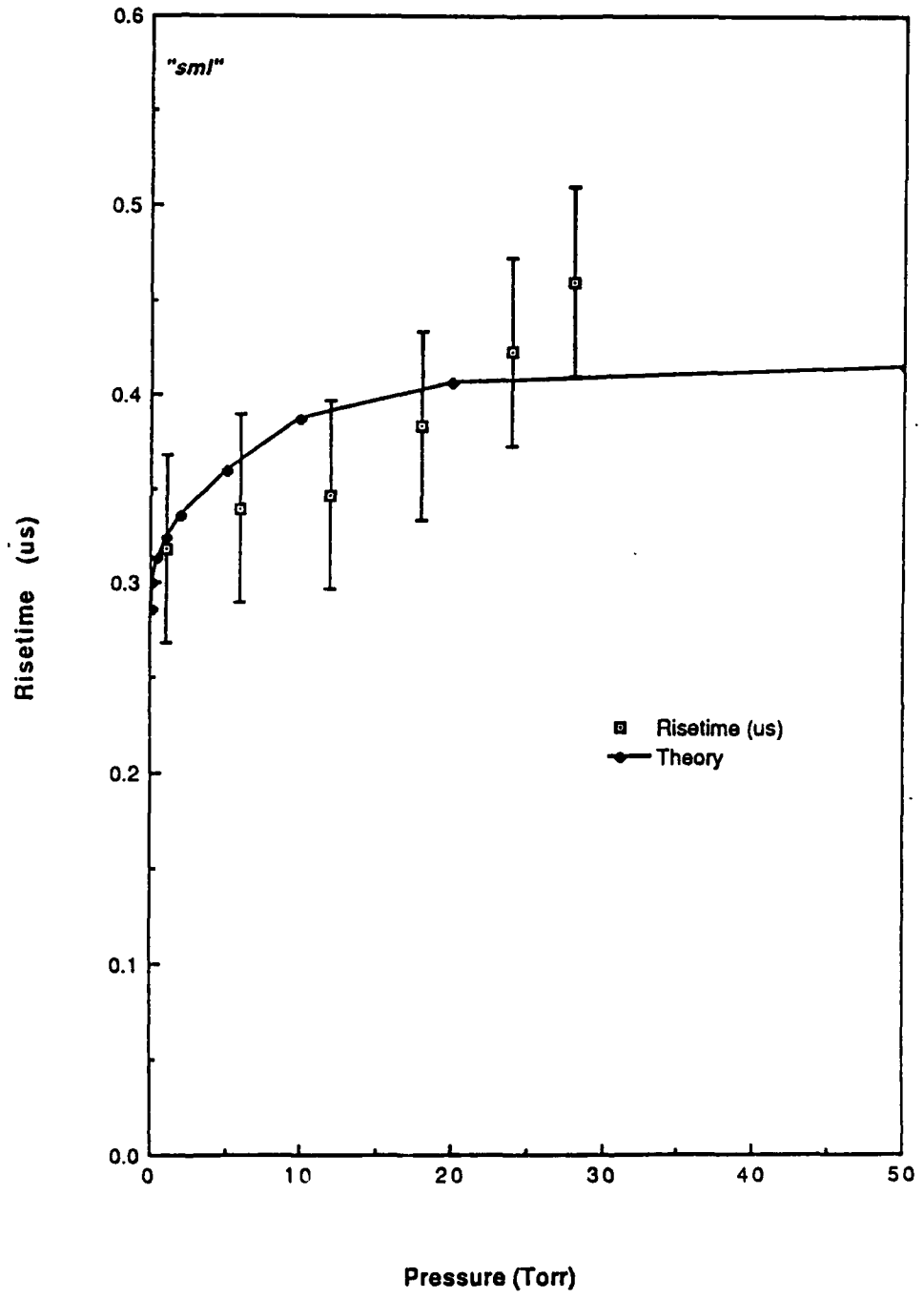

FIGURE 10. Risetime of the HCP spectral irradiance (squares) plotted as a function of fill gas pressure. The data are from Reference 24. The model results (solid line) are for risetime of the device current as predicted by the model. The system parameters are given in Table II and the fitting parameters in Table III.

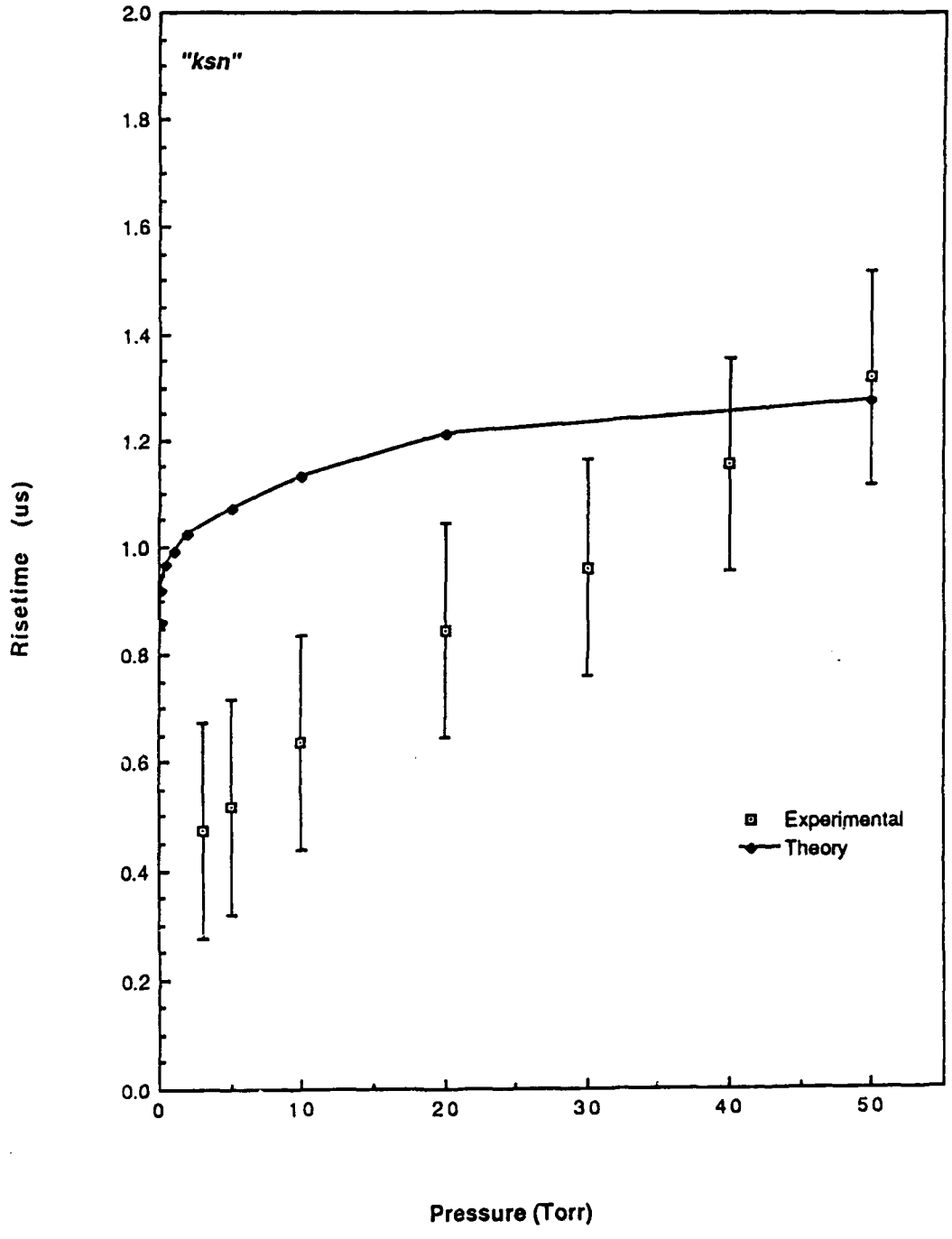

FIGURE 11. Same data as in Figure 10 but for the system described in Reference 25.

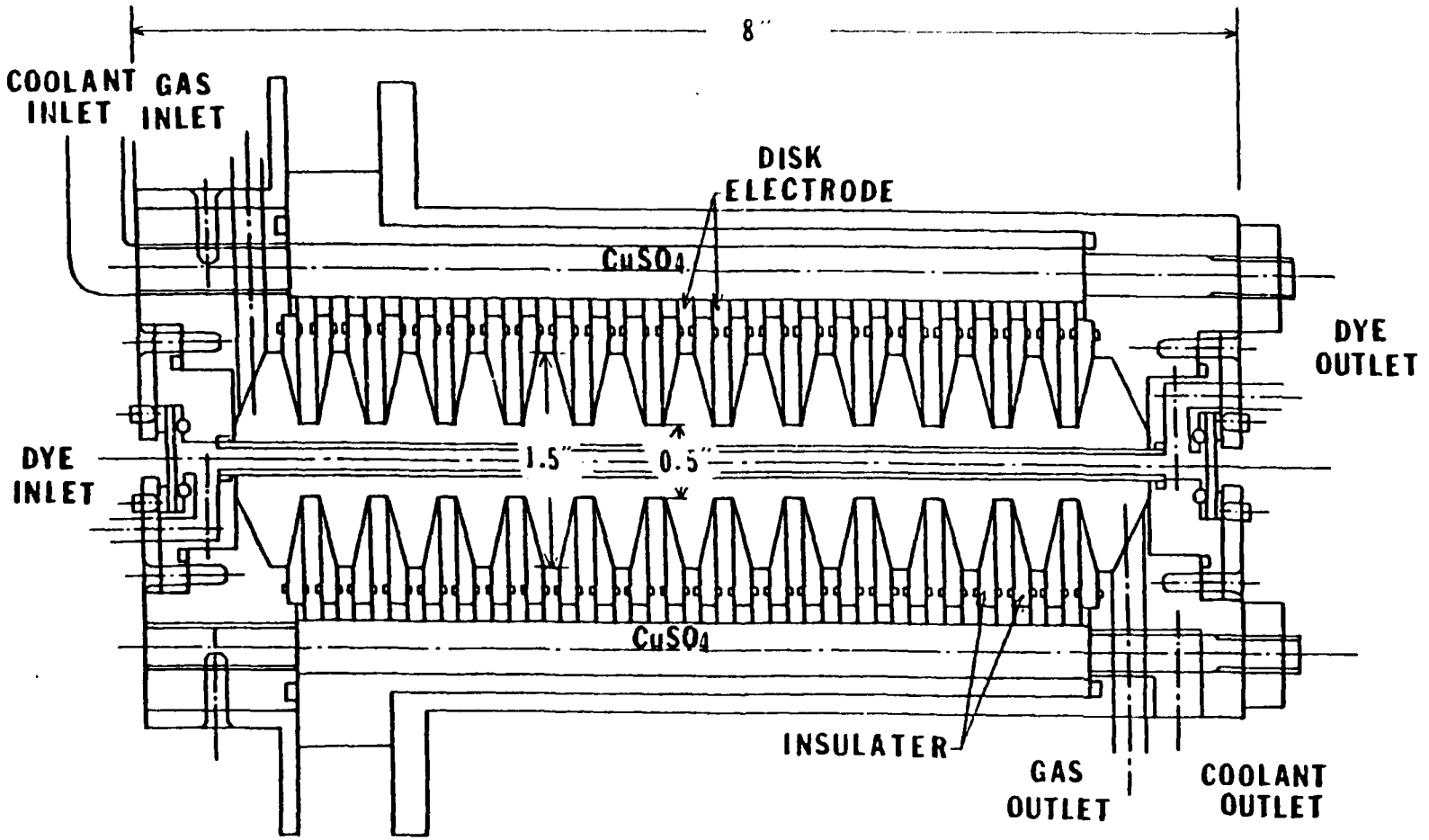

FIGURE 12. A detailed drawing of HCP device.

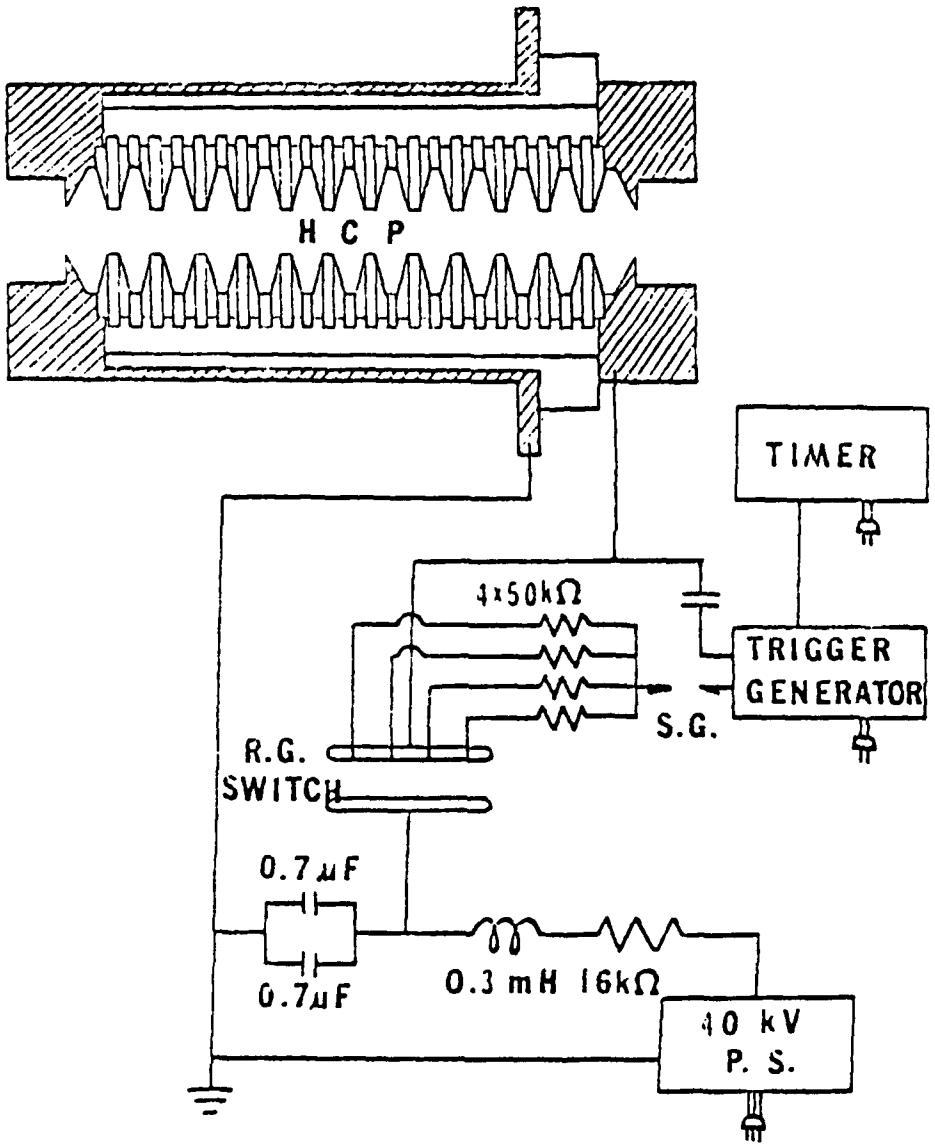

FIGURE 13. An electric circuit diagram for the HCP system.

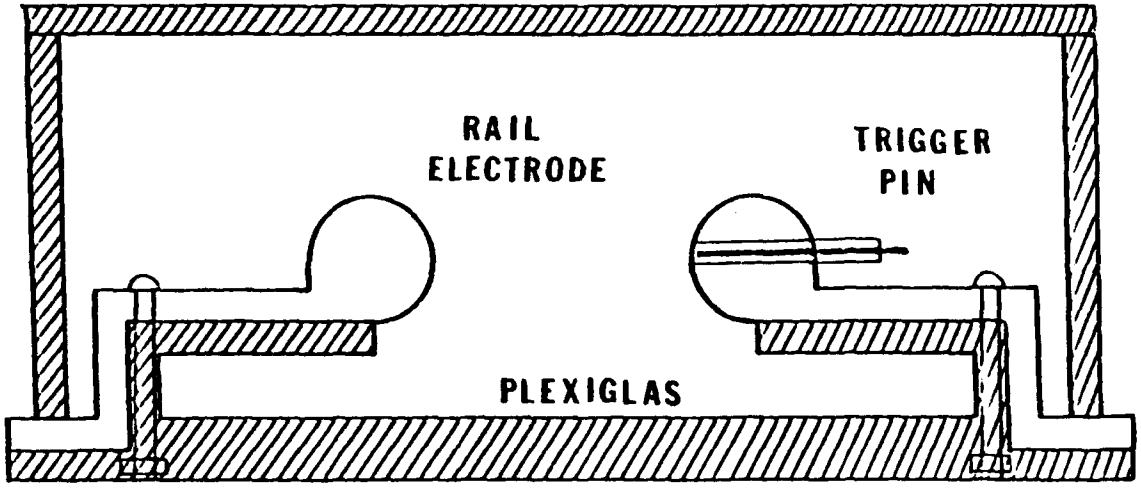

FIGURE 14. A cross section of the rail gap switch.

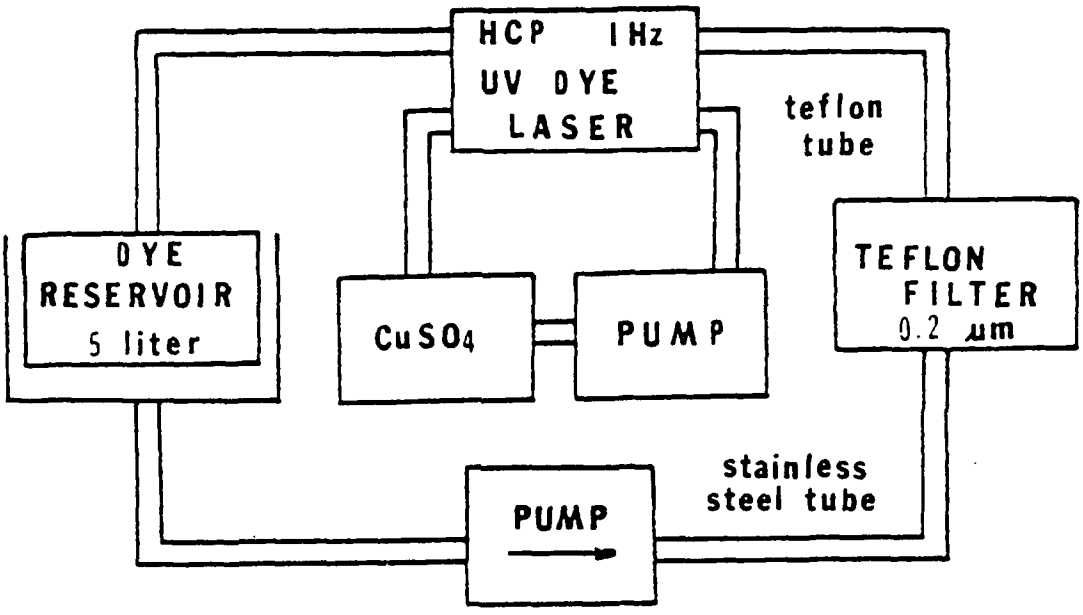

FIGURE 15. The schematic diagram for dye and $CUSO_4$ circulation.

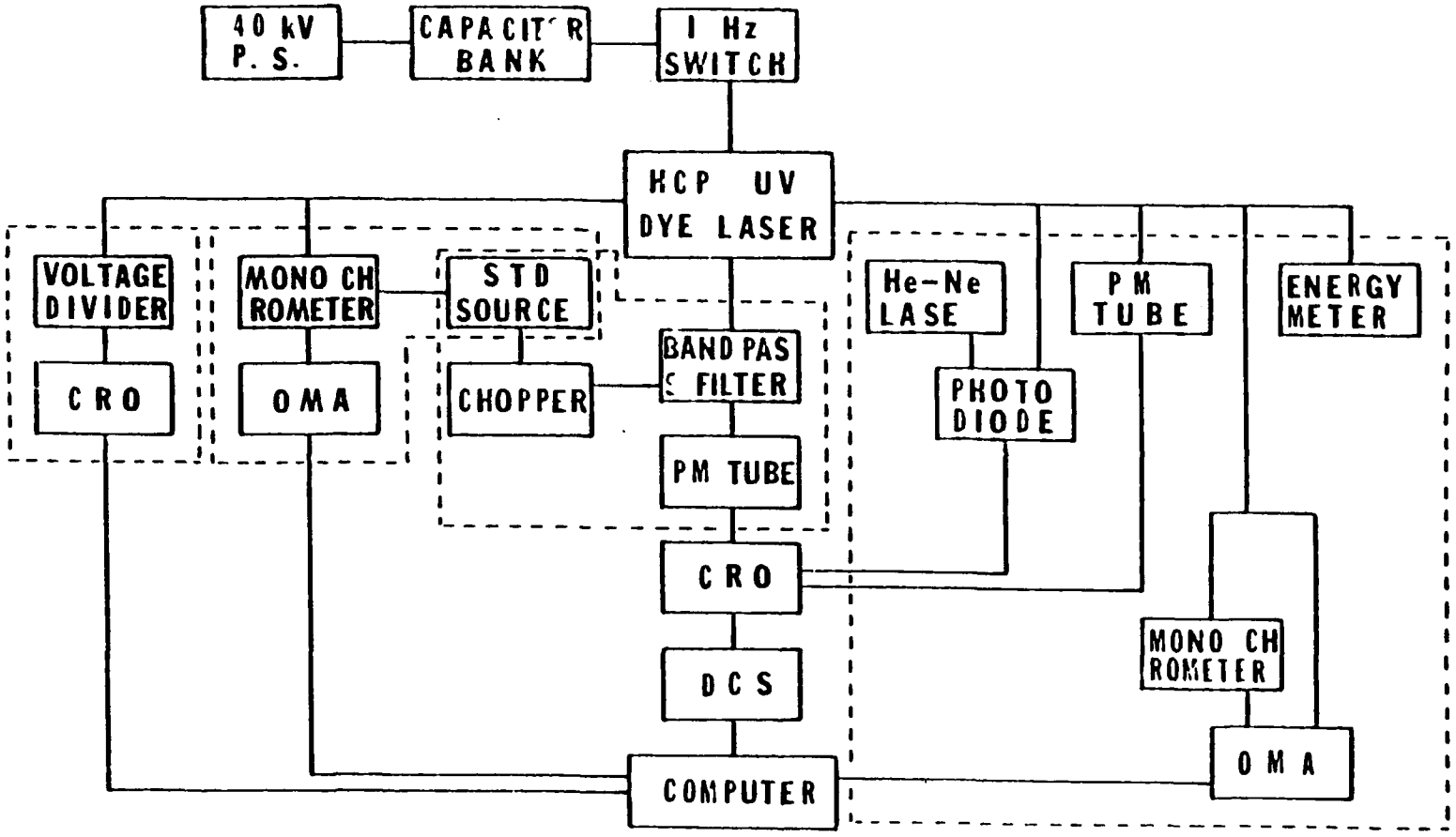

FIGURE 16. A block diagram for measurement systems.

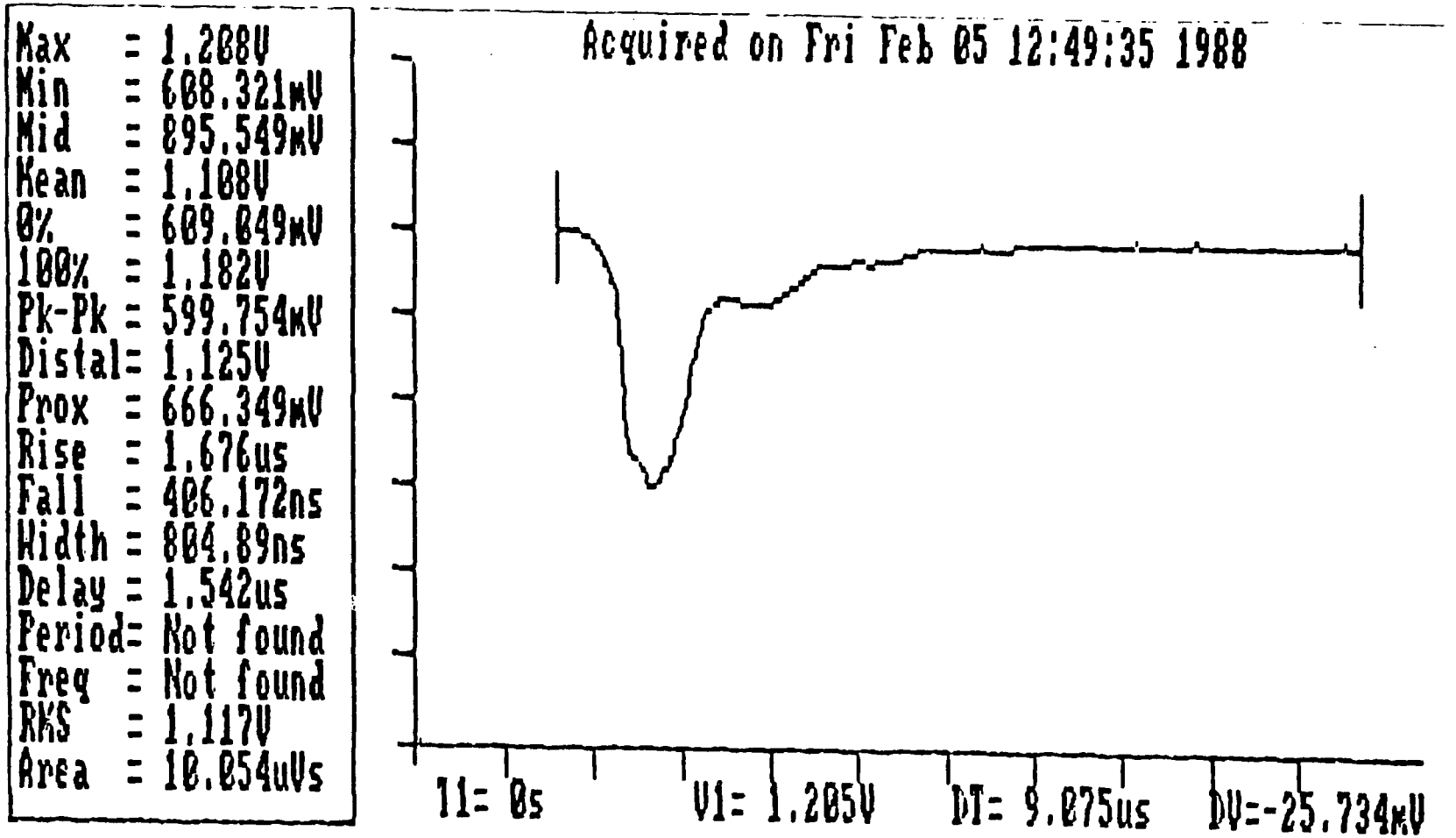

FIGURE 17. Temporal behavior of the pumping light.

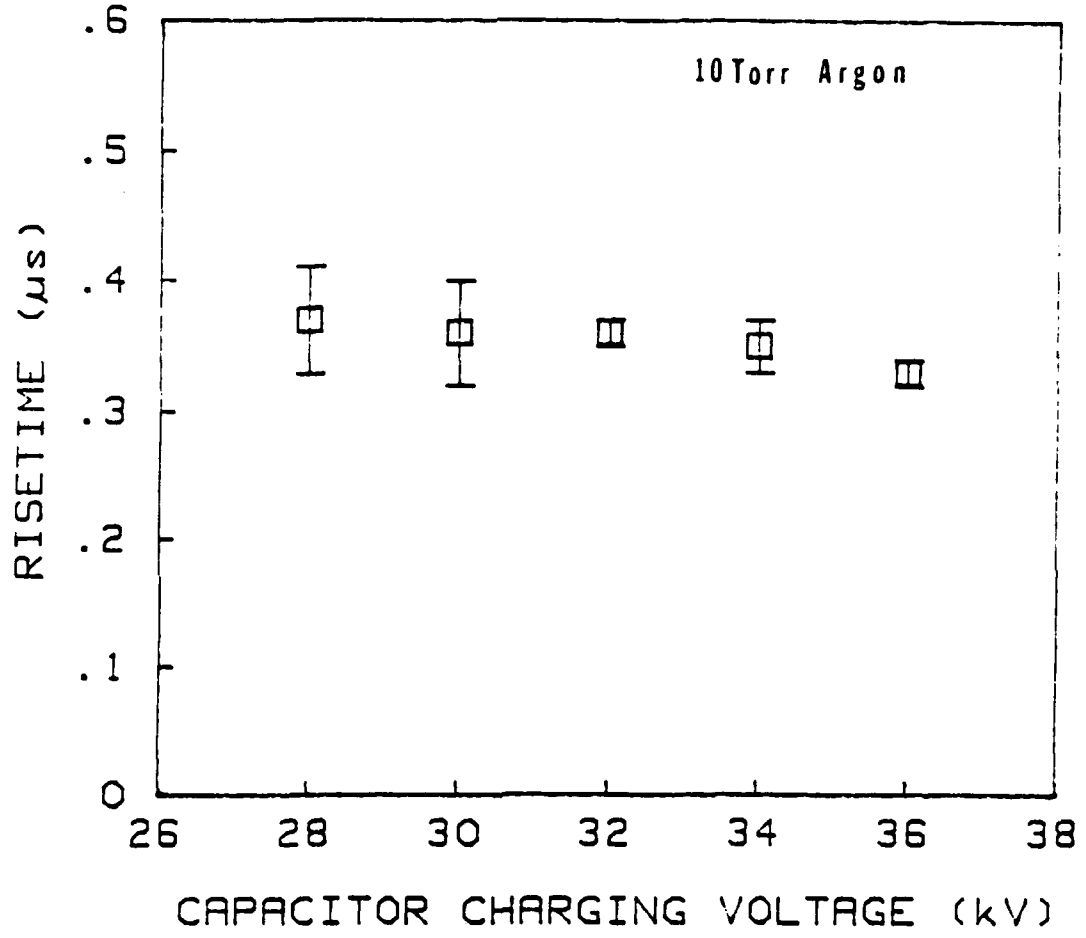

FIGURE 18. Risetime of the pumping light vs charging voltage.

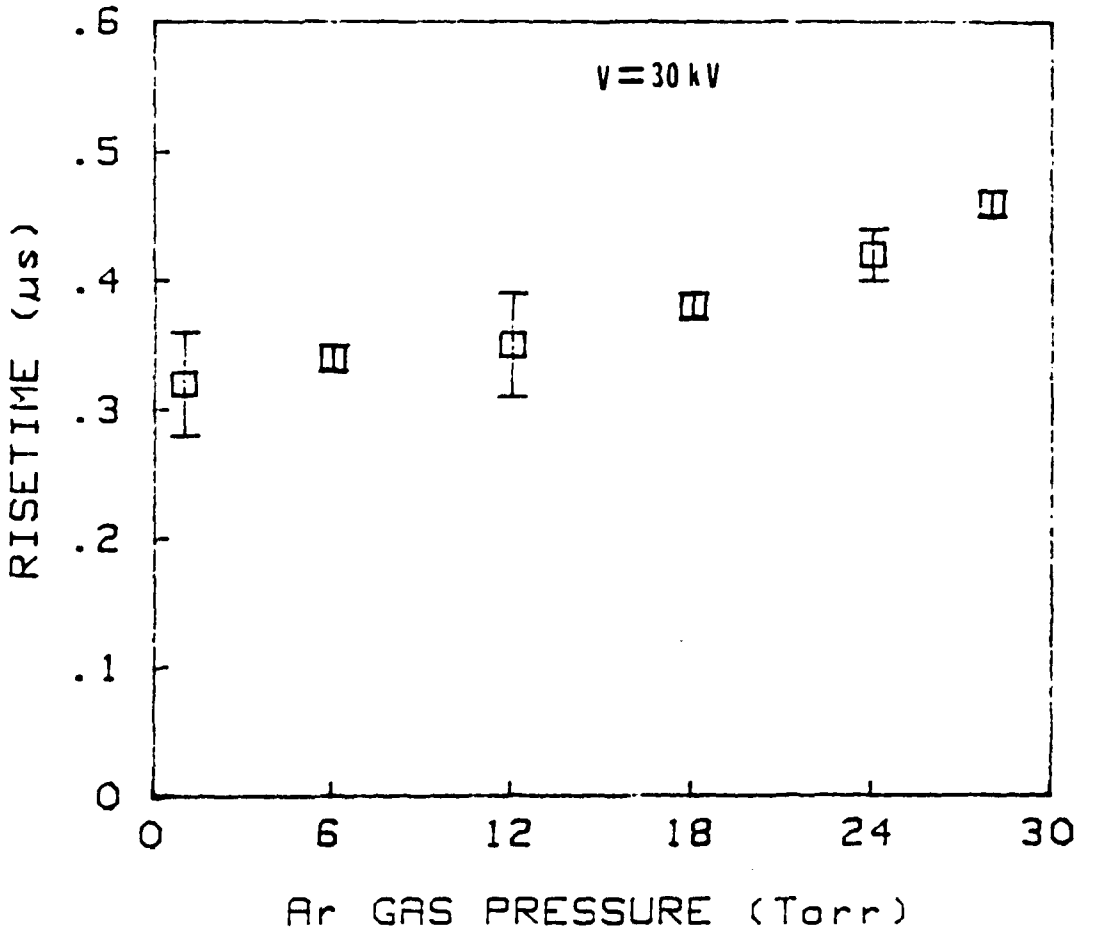

FIGURE 19. Risetime of the pumping light vs filling gas pressure.

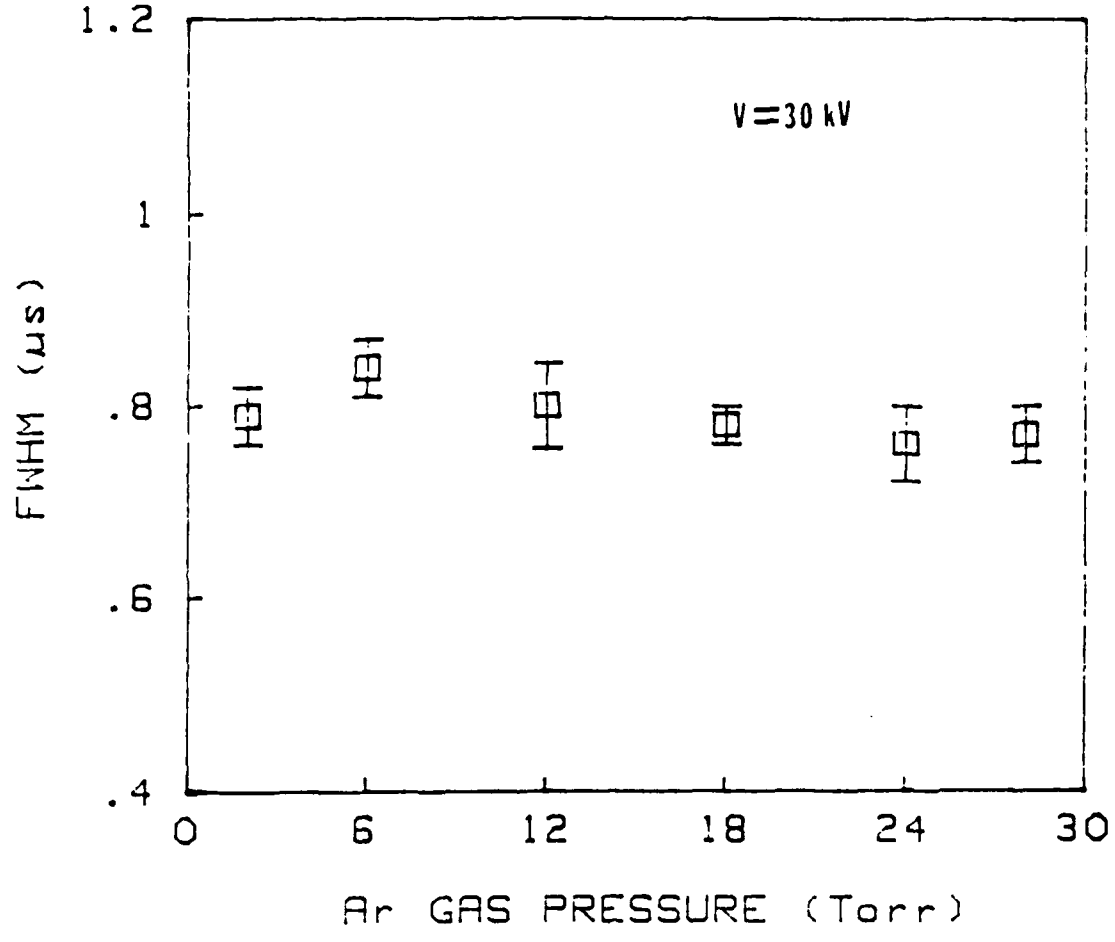

FIGURE 20. FWHM of the pumping light pulse vs filling gas pressure.

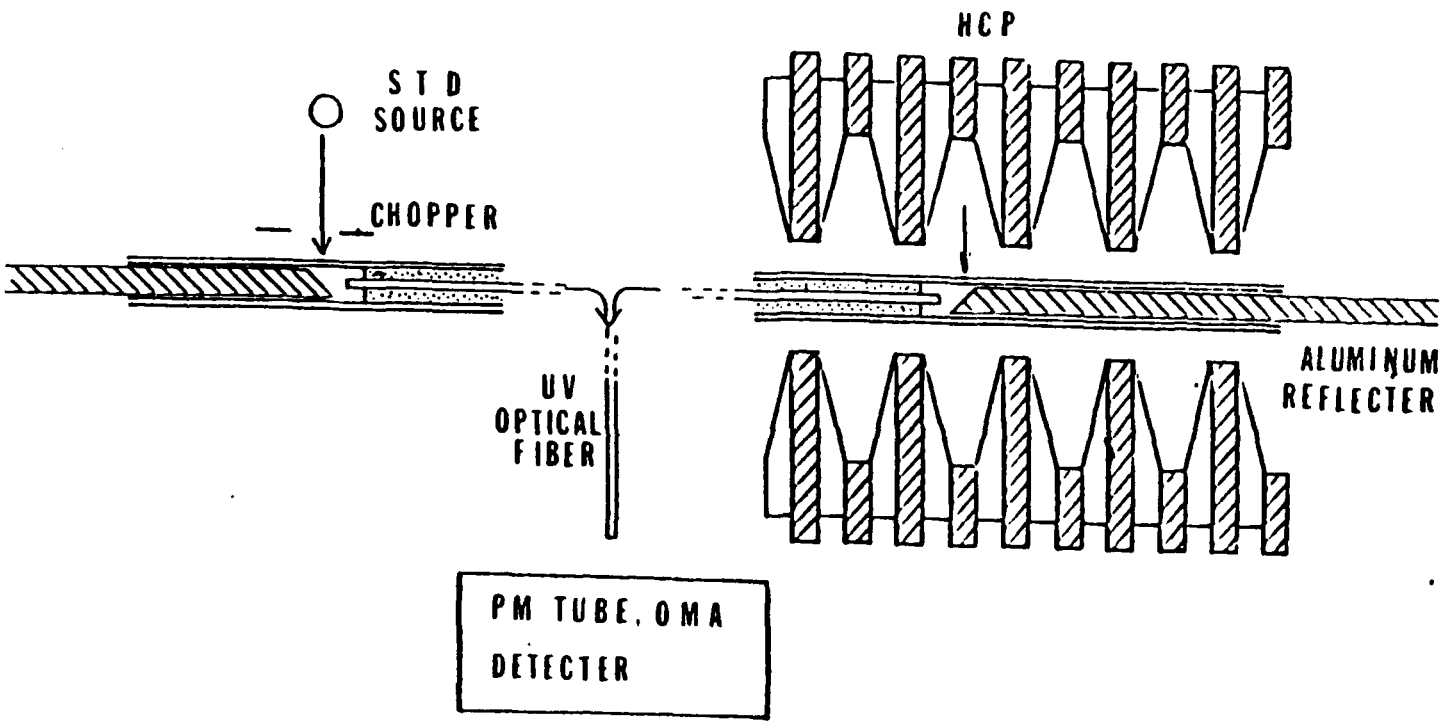

FIGURE 21. The arrangement for the absolute irradiance measurement system.

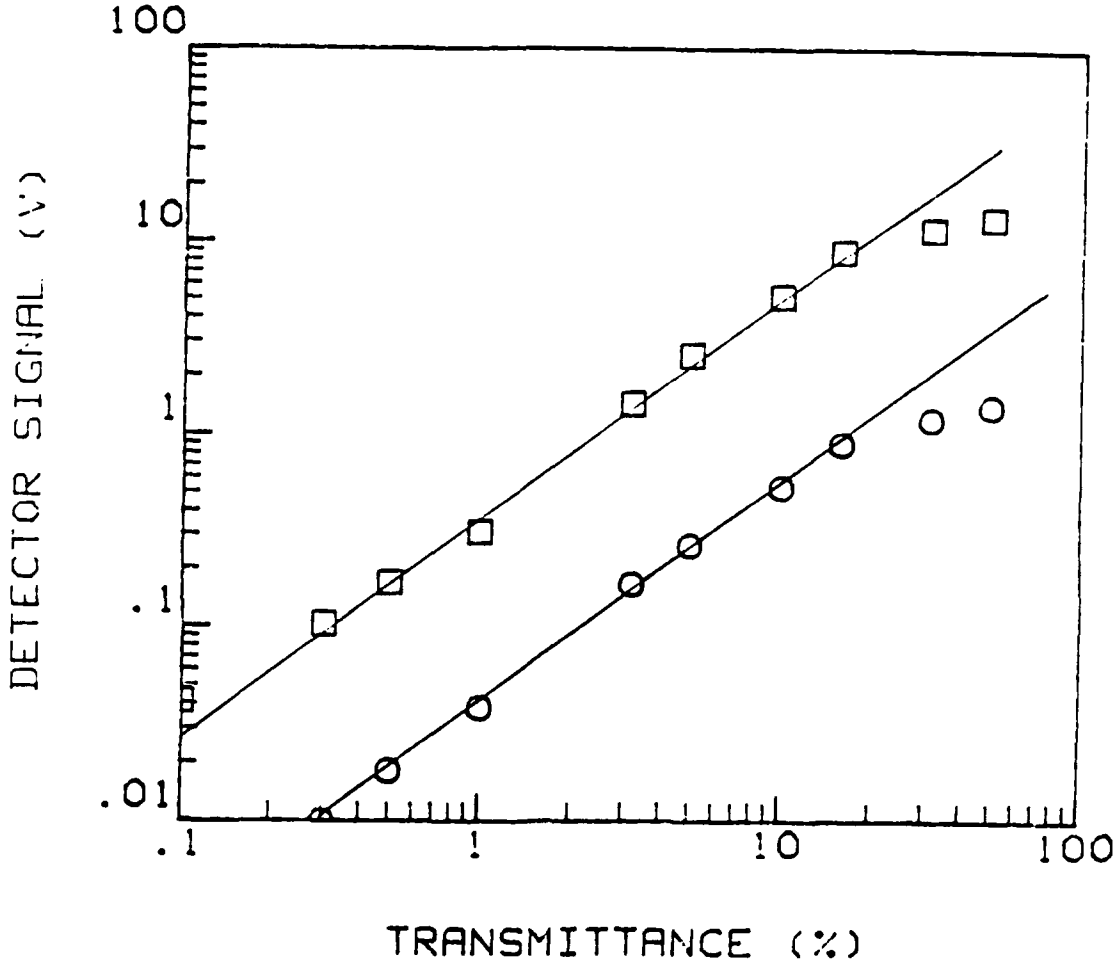

FIGURE 22. Results of PM tube linearity tests.

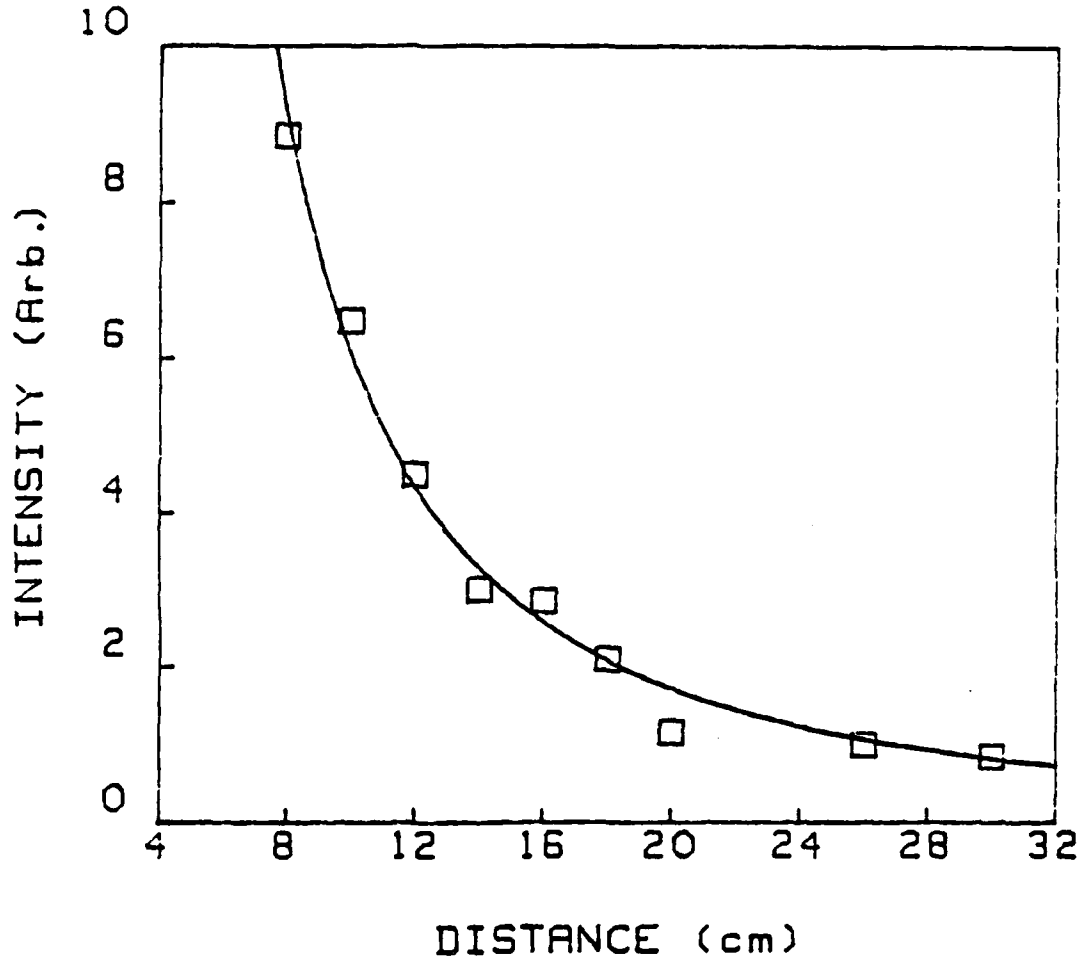

FIGURE 23. Test of secondary standard source intensity as a function of distance.

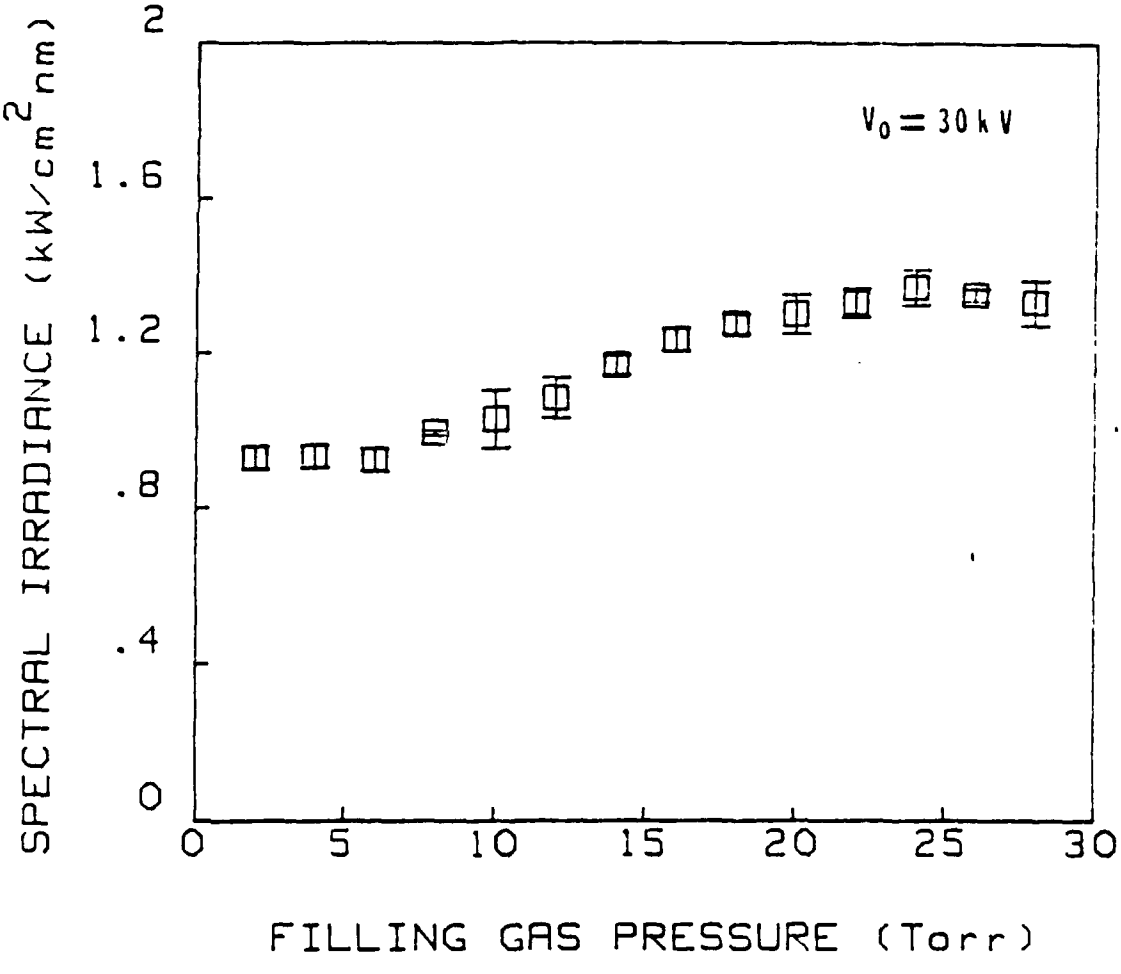

FIGURE 24. Spectral irradiance of the pumping light at λ=310 nm vs filling gas pressure.

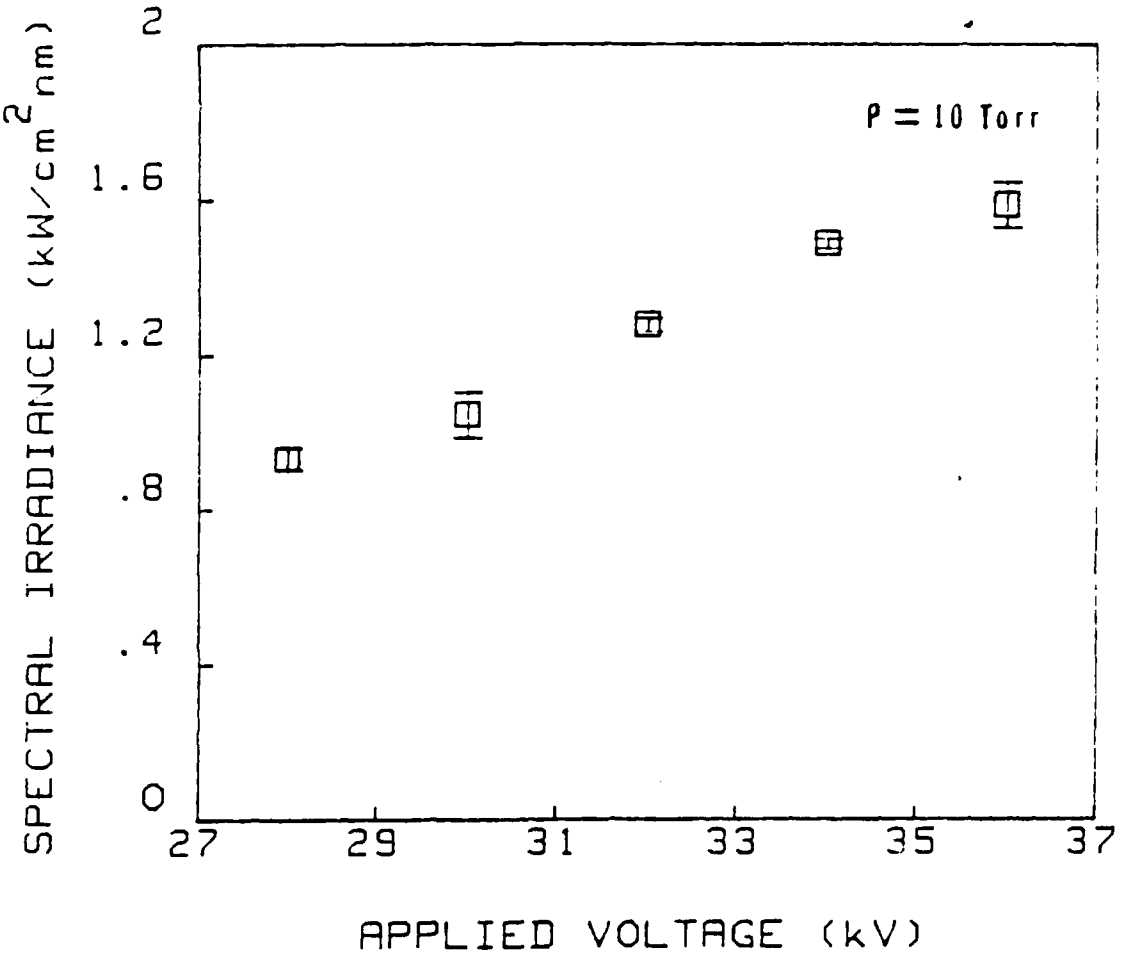

FIGURE 25. Spectral irradiance of the pumping light at λ=310 nm vs applied voltage.

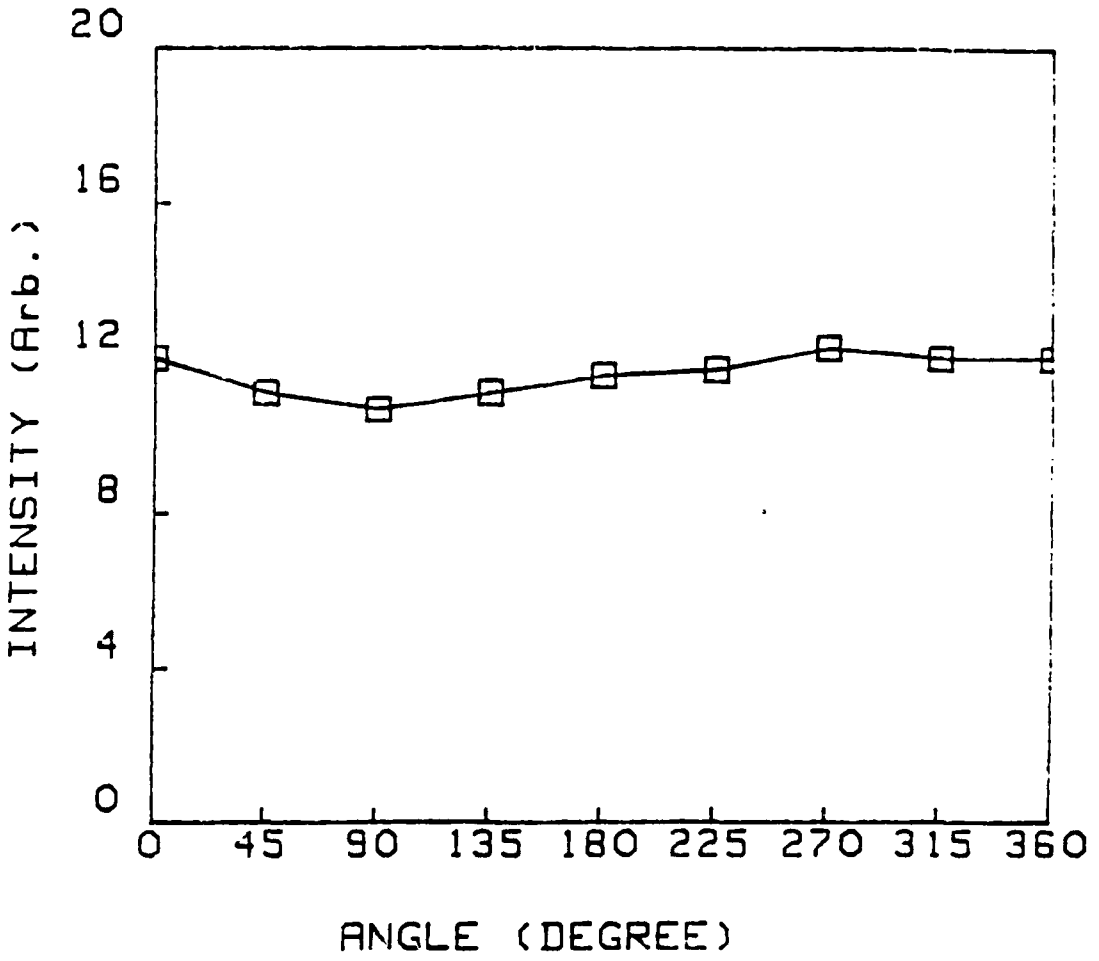

FIGURE 26. Angular distribution of HCP emission.

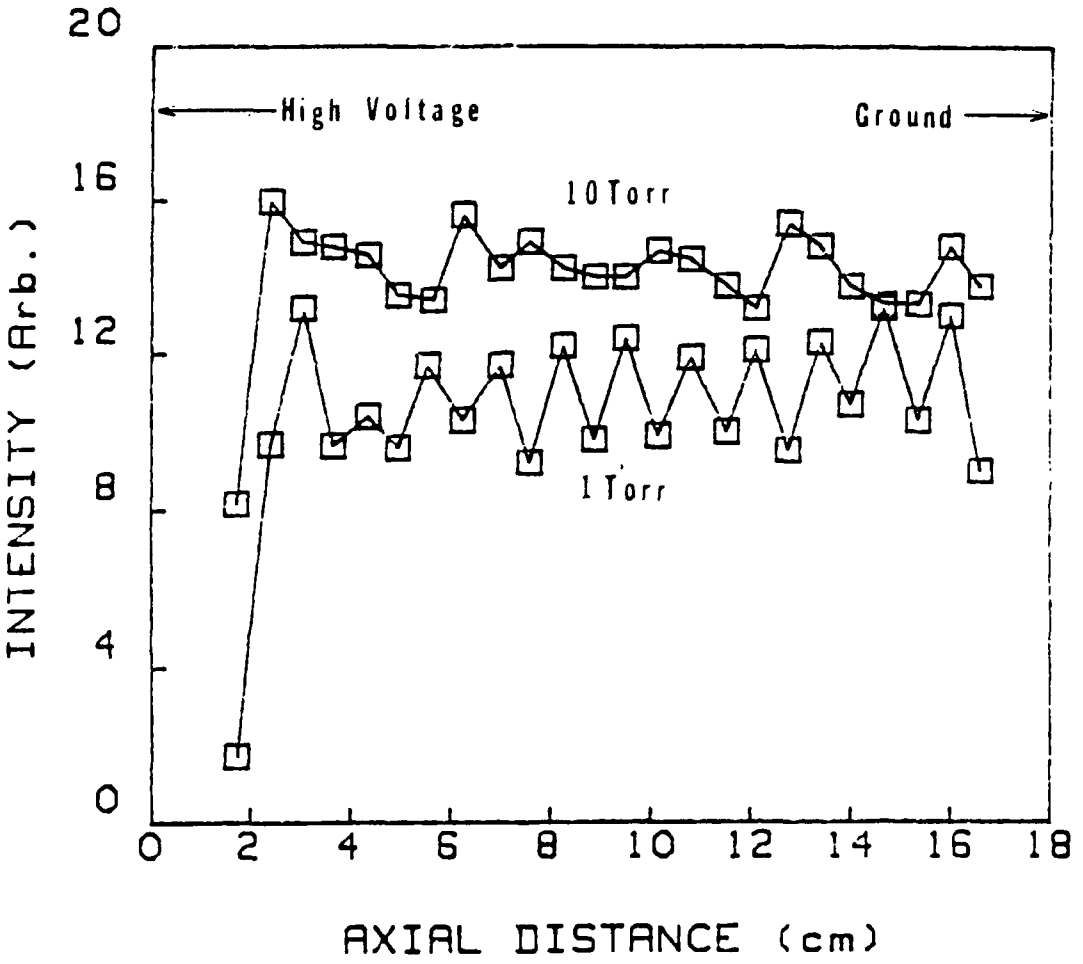

FIGURE 27. Axial distribution of HCP emission.

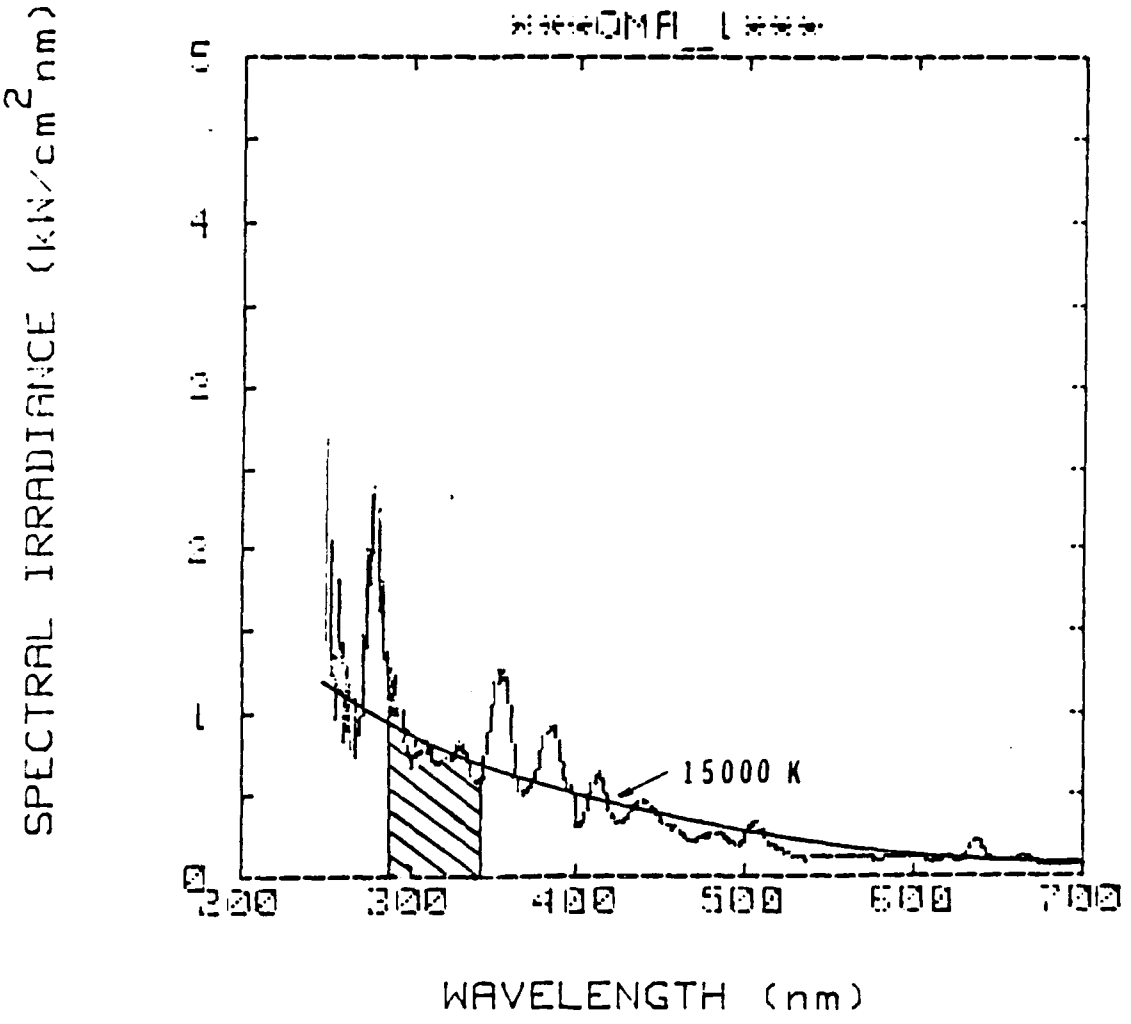

FIGURE 28. Spectral irradiance of HCP emission at 30 kV, 10 Torr with 1.4 µF capacitance.

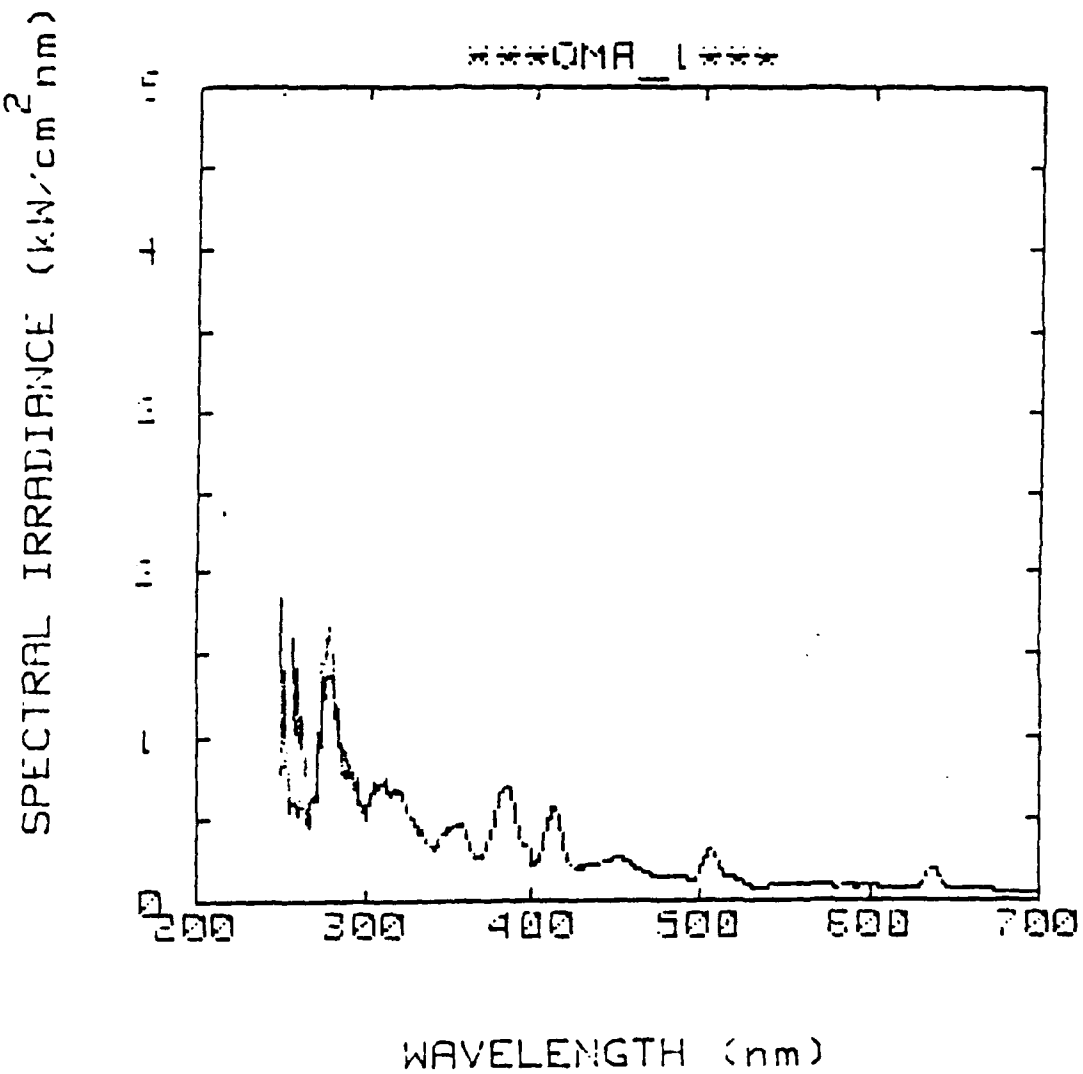

FIGURE 29. Spectral irradiance of HCP emission at 30 kV, 1 Torr with 1.4 µF capacitance.

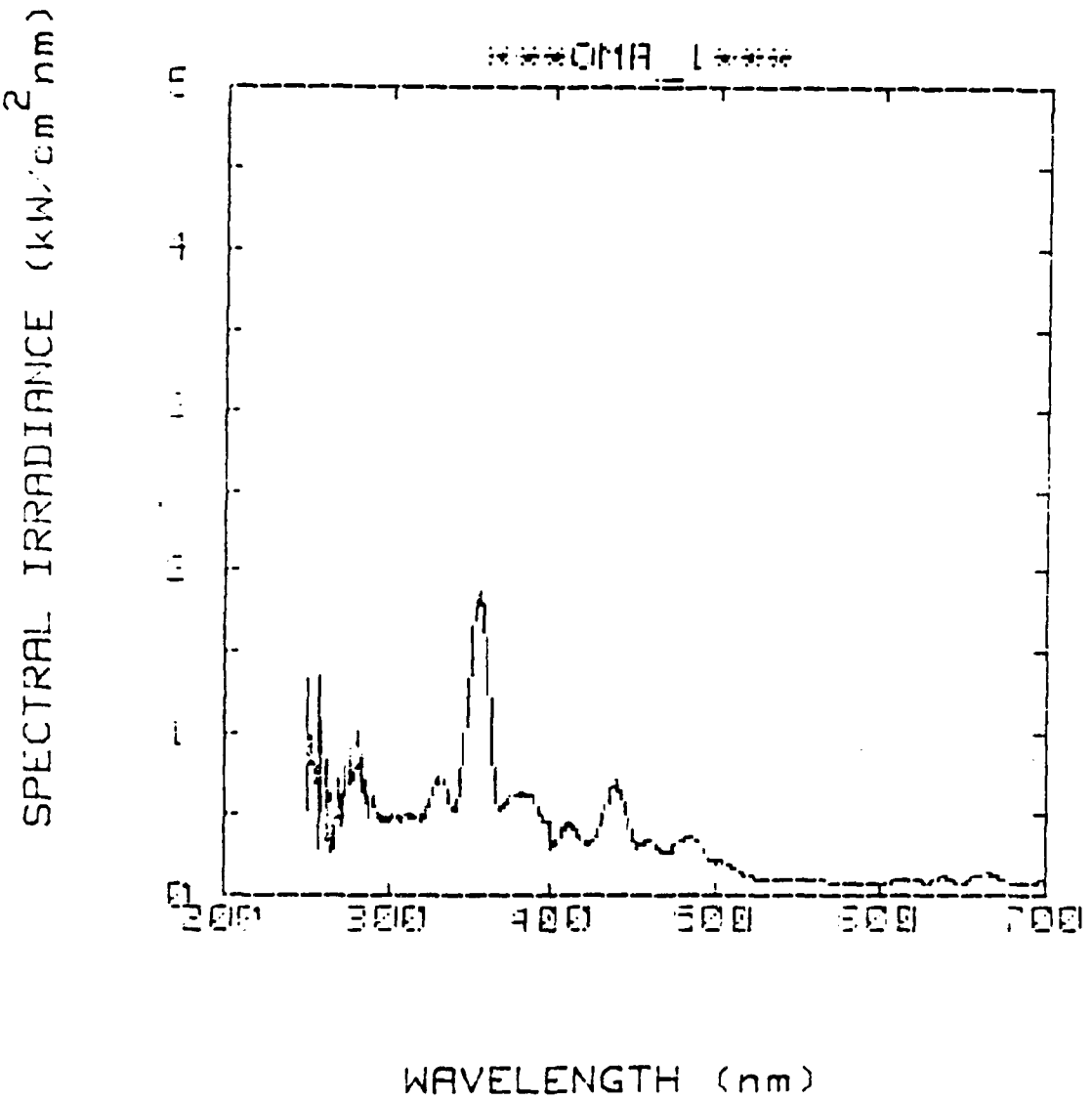

FIGURE 30. Spectral irradiance of HCP emission at 30 kV, 10 Torr with 0.7 μF capacitance.

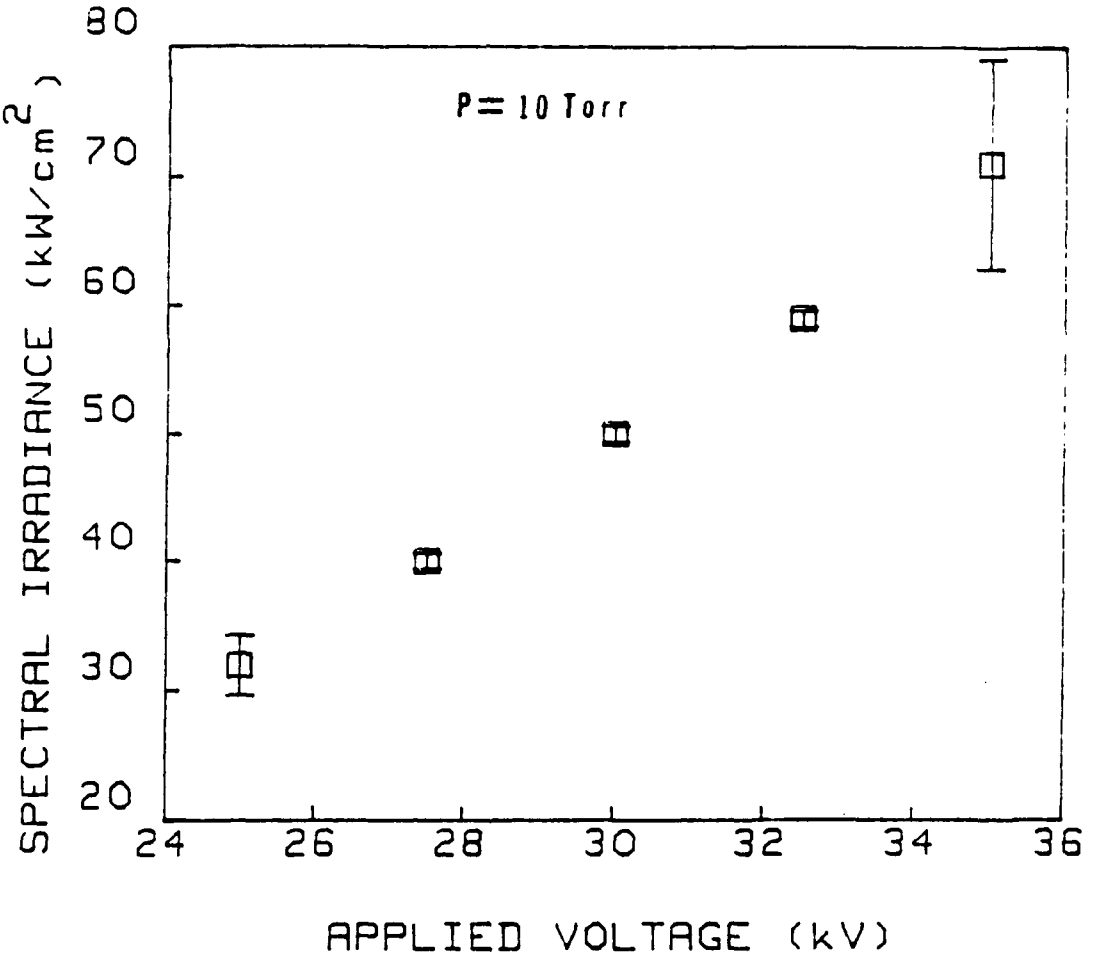

FIGURE 31. The time integrated spectral irradiance of HCP emission vs applied voltage in the region from 285 to 325 nm.

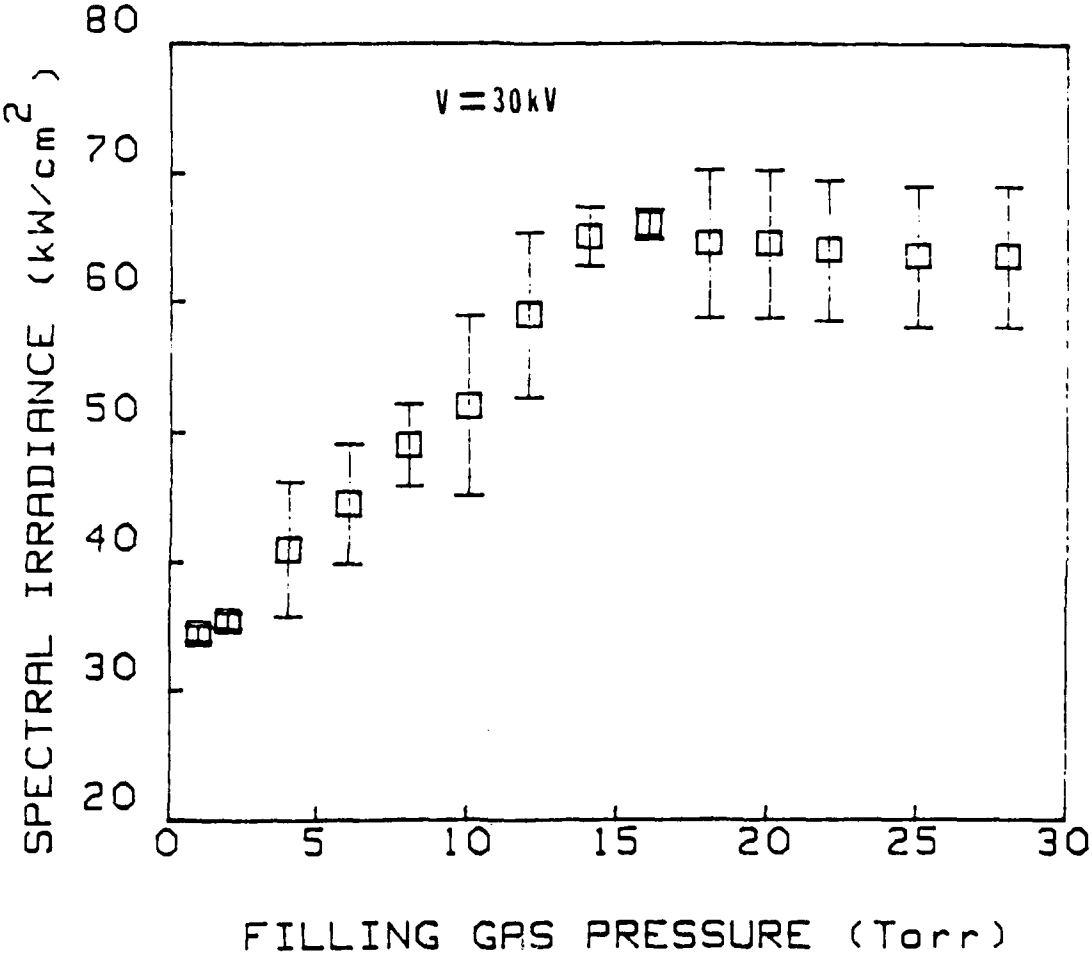

FIGURE 32. The time integrated spectral irradiance of HCP emission vs filling gas pressure.

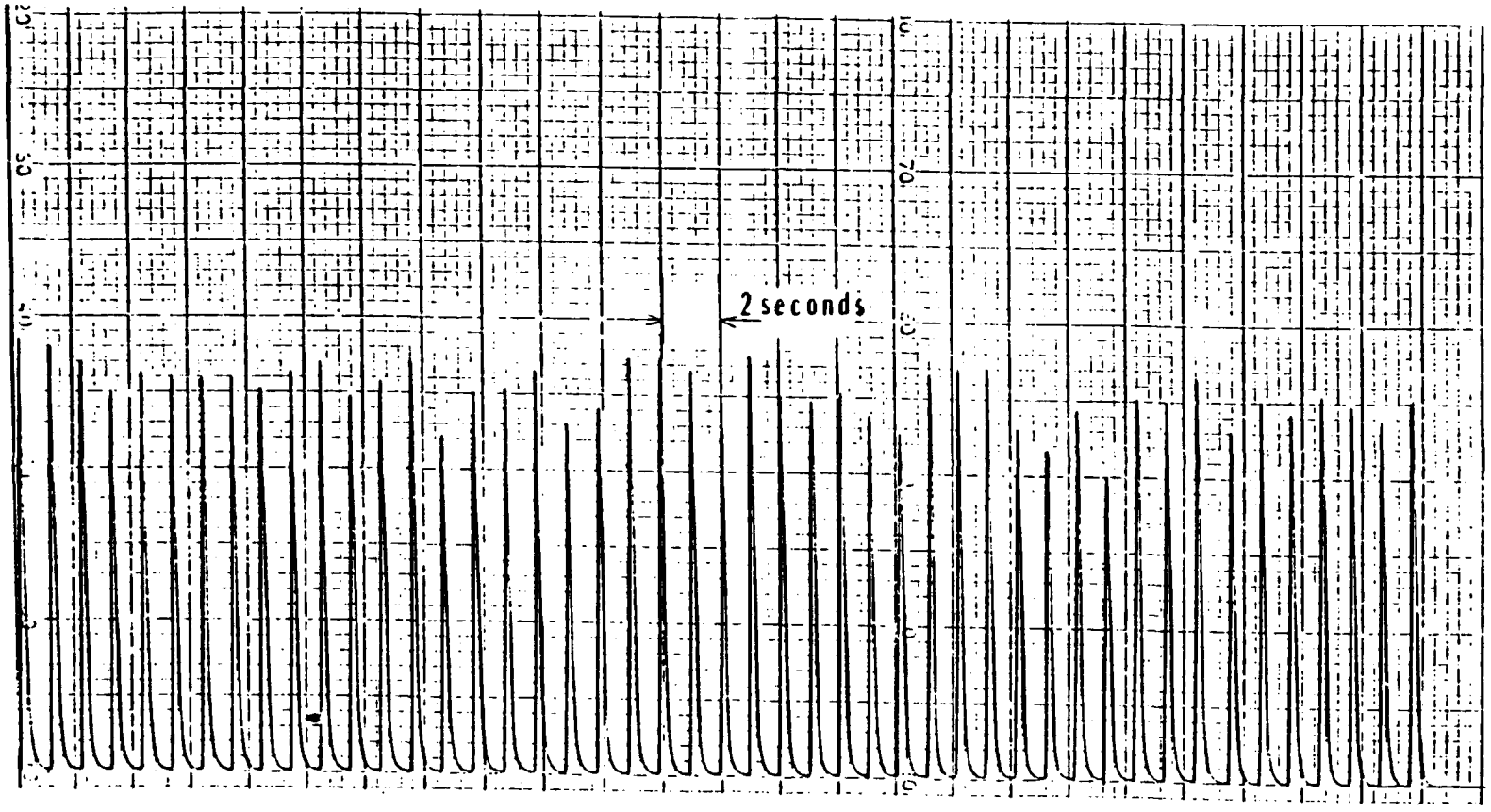

FIGURE 33. A strip chart recording of repetitive pumping light pulse.

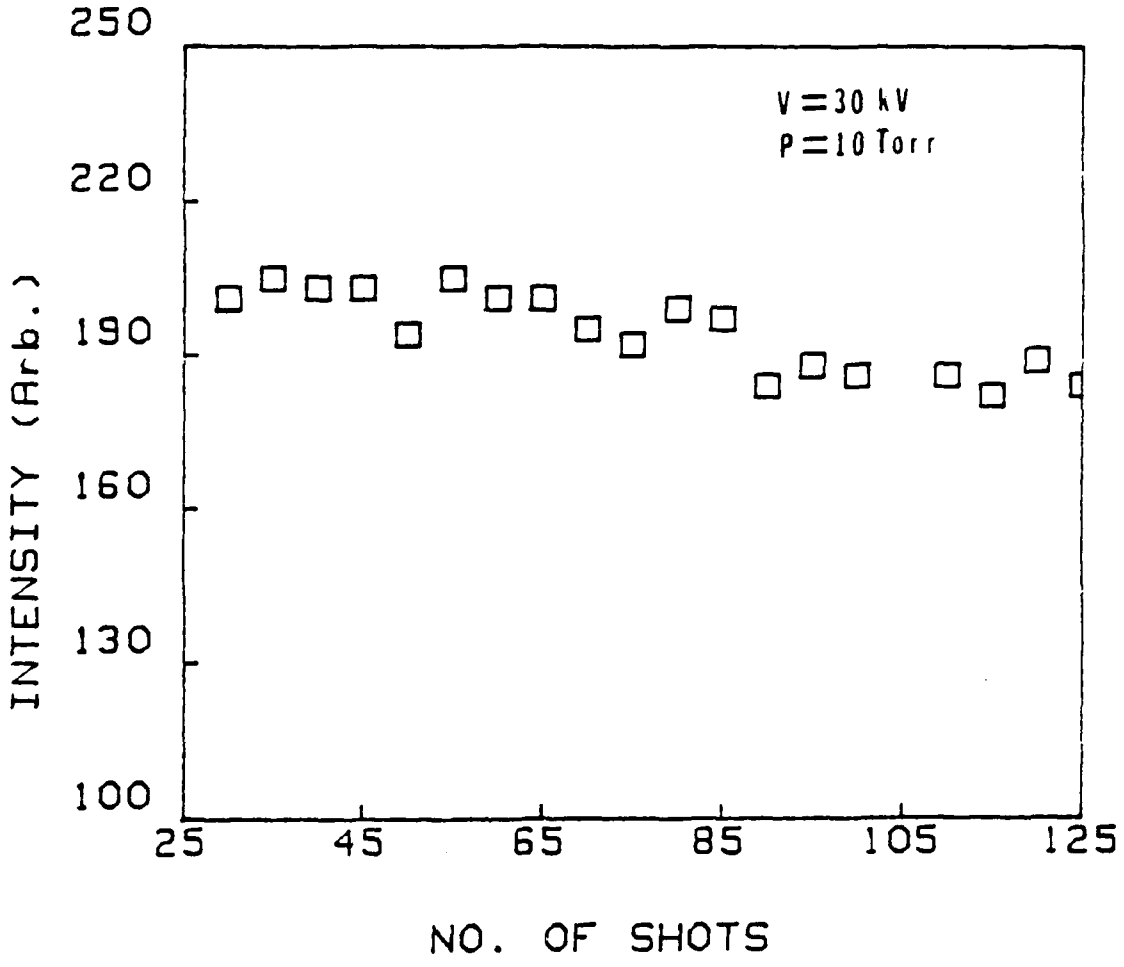

FIGURE 34. HCP emission intensity as a function of firing number of the device at 1 Hz operation.

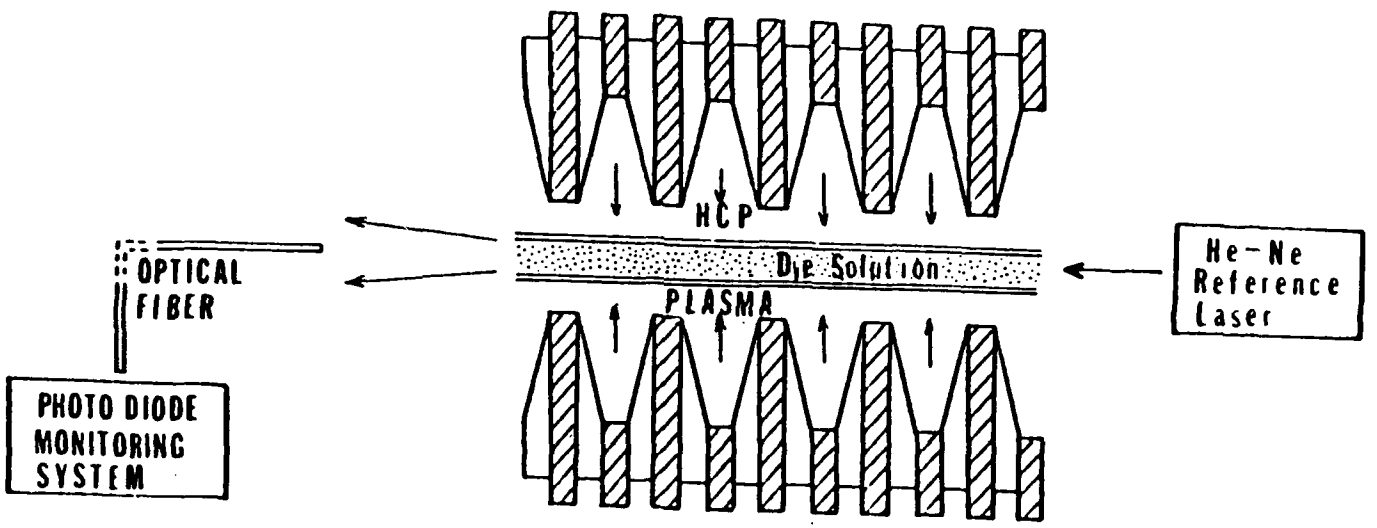

FIGURE 35. The schematic diagram of the arrangement for measurement of thermal effects.

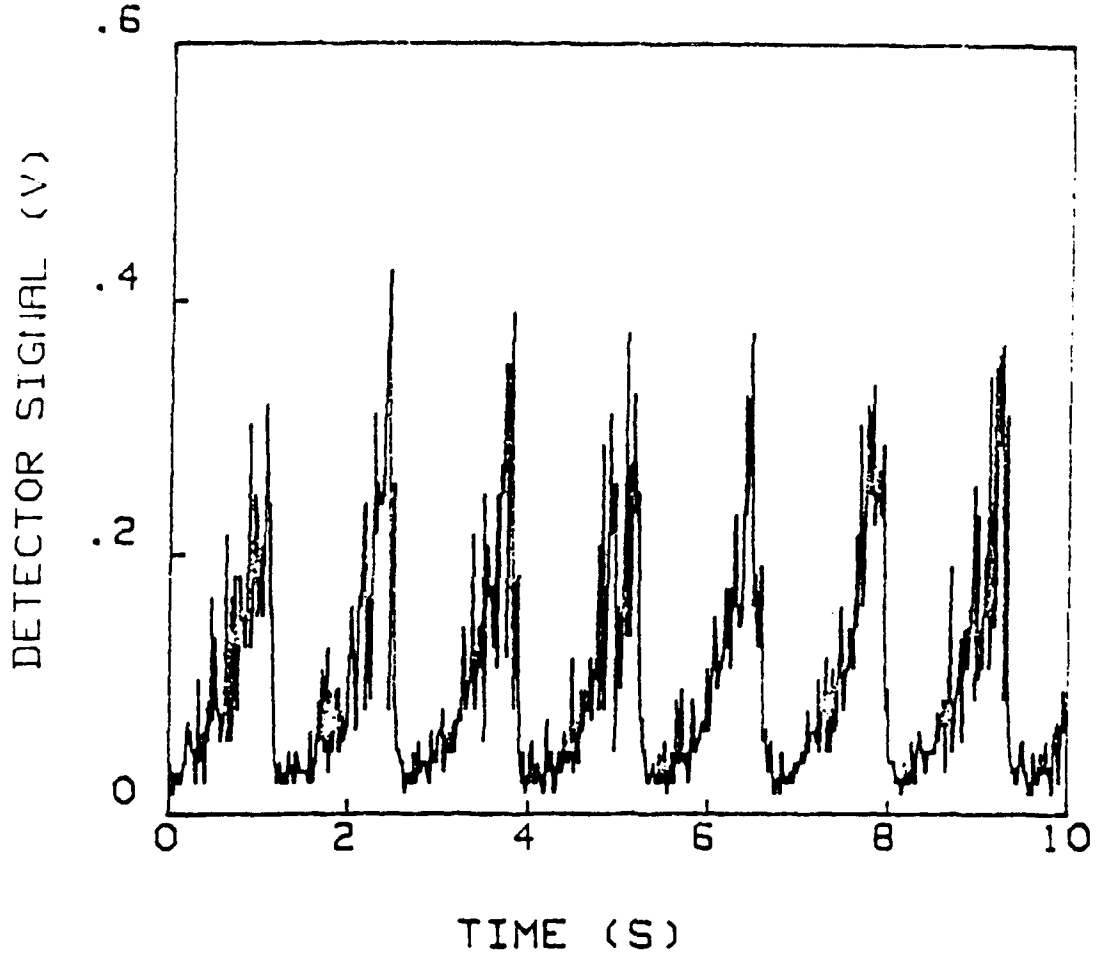

FIGURE 36. Temporal behavior of He-Ne laser beam monitored after passing through dye solution.

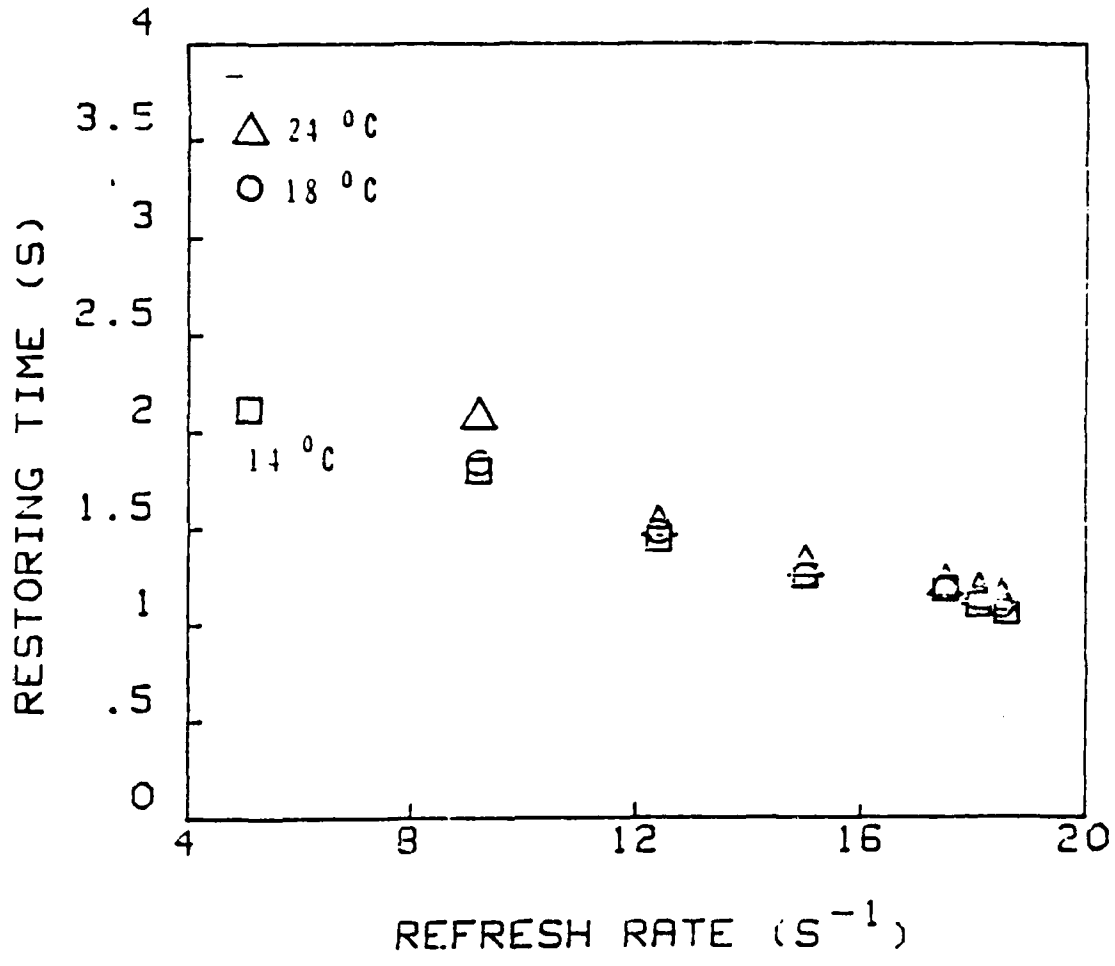

FIGURE 37. The restoring time as a function of refresh rate for different dye temperatures.

FIGURE 38. He-Ne laser intensity variation for numbers of firing at 1 Hz operation.

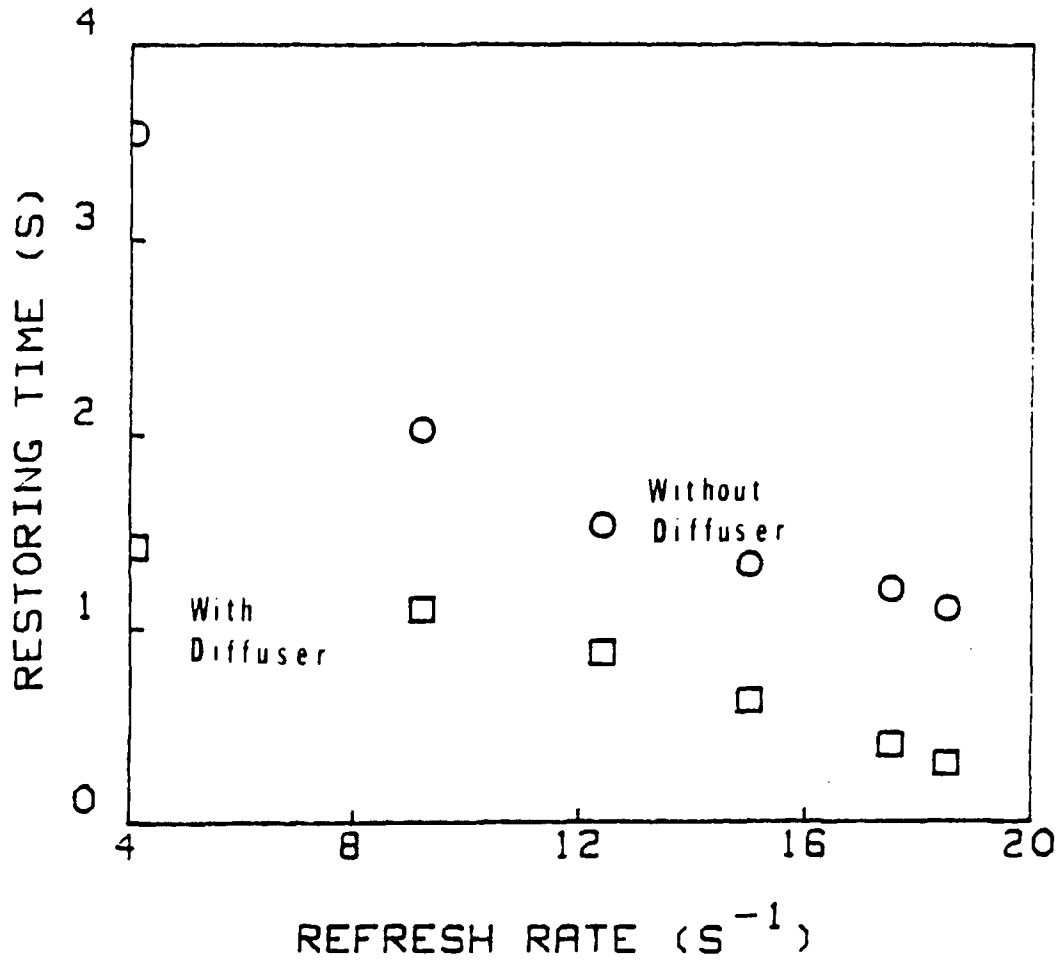

FIGURE 39. He-Ne laser intensity variation as a function of refresh rate with and without diffuser.

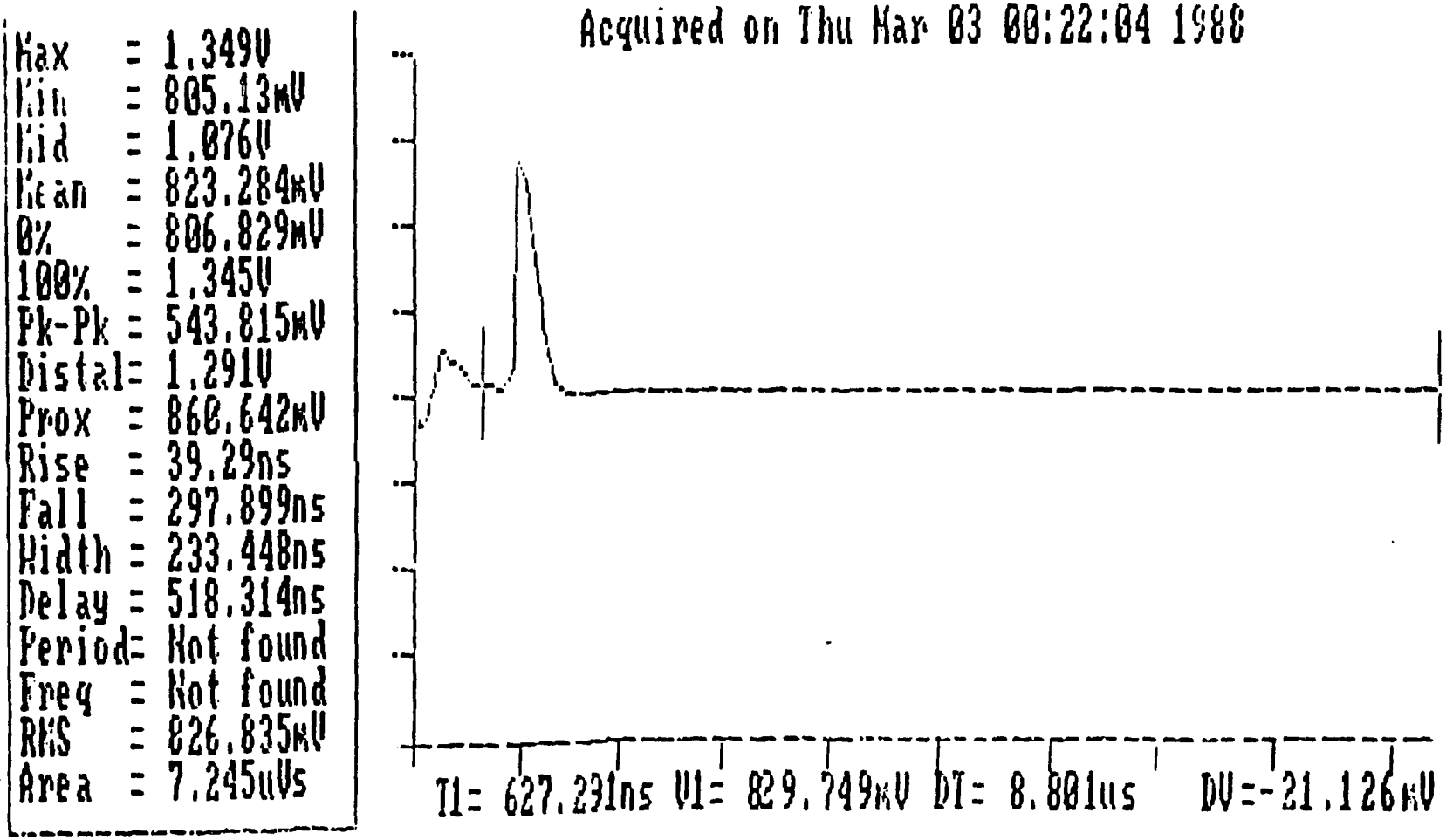

FIGURE 40. The temporal behavior of BBQ dye laser.

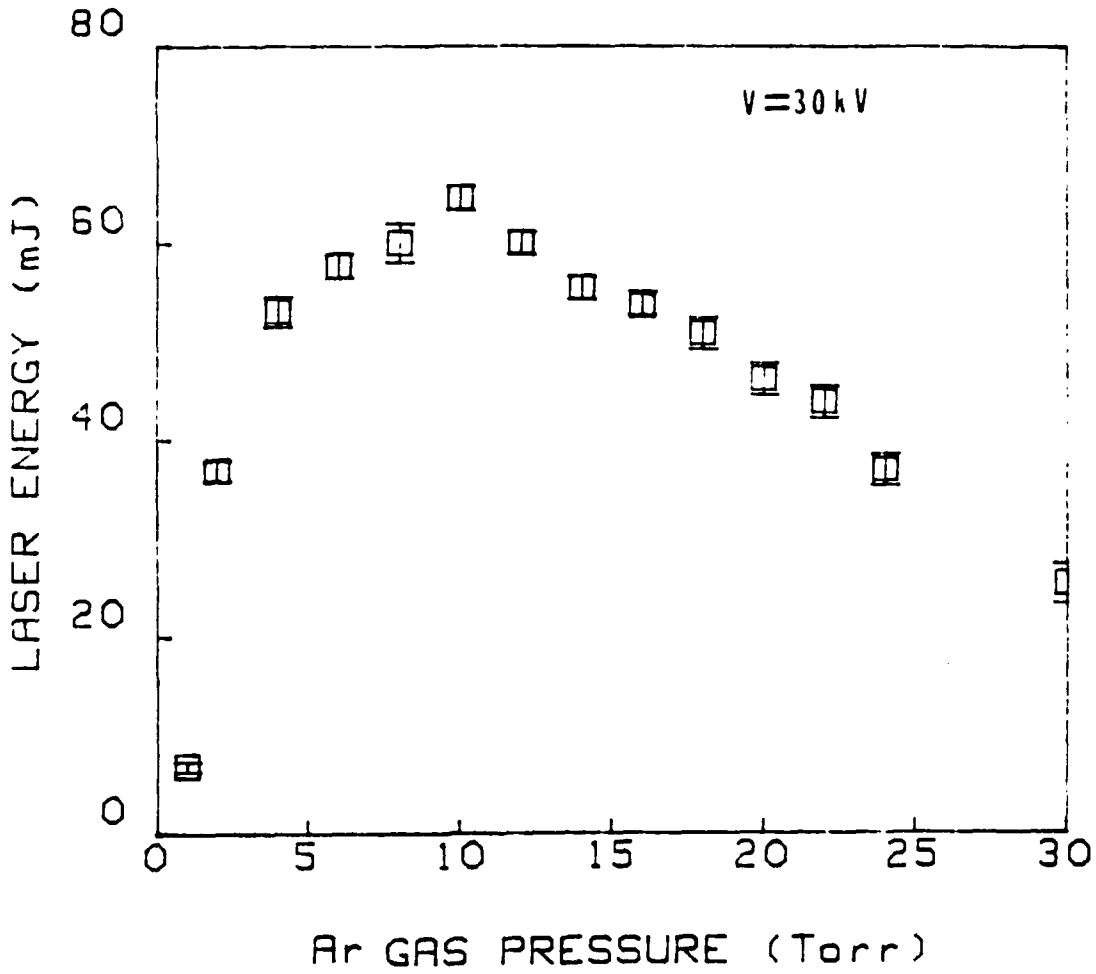

FIGURE 41. The laser output energy dependence on filling gas pressure.

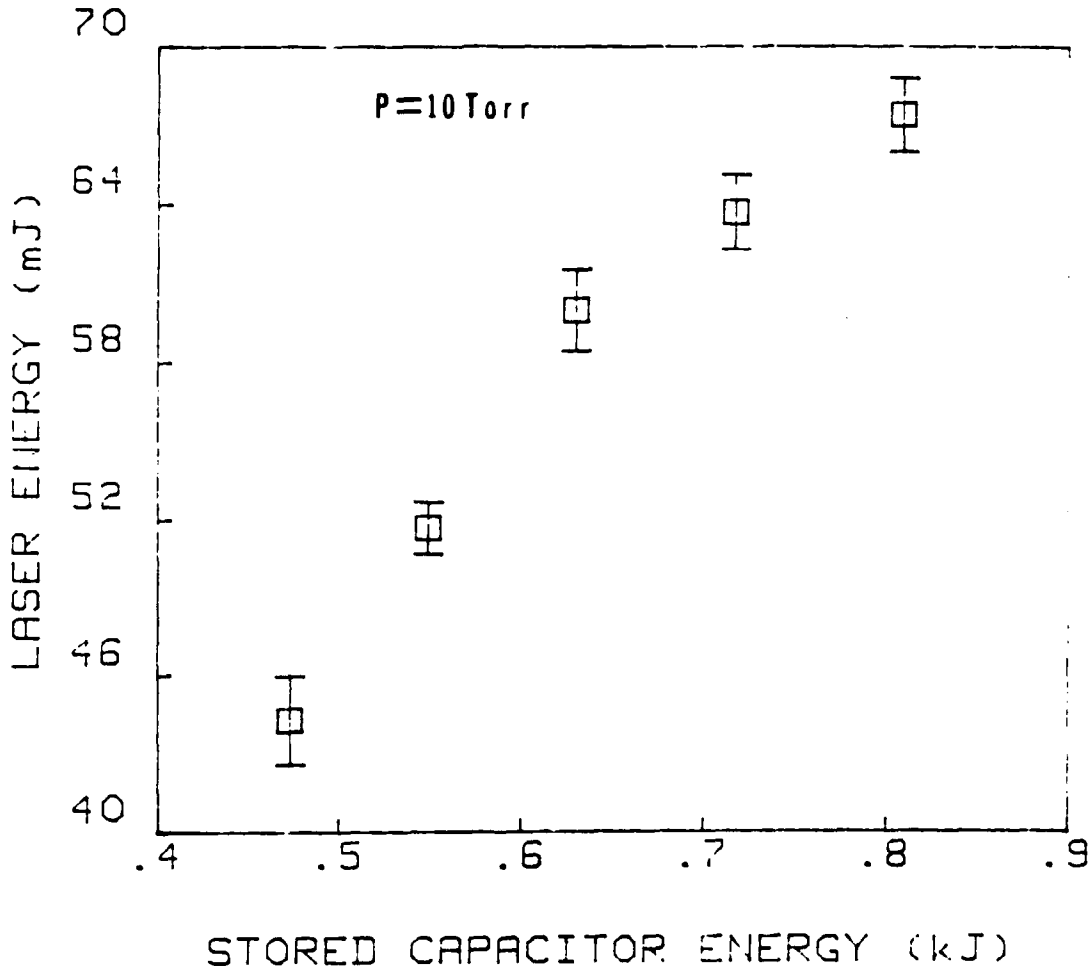

FIGURE 42. The output laser energy dependence on stored capacitor energy.

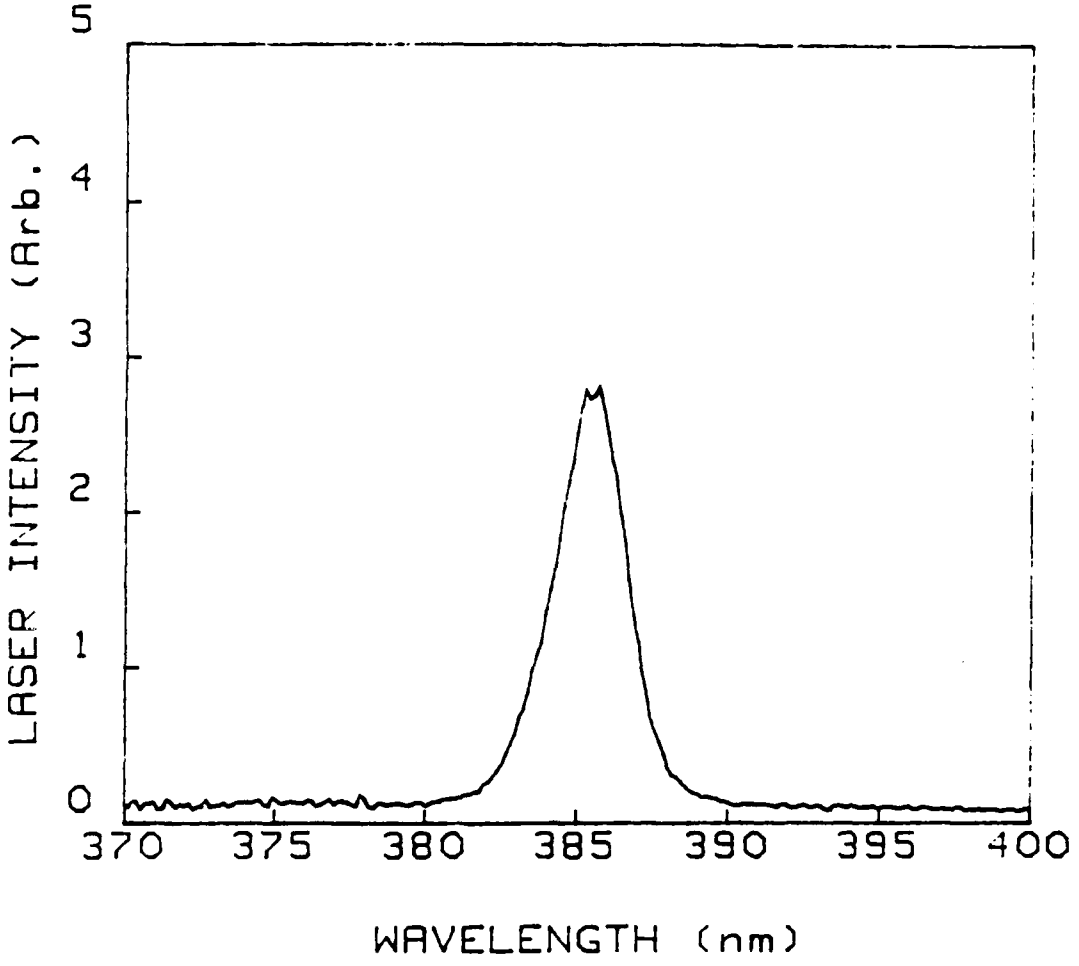

FIGURE 43. The untuned spectrum of the BBQ dye laser in p-dioxane solution.

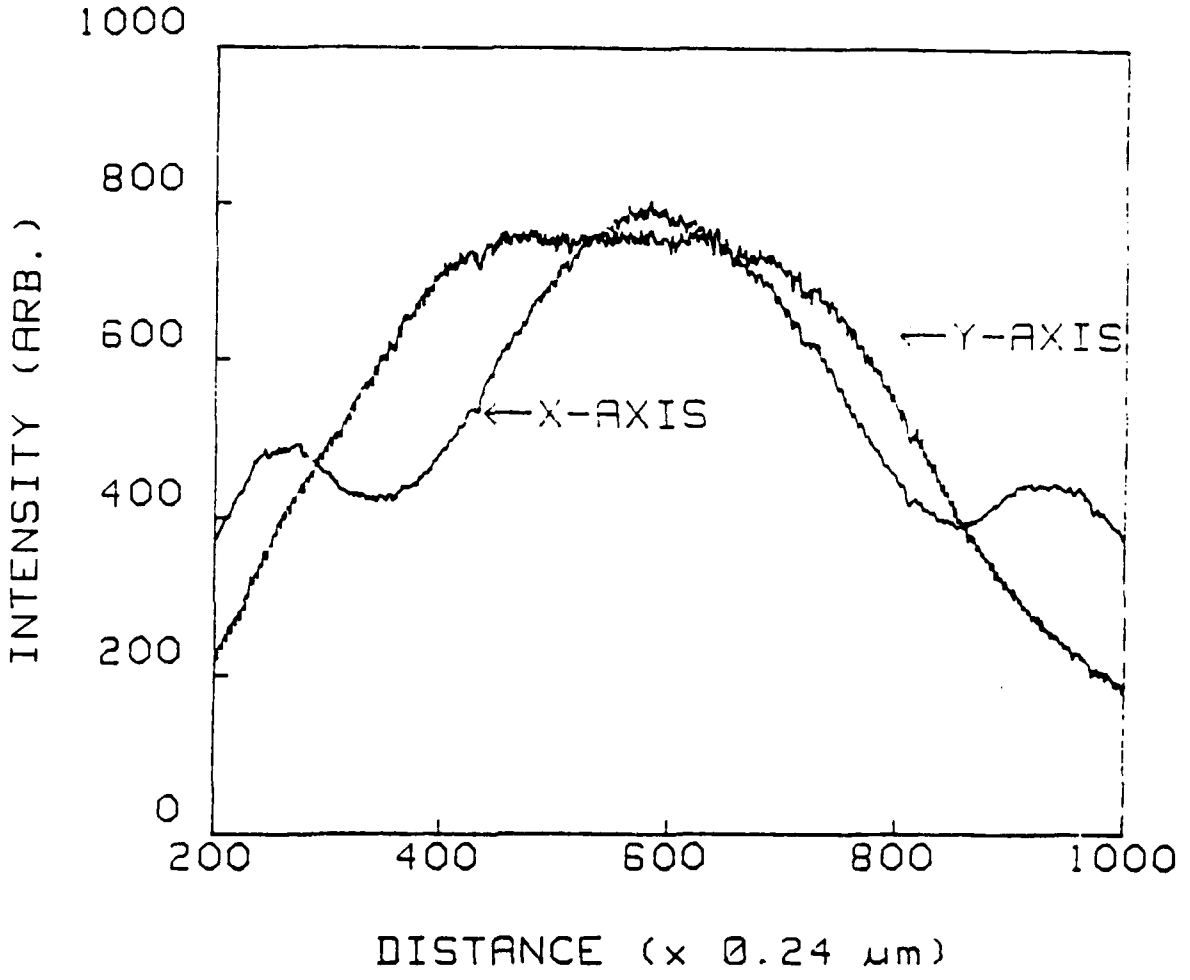

FIGURE 44. The measured beam profile for the BBQ dye laser.

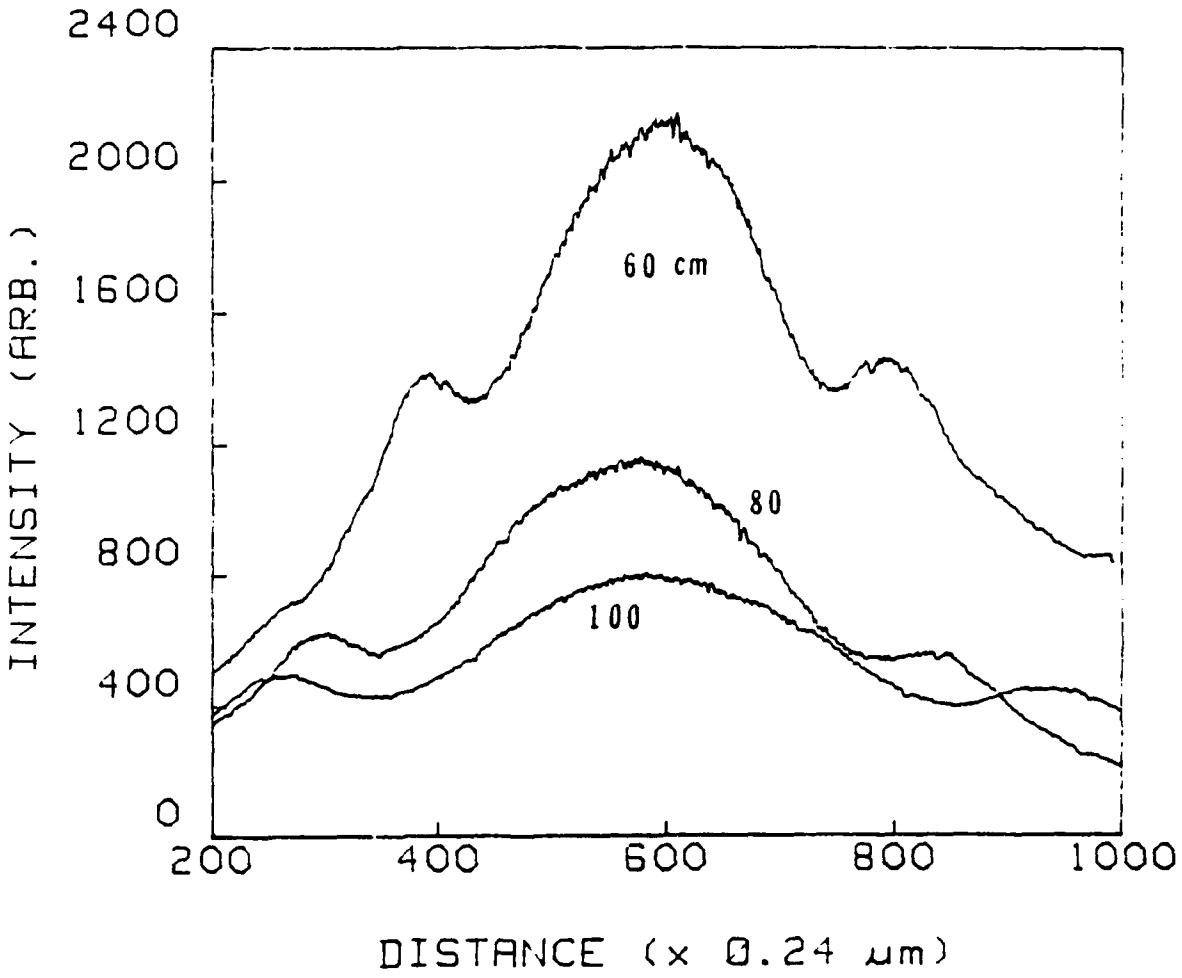

FIGURE 45. The measured beam profiles at 60, 80, and 100 cm distance from the output coupler.

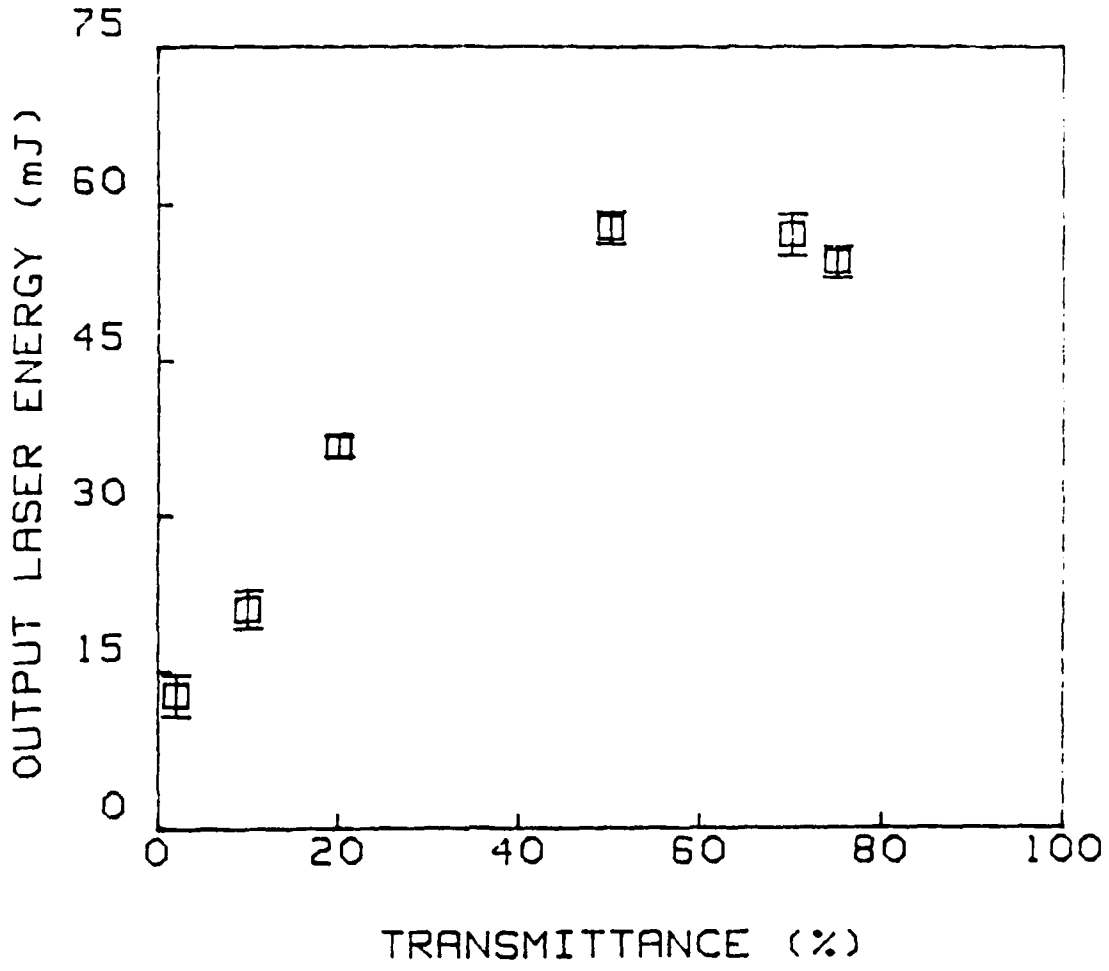

FIGURE 46. The output laser energy as a function of the output coupler transmittance.

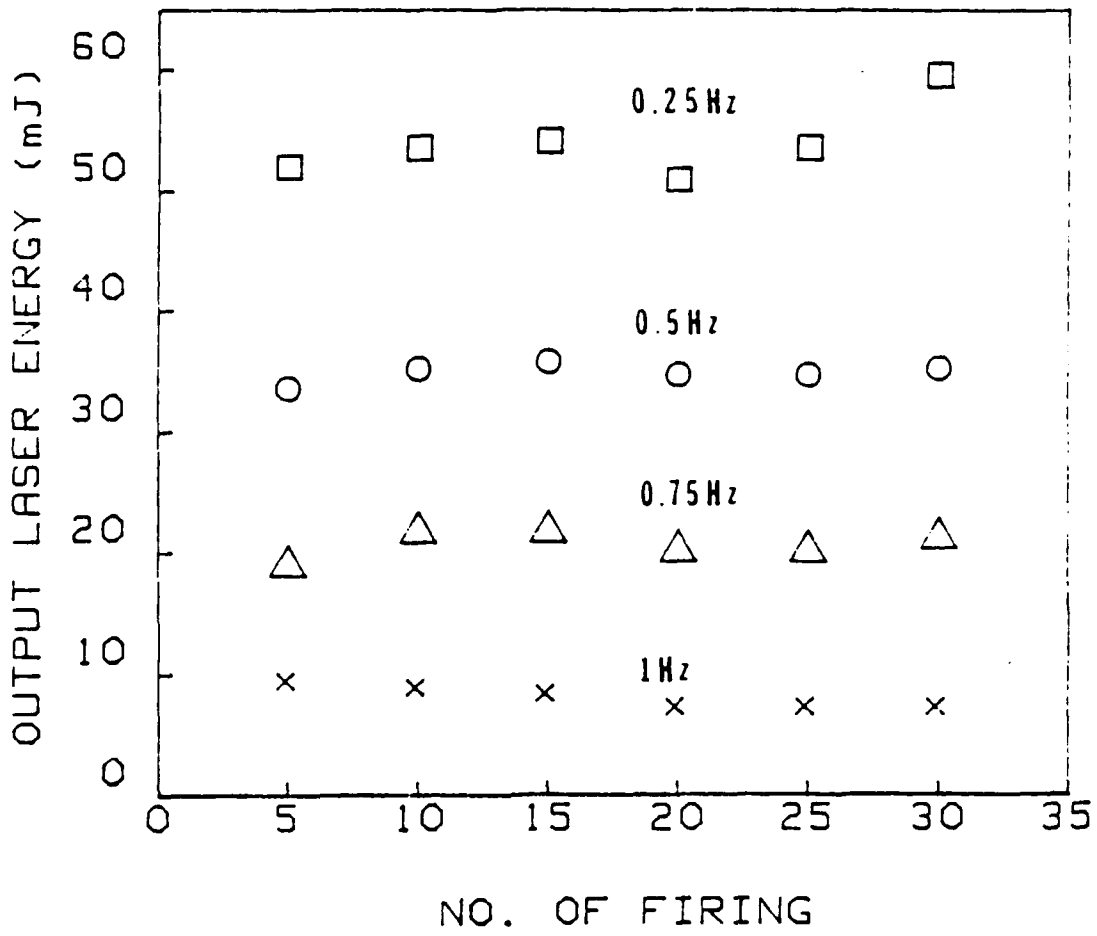

FIGURE 47. The stability of the output laser energy for the number of firings at different repetition rates.

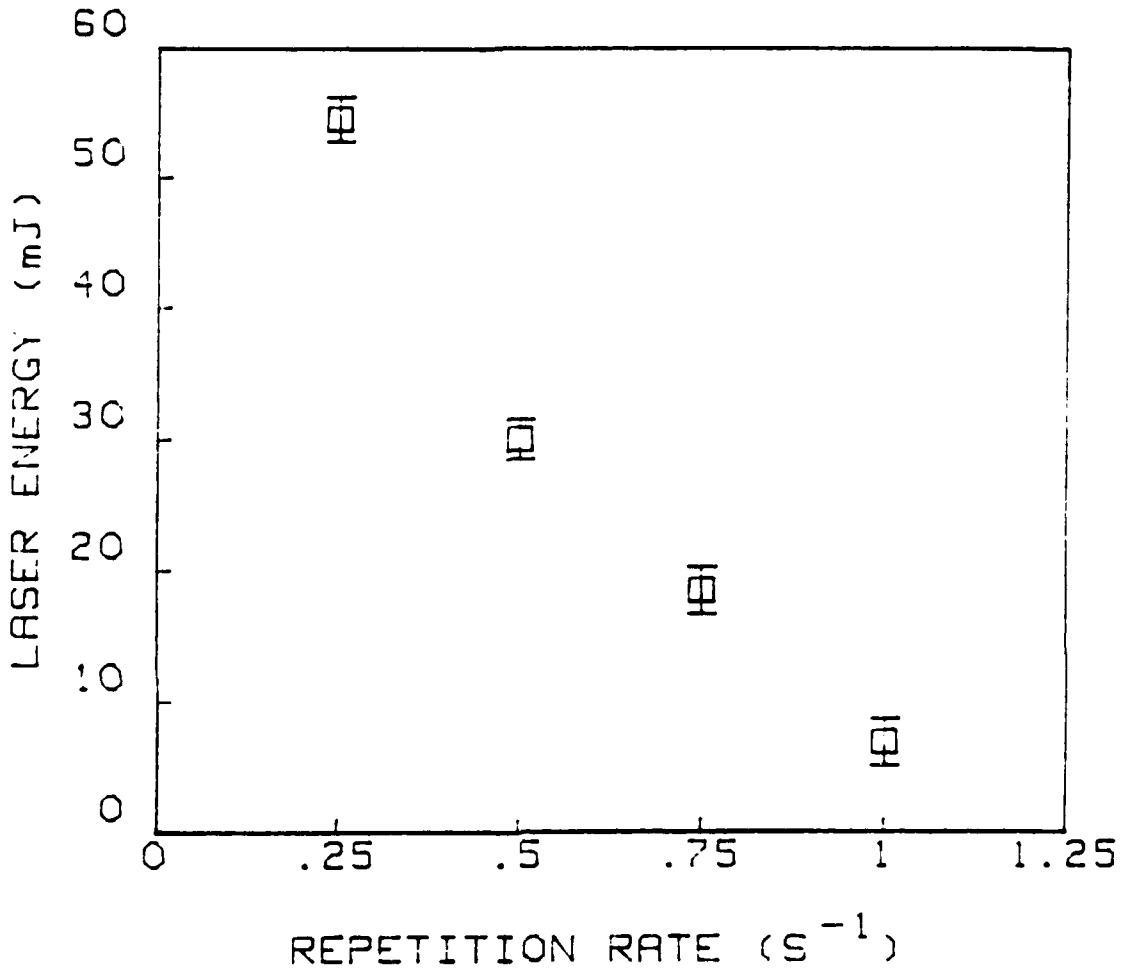

FIGURE 48. The output laser energy for variable repetition rates.

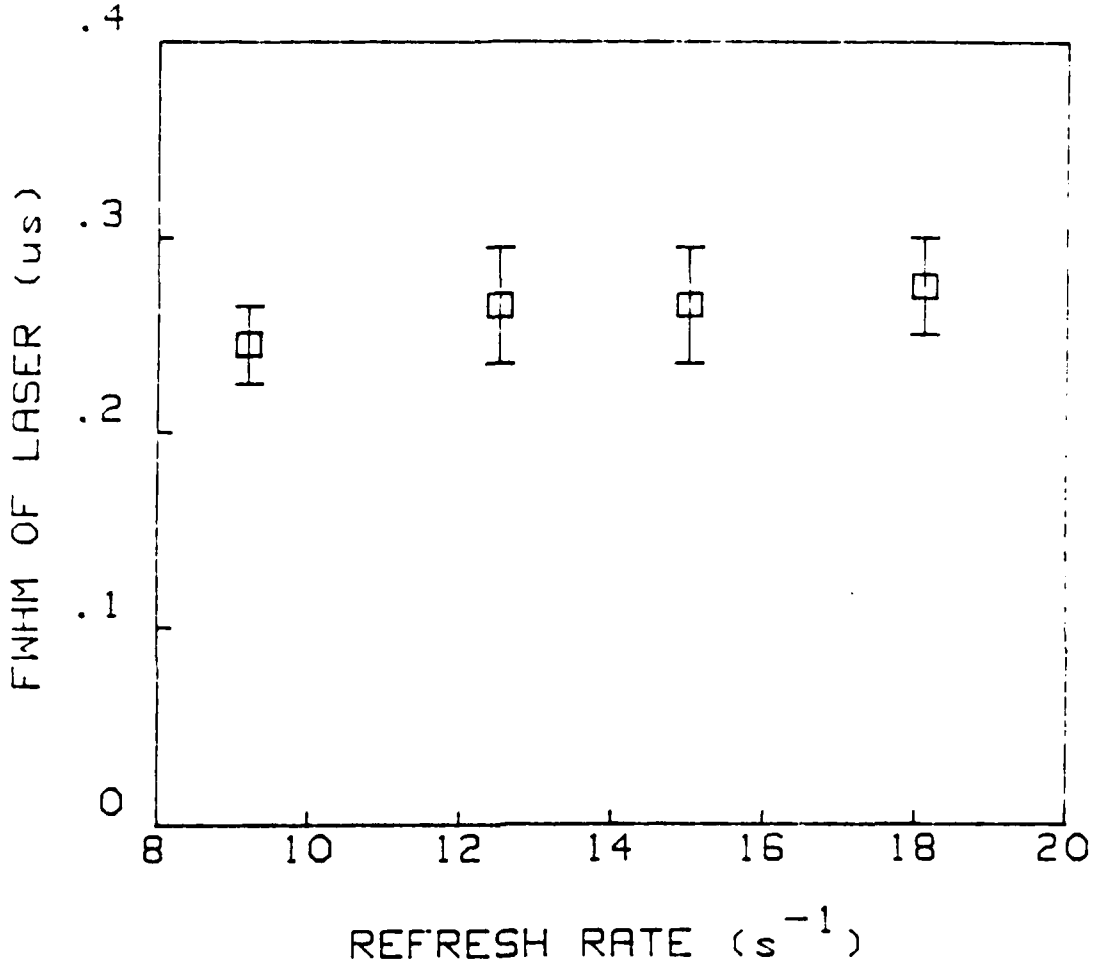

FIGURE 49. FWHM of the laser pulse for different refresh rates.

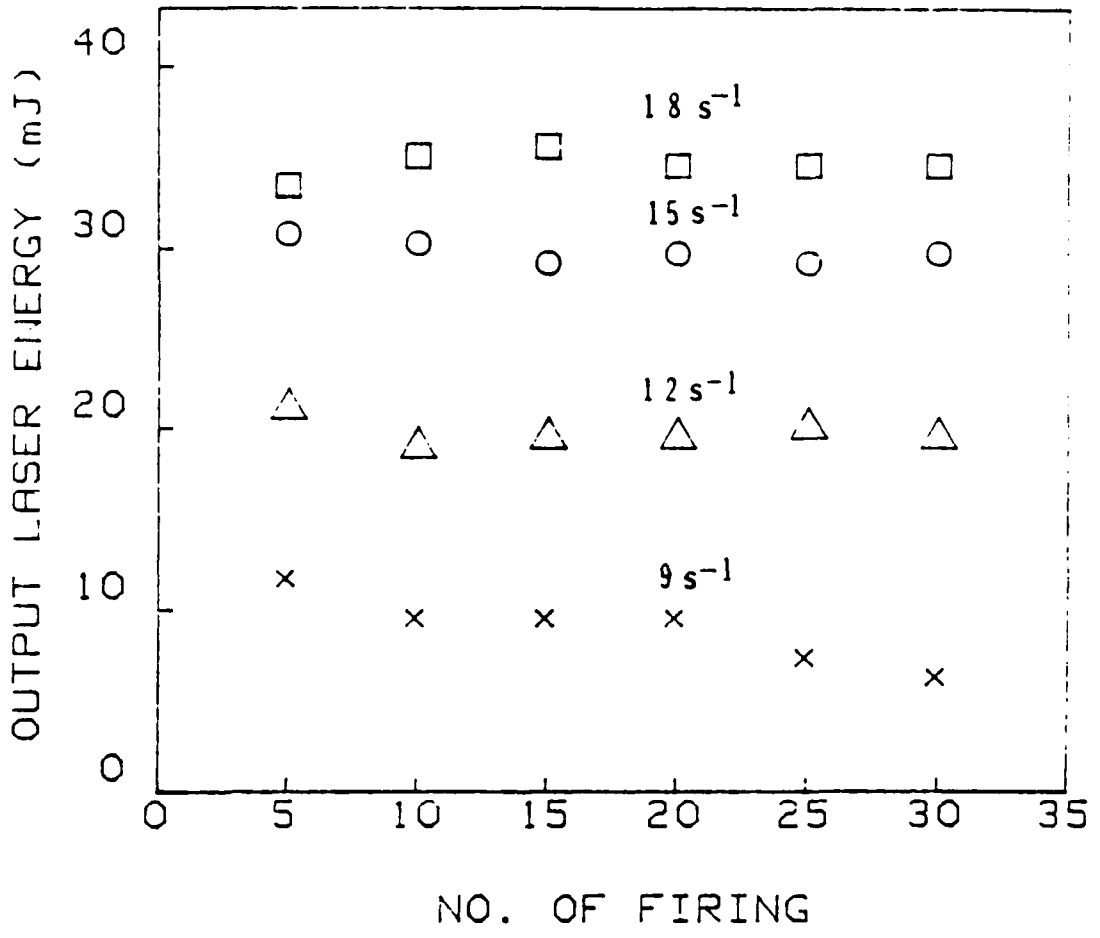

FIGURE 50. The stability of the output laser energy for the number of firings at different refresh rates.

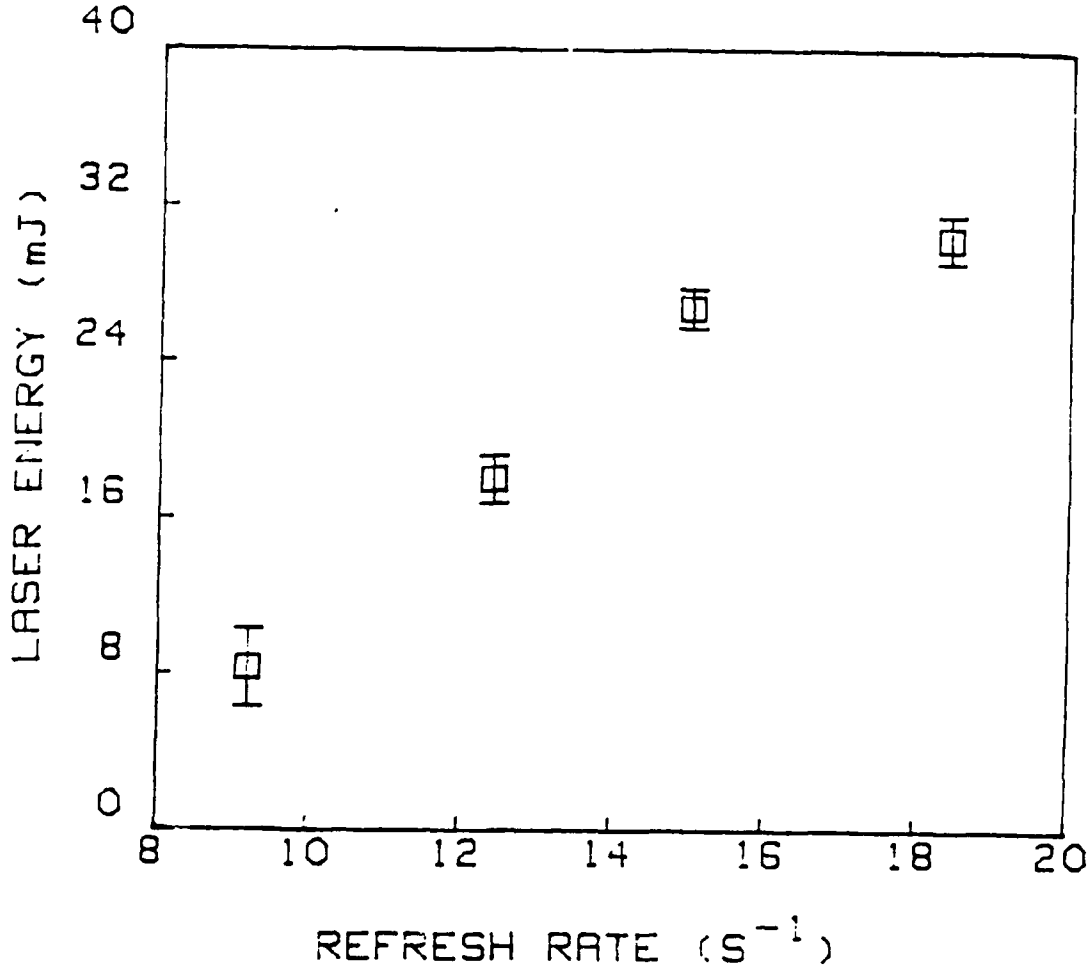

FIGURE 51. The output laser energy for variable refresh rates of the dye circulation.

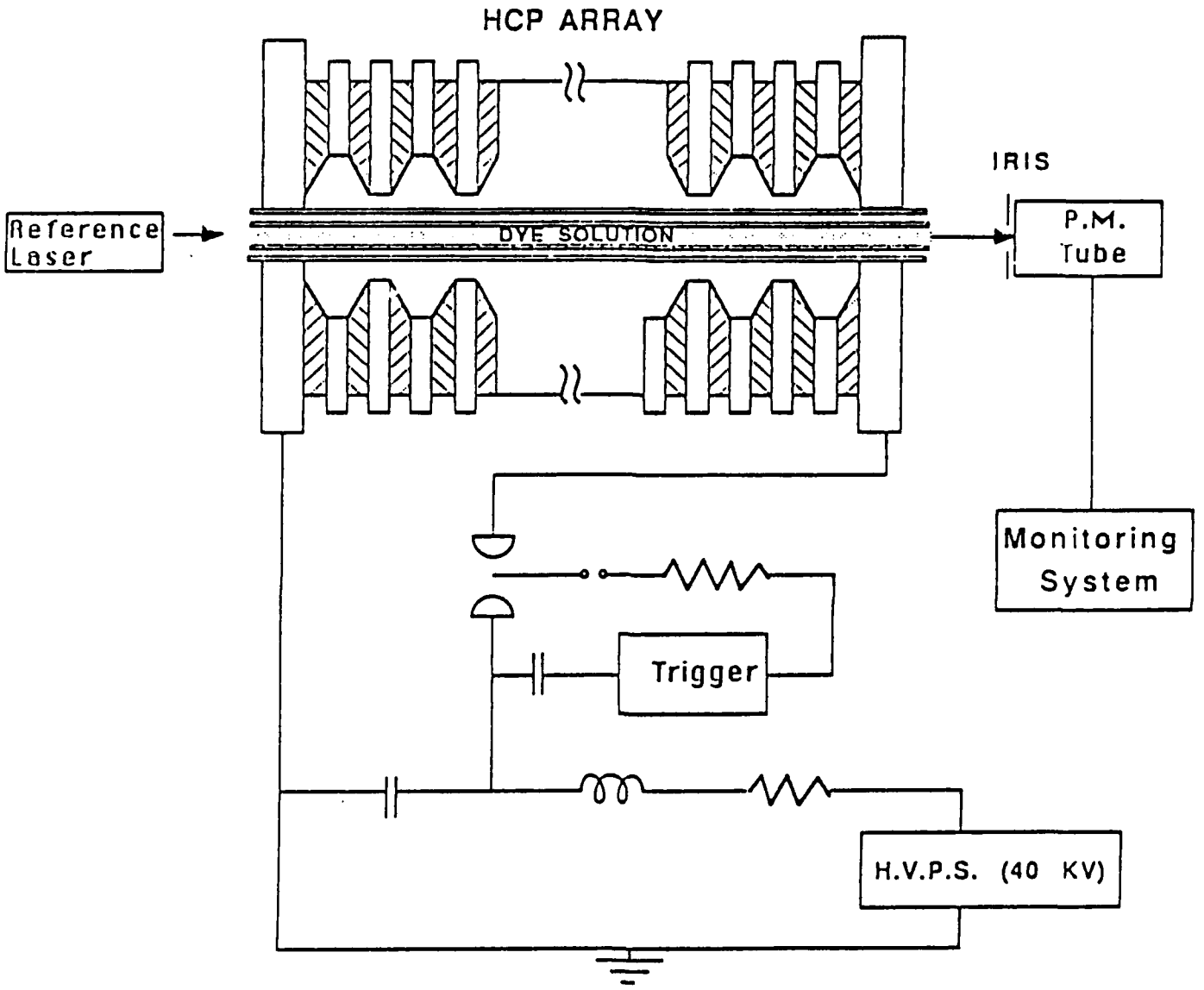

FIGURE 52. Experimental setup for thermal effect measurement.

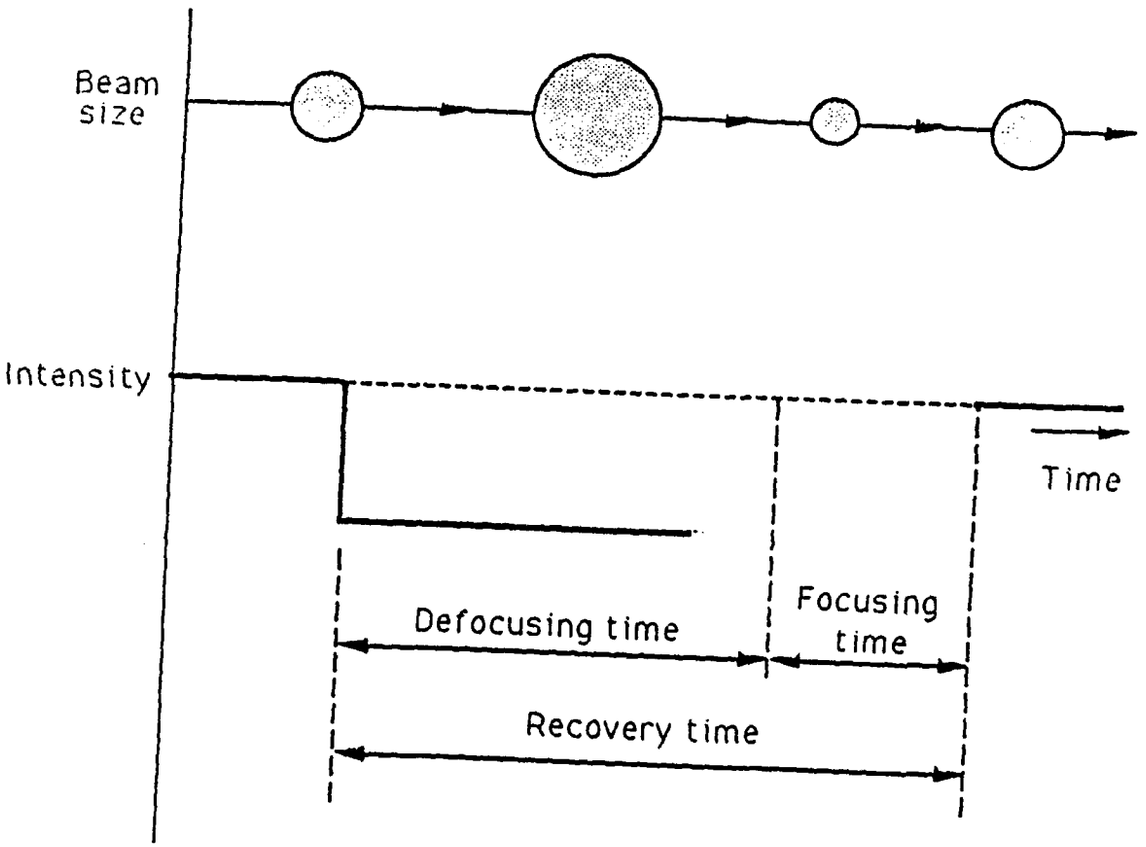

FIGURE 53. General characteristics of the thermal effect on the laser by the HCP plasma.

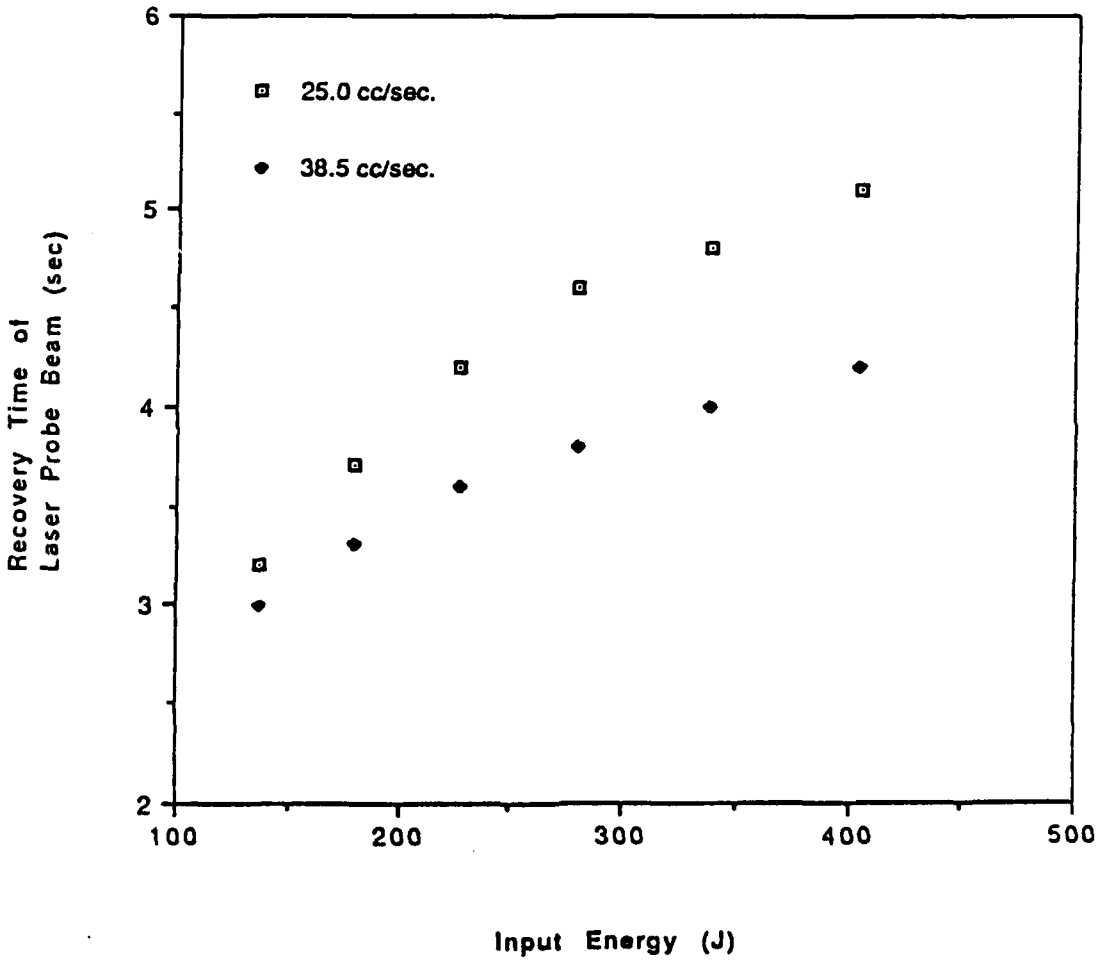

FIGURE 54. Recovery time of laser probe beam vs input energy to HCP with LD 490 dye in a cuvette. Full event covers defocussing, focussing and recovery.

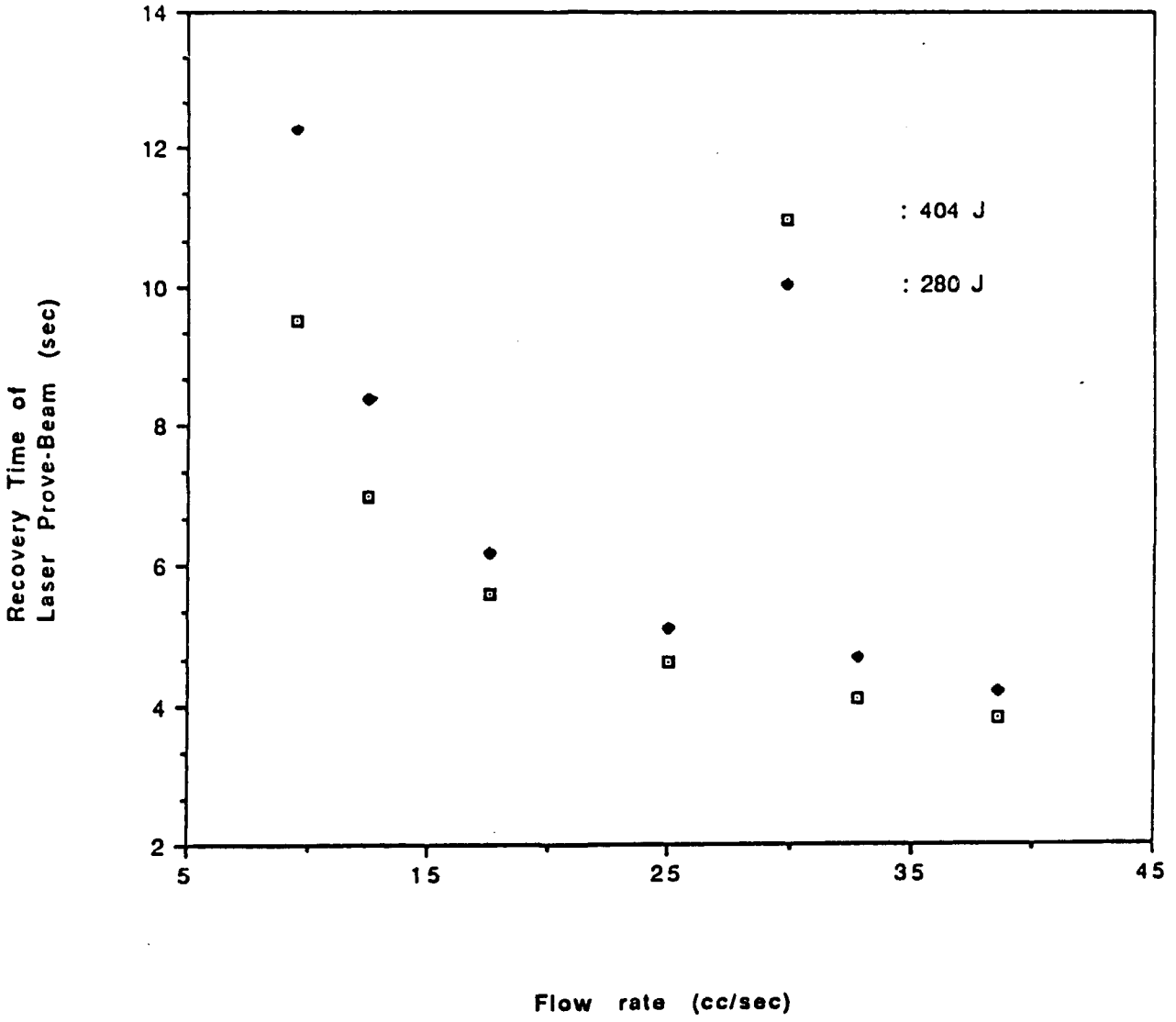

FIGURE 55. Recovery time of probe beam intensity vs flow rate in the HCP with LD 490 dye solvent in the cuvette.

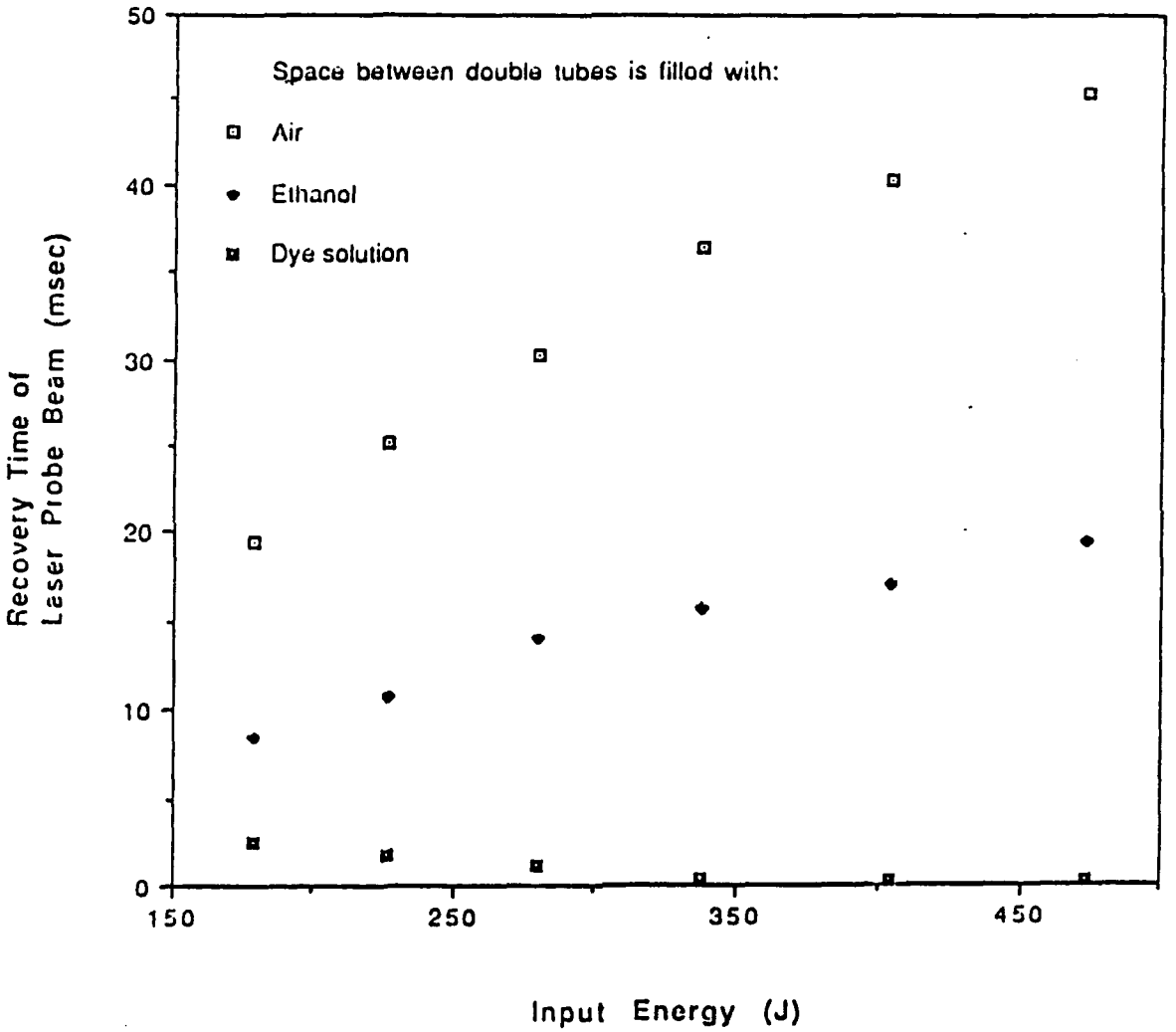

FIGURE 56. Recovery time of laser probe beam vs input energy to HCP with double tubes. Dye flow rate is 25 cc/sec.

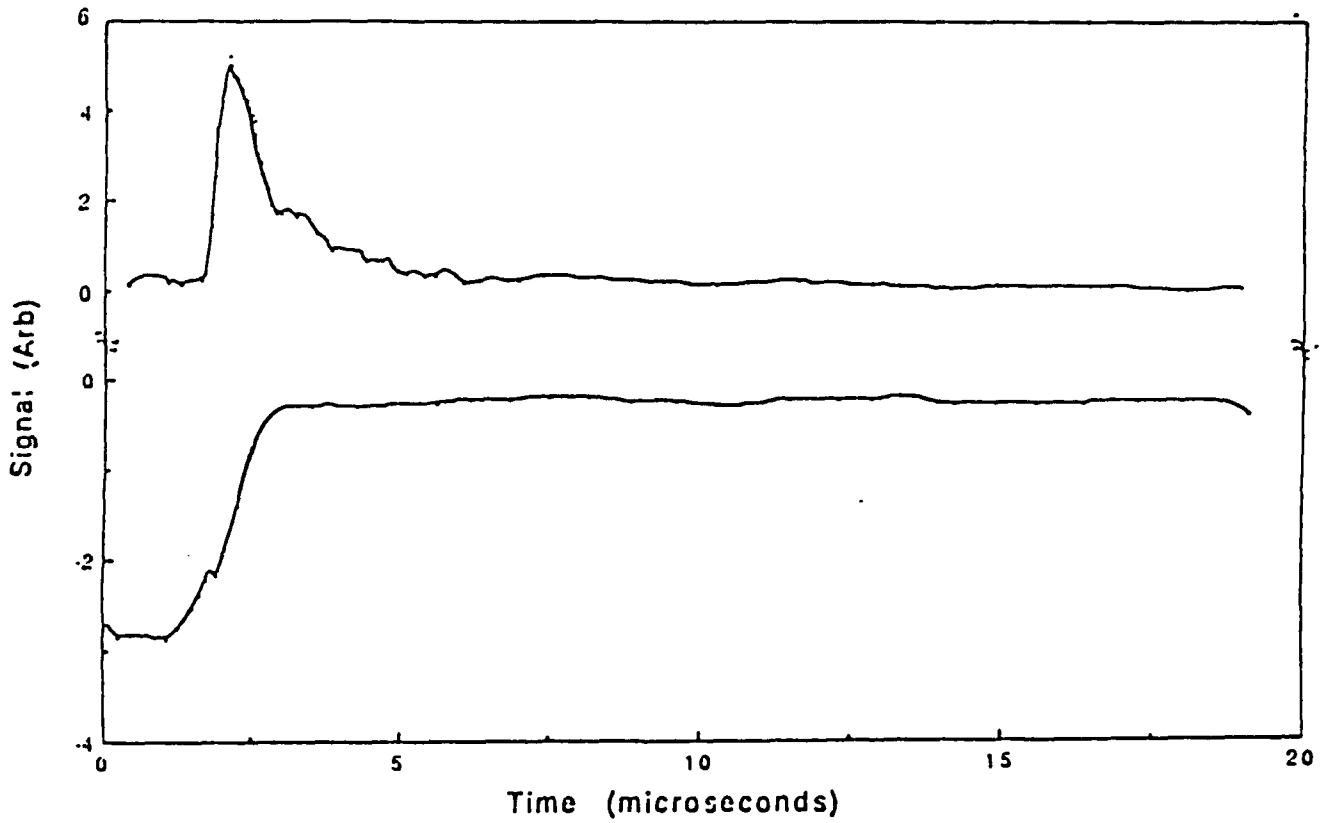

FIGURE 57. Typical oscilloscope signals for HCP pumping light (upper trace) and the probe-beam transmission (lower trace).

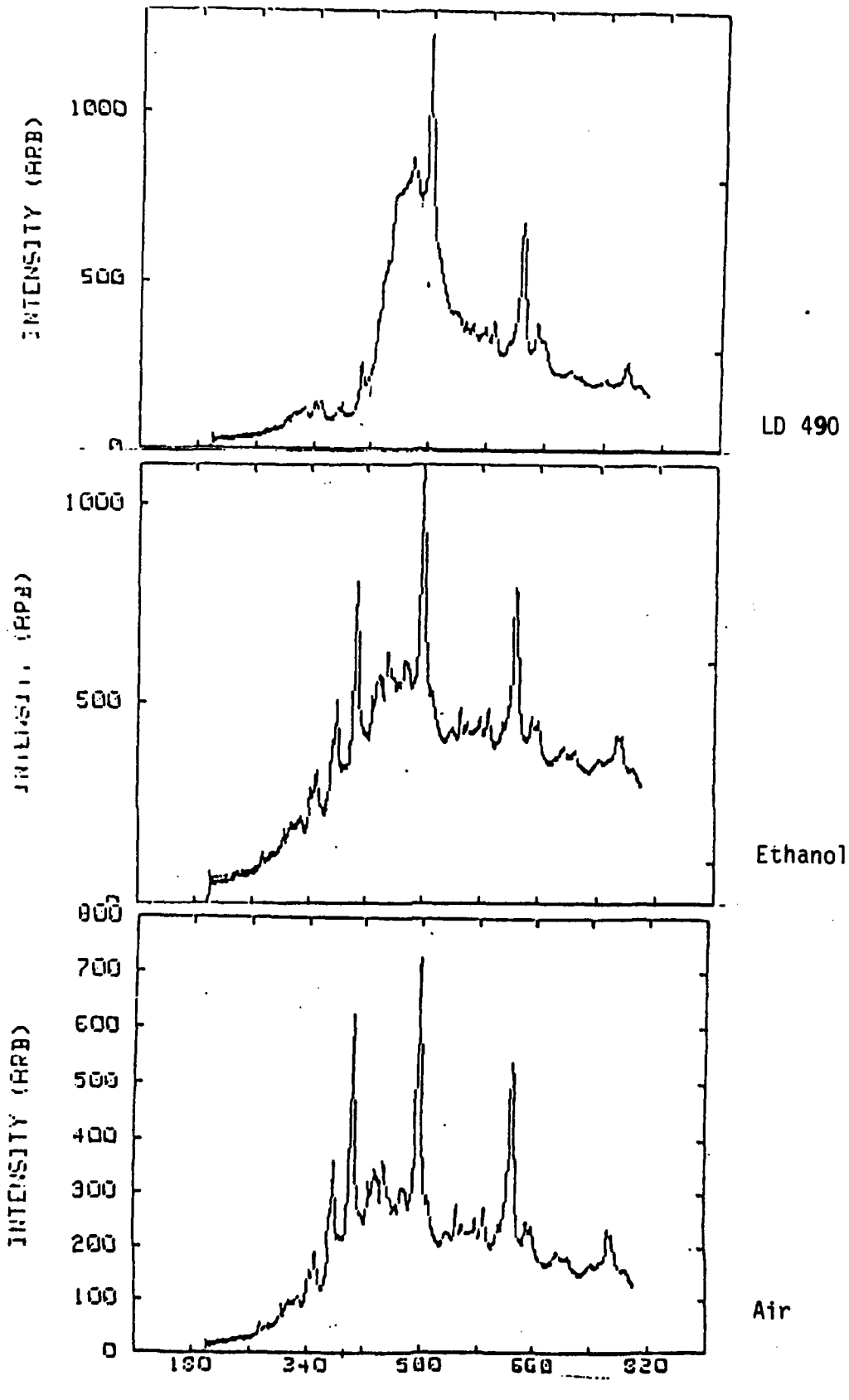

FIGURE 58. Spectra of plasma light source.

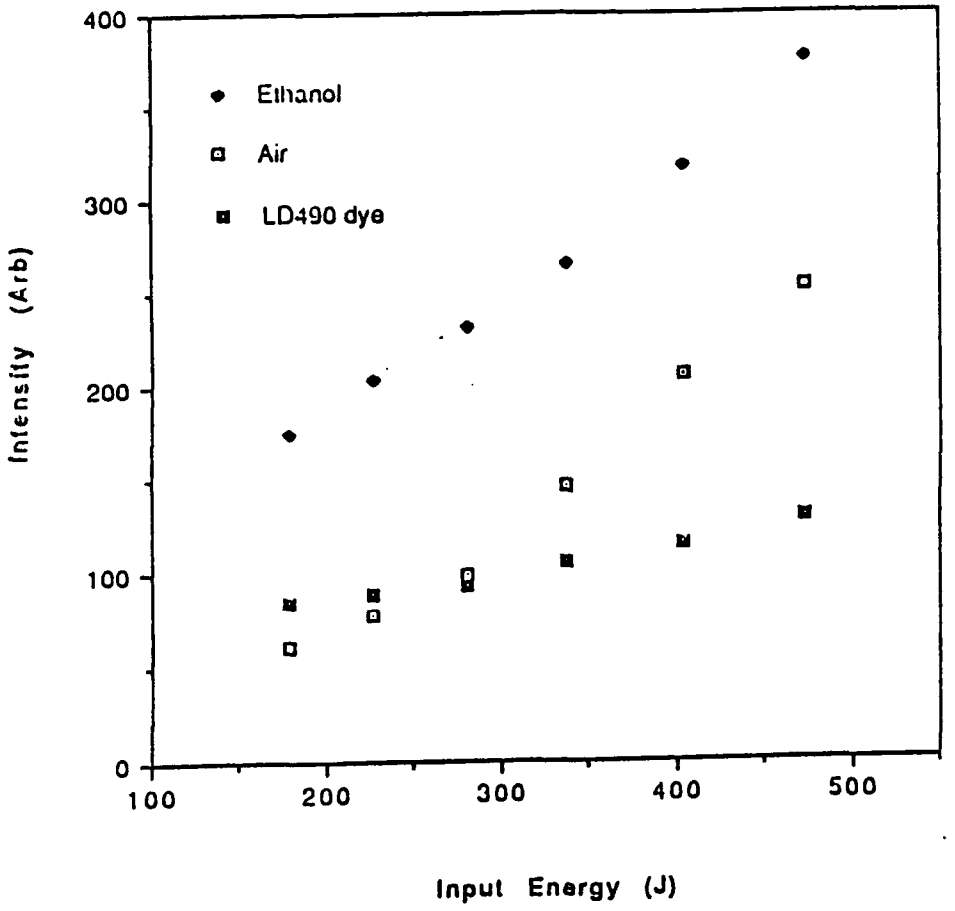

FIGURE 59. Relative light intensity at wavelength 396 nm vs input energy. The jacket space between double cuvette is filled with Ethanol, air or dye solvent.

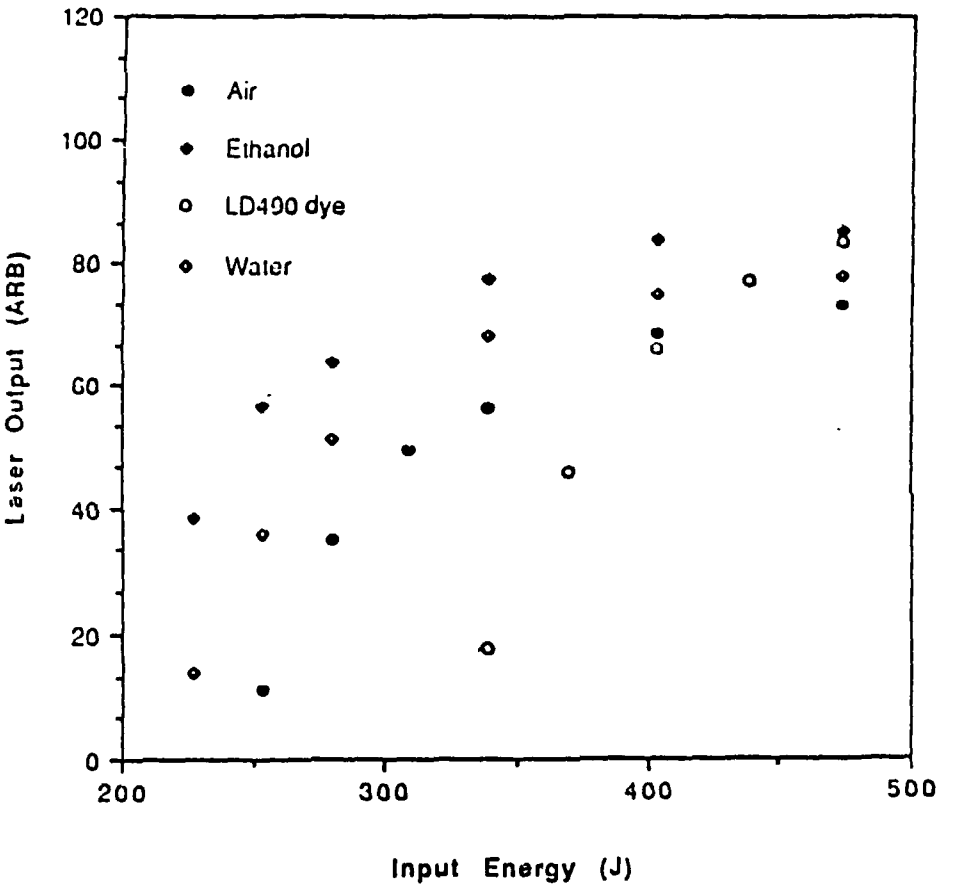

FIGURE 60. Laser output intensity vs input energy. The space between a double tube is filled with air, Ehtanol, LD 490 dye or water.

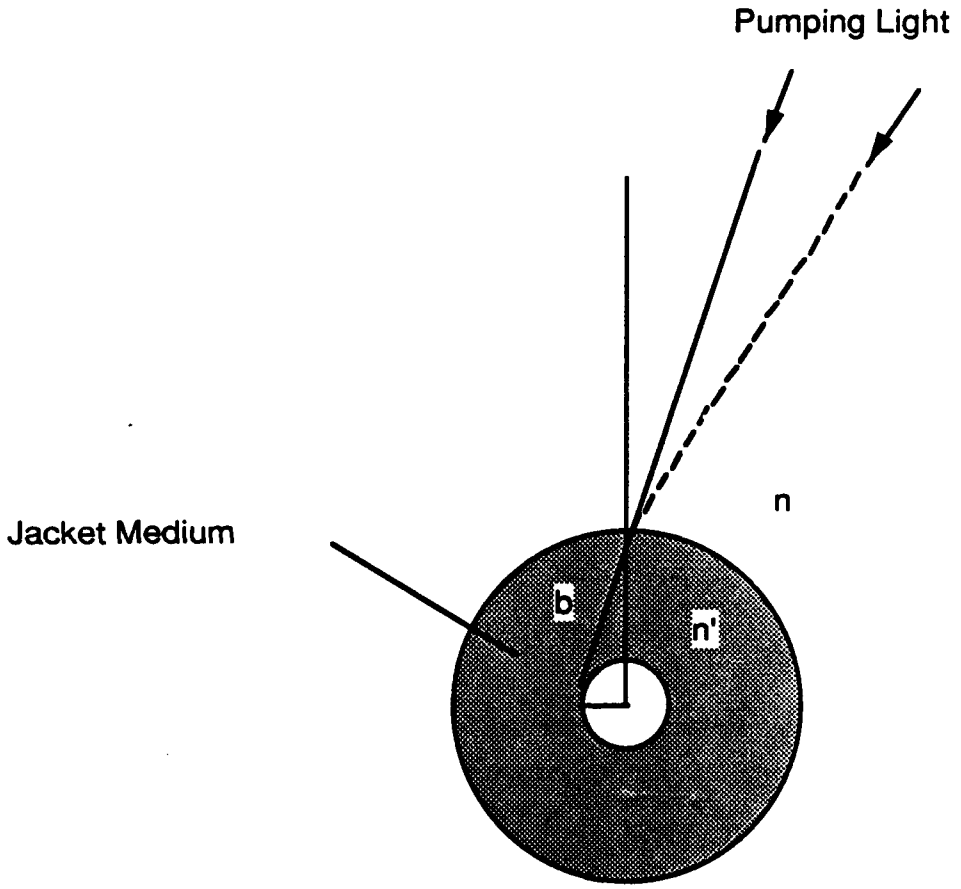

FIGURE 61. Refraction in double-wall cuvette.

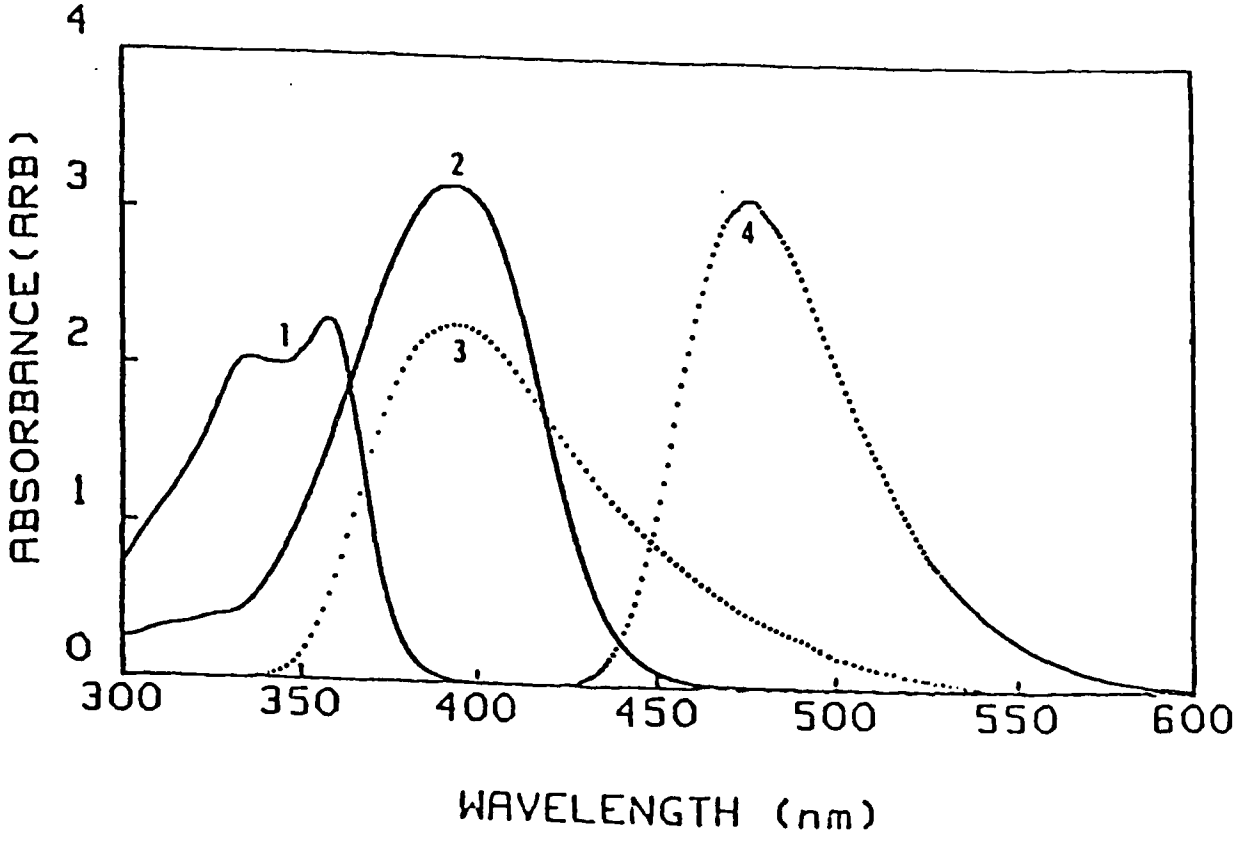

FIGURE 62. Absorbance and fluorescence spectra for the dyes LD390 (1,3) and LD490 (2,4) in methanol.

APPENDICES

ULTRAVIOLET DYE LASERS PUMPED BY HYPOCYCLOIDAL PINCH PLASMAS

W.J. Yi, D.D. Venable, and J.H. Lee

Department of Physics, Hampton University
Hampton, VA 23668

Abstract

A hypocycloidal pinch (HCP) device was utilized to pump dye lasers in the near ultraviolet region of the optical spectrum. The spectral irradiance of the HCP light was found to be dependent on the input energy and the working gas (argon) pressure. This paper reports on the optimum conditions for achieving lasing for the dyes p-terphenyl, BBQ and POPOP. Specifically, for the case of p-terphenyl which has an absorption maximum at 276 nm, we determined an optimum pressure of 1 Torr of argon. For an electrical input energy of 900 J, we obtained a laser output of 8 mJ at 337 nm. Our results with three dyes compare favorably with those obtained for a coaxial flashlamp system.

Introduction

Tunable ultraviolet (uv) lasers are important for many aspects of photochemical research. Frequency doubled or tripled high power lasers such as ion, ruby, Nd^{3+}, and visible dye lasers as well as short wavelength excimer lasers have been employed for pumping uv dye lasers. However, these pump sources are complex and expensive laser systems themselves. Consequently their applications are limited. Broadband flashlamp-pumped high power dye lasers would be desirable for the uv range. These devices are currently available only for wavelengths above 330 nm. Additionally, their output energies are limited to values of typically less than 1 J. This limitation is due to the lack of intense uv emission from the flashlamp. New light sources such as exploding wires or foils [1] and dense plasmas [2-6] have been studied as intense uv pump sources for an iodine laser which also requires uv excitation. The dense plasmas produced in hypocycloidal pinch (HCP) arrays and coaxial gun type devices have recently been used to pump visible and blue-green laser systems.[5-6]

This paper reports on results obtained using the HCP as a broadband pump source for uv dye lasers with emission wavelengths below 420 nm.

Experimental Arrangement

A block diagram of our experimental set-up for the HCP dye laser system is shown in Figure 1. Nine hundred (900) J of energy was provided to the HCP laser system. The laser system parameters were simultaneously monitored by three different methods: (1) electrical parameters were monitored using a voltage divider; (2) the HCP emission was monitored by a monochrometer and a photomultplier tube that were coupled to the HCP by a uv enhanced optical fiber; and (3) laser output parameters were measured with an energy meter and with a uv enhanced photodiode. In addition to these simultaneous measurements, an optical multichannel analyzer was used to analyze the emission of the HCP. Each of these instruments was interfaced to a microcomputer for analysis of data.

A cross sectional view of the HCP device is shown in Figure 2. Resistor chains were used to uniformly distribute voltage in the system. The gas breakdown over the surface of the insulators produced a strong uv light and the current buildup caused a current sheet to move radially inward in an inverse pinch mode by the action of the JXB force. The dotted curves represent the final position of the current sheet which produced an array of plasma rings concentric with the dye tube. These plasma rings emitted intense radiation over a wide range of the spectrum. The intense light produced by the early surface discharge and the later plasma modes, which depended on the pressure of the working gas, served as a pump for the active medium of the dye laser tube placed on the axis.

The HCP emission spectrum is shown in Figure 3. The spectrum is seen to be composed of characteristic lines superimposed on a continuum. The characteristic lines are produced by the working gas, argon, and by the surface discharge. The line spectra are very intense in the region below 300 nm. The continuum spectrum has a maximum at approximately 280 nm which, according to the Wien displacement law, corresponds to a blackbody temperature of 10,500 K. A typical emission spectra for a xenon flashlamp is shown as a dotted line for comparison. The continuum produced by the flashlamp has a peak at longer wavelength and therefore corresponds to a lower blackbody temperature. Thus, the combination of strong line emission and strong continuum radiation in the uv

BLOCK DIAGRAM OF EXPERIMENTAL SET UP

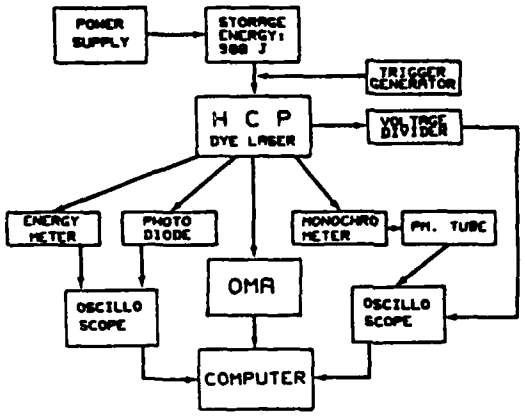

Figure 1: Block diagram of the experimental arrangement for the HCP uv dye laser system.

CROSS-SECTION OF HCP DEVICE

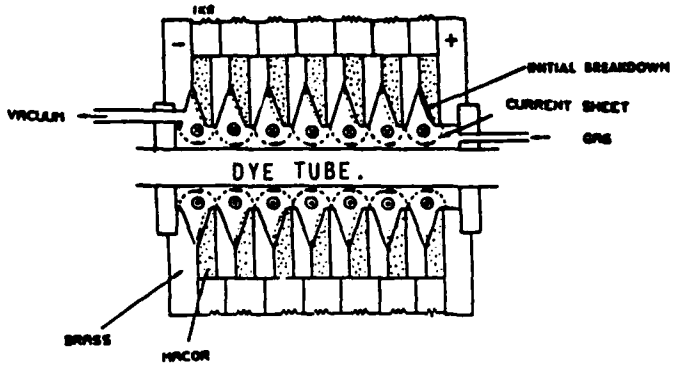

Figure 2: Cross sectional view of the HCP device. The device consists of six coaxial electrodes separated by ceramic insulators. The dotted curves represent the initial breakdown and final positions of the current sheet.

band of the spectrum indicates the HCP is a more efficient pump source for uv lasers than typical flashlamps.

The ability to produce a uv laser using the HCP as the pump source will strongly depend on two parameters: (1) the intensity of the HCP emission spectra within the pumpband of the selected dye; and (2) the risetime of this pump light. These parameters depend on the pressure of the working gas and could thus be optimized for a particular lasing dye. In Figure 4, we show the intensity of the HCP pump light as a function of working gas pressure. Light intensity was measured at a wavelength of 276 nm. The spectrometer used to select this wavelength has a spectral bandwidth of 2 nm. This wavelength corresponds to the absorption peak of the dye p-terphenyl. The measured intensity was compared to a deuterium standard source and it was found that at 1 Torr pressure the spectral irradiance of the HCP emission was 18 W/cm²nm. Figure 5 shows the dependence of risetime of the HCP pump light on the pressure of the working gas. The fastest risetime for these conditions was 40 ns and was obtained at a pressure of 0.1 Torr. It is observed that above pressures of 0.5 Torr the risetime is linearly dependent on pressure with a constant of proportionality of 0.08 microseconds per Torr. The risetimes in Figure 5 were measured for the same conditions as the intensities in Figure 4. Risetime was defined as the time required for the signal to grow from 10% to 90% of the peak height.

Results

In Figures 6 through 8, we show typical output characteristics for the case of the p-terphenyl dye laser with peak laser output at 337 nm, pumped by the HCP device. In Figure 6, we show typical temporal oscillograms of the laser output and the HCP pump light. The oscillograms are shown for four different pressures as indicated in the figure. A comparison of the cases for 0.5 and 2.0 Torr shows that the pump light (lower traces) is less intense for lower pressures. However, the lower pressure case produces the more intense laser signal (upper traces). This can be explained by observing that the risetime is faster for the case of 0.5 Torr than for the case of 2.0 Torr. Thus the laser output can be enhanced by optimizing the risetime of the pump light as required by the dye-laser kinetics.

Figures 7 and 8 show laser output energy and laser power, respectively, as a function of working gas pressure. An output coupler of 70% transmittance was found to give maximum output energy and was utilized for the data presented in Figures 7 and 8. A maximum output energy of 8 mJ was observed at a pressure of 1 Torr. The maximum output power of 160 kW was observed at a pressure of 0.75 Torr. The maximum output power occurred at a lower working gas pressure than the maximum output energy. The lower pressure corresponding to faster risetime results in a laser pulse of shorter duration and consequently more power. The solid line in Figure 8 shows the pump rate vs. pressure. The pump rate P is defined by $P = I/T$ where I is the peak intensity of the

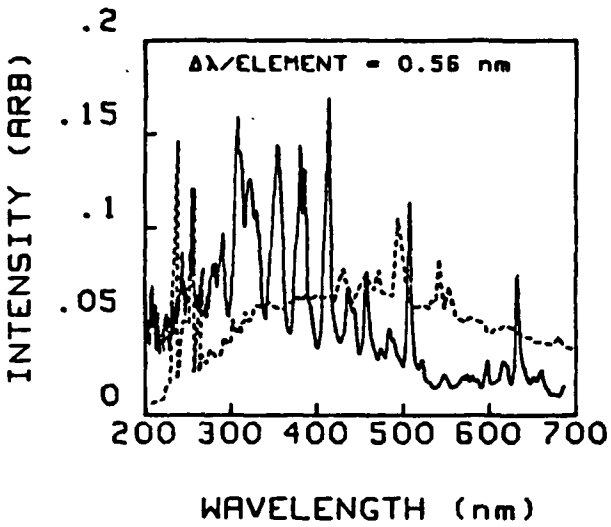

Figure 3: HCP emission spectrum. Emission spectrum of the HCP pump source is represented by the solid line. The dashed line represents emission for a typical xenon flashlamp. These data were obtained using an optical multichannel analyzer with a wavelength resolution of 0.56 nm per element.

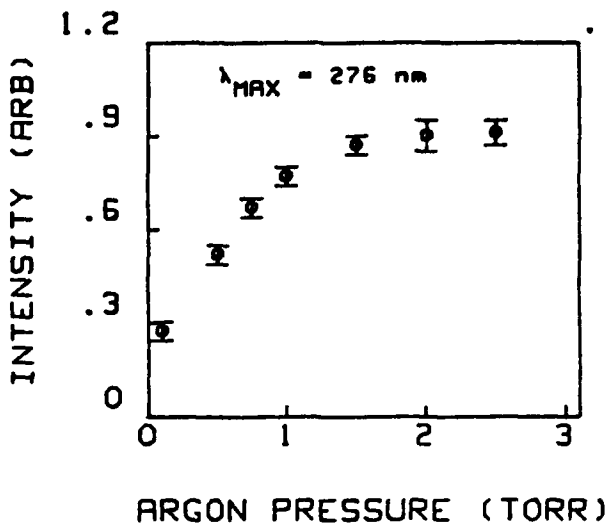

Figure 4: Intensity of HCP pump light as a function of working gas (argon) pressure. These data were measured at a wavelength of 276 nm which corresponds to the absorption peak of p-terphenyl dye.

pump light and T is the risetime of the pump light. The pump rate relationship reasonably predicts the location of the optimum when the laser power is measured as a function of working gas pressure.

These results, as well as the results for the other two uv dyes tested, are summarized in Table 1. The three dyes tested were p-terphenyl, BBQ, and POPOP. These dyes have peak absorption at 276, 307, and 358 nm, respectively. Correspondingly, our system was adjusted to produce optimum emission at each of these wavelengths. The maximum output energies obtained for the three dyes were 8, 30, and 1.3 mJ, respectively. For the case of p-terphenyl the maximum energy was obtained at a pressure of 1.0 Torr. At this pressure the risetime of the pump light at 276 nm was 100 ns. The BBQ laser produced maximum output energy for an optimum risetime of 300 ns for pump light in the 307 nm region of the spectrum. This risetime was obtained for an argon pressure of 2.5 Torr. Optimization of the system for POPOP required the fastest risetime of 40 ns which was obtained at a pressure of 0.1 Torr. The maximum output power for the lasers occurred at different pressures as explained earlier.

The extracted energy density for our system was measured and compared to the perfomance of typical coaxial dye lasers. For our system, we obtained an extracted energy of 20 mJ/cm³ for p-terphenyl. This value was found to be about 3 times higher than that obtained for coaxial laser systems. For the case of BBQ, we measured an extracted energy density of 63 mJ/cm³ which was 5 times higher than the corresponding value for coaxial flashlamp lasers. Finally, we determined that the overall slope efficiencies for our system were 0.0012%, 0.015%, and 0.0008% for p-terphenyl, BBQ, and POPOP, respectively.

Summary

In summary, we have used an HCP device to pump uv dye lasers for p-terphenyl, BBQ, and POPOP dyes. We conclude the following:

1. The spectral irradiance of the HCP device can be optimized by varying the working gas pressure.

2. The spectral irradiance of the HCP pump source is sufficiently intense to pump dyes in the uv region of the spectrum.

3. The risetime of the system can be easily optimized for various dyes. Risetimes were measured as fast as 40 ns.

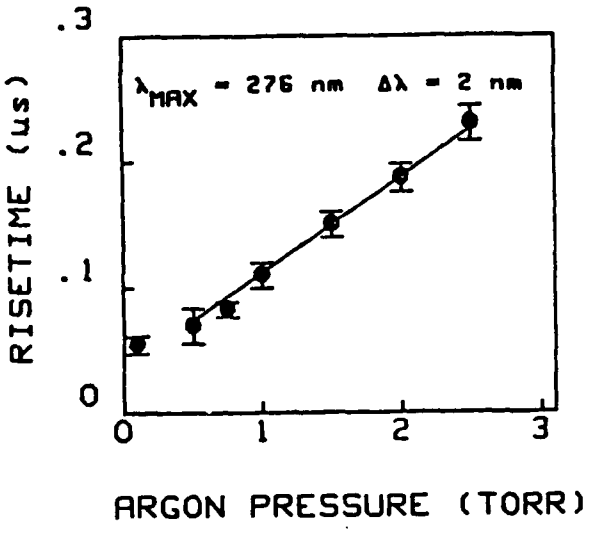

Figure 5: Risetime of the HCP pump light as a function of working gas (argon) pressure. The solid line indicates linear dependence above pressures of 0.5 Torr with a constant of proportionality of 0.08 μs/Torr. These data were obtained at 270 nm which corresponds to the absorption peak for p-terphenyl laser dye.

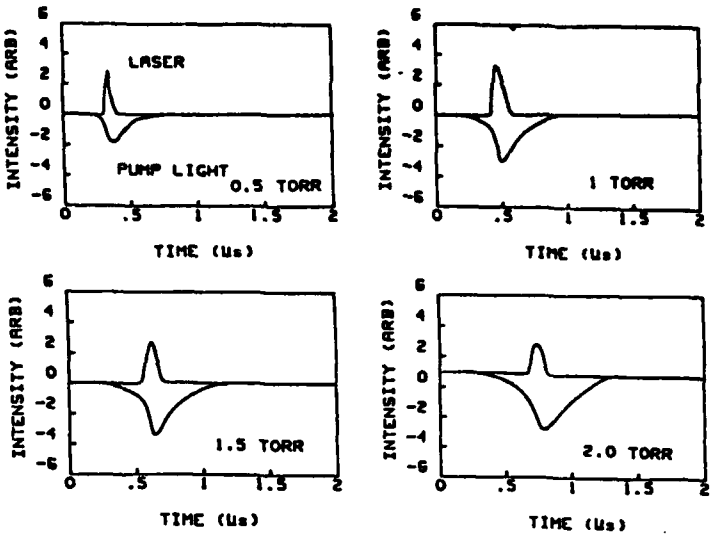

Figure 6: Oscillograms showing temporal response of the output laser signal (upper traces) and the HCP pump light (lower traces) for pressures of 0.5, 1, 1.5 and 2.0 Torr. Analysis of these oscillograms indicates that laser peak power depends on both the pump light power and risetime.

4. Finally, we compared the HCP system to coaxial dye lasers in the uv part of the spectrum and found the HCP system extracts 3 to 5 times more energy per unit volume of lasant dye.

References

1. Jones, C.R. and K.D. Ware, "Optically Pumped Ultraviolet and Infrared Laser Driven by Exploding Metal Films and Wires." SPIE, 308, 160 (1983).

2. Rozanov, V.B. and A.A. Rukhadze, "Plasma Pump Source for Lasers." Sov. J. Quantum Electronic, 13, 73 (1983).

3. Kashnikov, G.N., V.K. Orlov, A.N. Panin, A.K. Piskunov and V.A. Reznikov, "Pulse-Periodic Iodine Photodissociation Laser Pumped with Radiation from Magnetoplasma Compressions." Sov. J. Quantum Electron, 10, 1193 (1983).

4. Kamrukov, A.S., G.N. Kashnikov, N.P. Kozolov, V.A. Malashchenko, V.K. Orlov, and Yu. S. Protasov, "Investigation of an Iodine Laser Excited Optically by High Current Plasmadynamic Discharge." Sov. J. Quantum Electron, 6, 1101 (1976).

5. Lee, J.H., D.R. McFarland, and F. Hohl, "Ultraviolet Laser Excitation Source." Applied Optics 19, 3343 (1980).

6. Han, K.S., S.H. Nam, and J.H. Lee, "High Power Blue-Green Laser by Hypocycloidal-Pinch Plasma." J. Appl. Phys. 55, 4113 (1984).

7. Reiger and K. Kim, "Performance of an Array of Plasma Pinches as a New Optical Pumping Source for Dye Lasers." J. Appl. Phys. 54, 99 (1983).

8. Kim, K. and J.J. Fanning, "New Short-Wavelength Optical Pump Consisting of Mather-Type Dense Plasma Focus." CLEO'84 Tech. Digest, Paper TUB33.

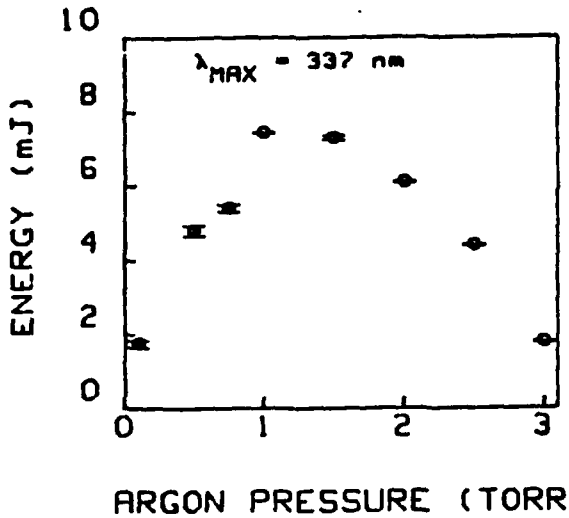

Figure 7: Output energy of the p-terphenyl dye laser as a function of working gas (argon) pressure. The input electrical energy to the laser system was 900 J and the laser dye concentration was 1X10⁻³ M. An output coupler of 70% transmittance was used to obtain these results. P-terphenyl's peak lasing wavelength occurs at 337 nm.

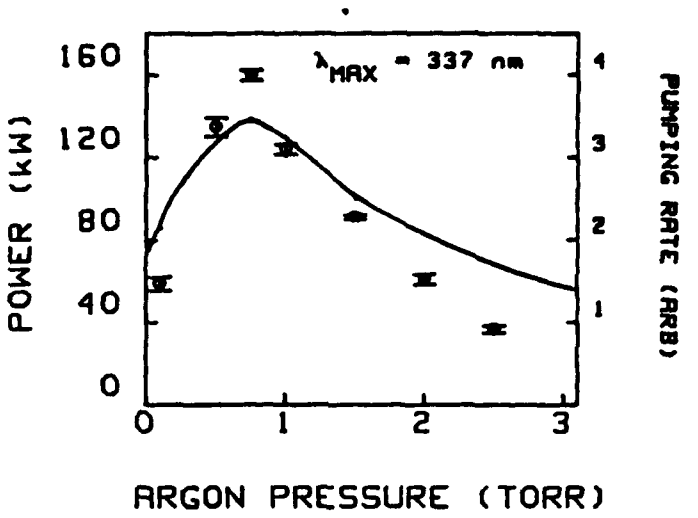

Figure 8: Output power of the p-terphenyl laser as a function of working gas pressure. The system parameters are the same as those given for Figure 7, however, optimum performance occurred at a lower pressure than that observed for the output energy. The solid line gives the pump rate for the system.

TABLE 1

PERFORMANCE OF HCP-PUMPED DYE LASERS

	P-TERPHENYL	BBQ	POPOP
Absorption Peak Wavelength (nm)	276	307	358
Lasing Peak Wavelength (nm)	337	383	417
Maximum Energy (mJ)	8	30	1.3
Pressure (Torr) Argon	1.0	2.5	0.1
Risetime (μs)	0.1	0.3	.04
Concentration (1X10⁻³ M)	1.0	0.4	1.5
Input Energy (J)	900	900	900
Output Coupler (% T)	70	80	80
Extracted Energy Density (mJ/cm³)	20	63	3.3
(Typical Coaxial Flashlamp)	(7)	(13)	(*)
Maximum Power (kW)	160	250	30
Pressure (Torr) Argon	0.75	0.50	0.10
Slope Efficiency (1X10⁻³%)	1.2	15	0.8

*Data not available

SECTION Astronomy, Mathematics and Physics .

ABSTRACT FOR PUBLICATION IN THE VIRGINIA JOURNAL OF SCIENCE

Read the instructions on the reverse side with care and follow them precisely.

Abstracts will be reproduced directly from the form below for publication by photo offset in the Proceedings issue of the Virginia Journal of Science. Abstracts must follow format to be acceptable for publication. Those deemed unsuitable for direct reproduction will be retyped and the authors charged $5.00.

MAIL THE UNFOLDED FORM TOGETHER WITH TWO XEROX (OR EQUIVALENT) COPIES TO YOUR SECTION SECRETARY BY THE DATE SPECIFIED IN THE COVERING MEMO.

ULTRAVIOLET EMISSION OF A ONE-HERTZ HYPOCYCLOIDAL PINCH DEVICE. S. M. Lee, D. D. Venable, J. H. Lee, and K. S. Han, Dept. of Physics, Hampton University, Hampton, VA 23668. We have developed a 1 Hz hypocycloidal pinch (HCP) system with maximum charging energy of 1.1 kJ and have utilized this system as an ultraviolet (uv) broadband optical pump source for dye lasers. When operating at 630 J with 10 Torr Ar pressure, our HCP has a stored-energy efficiency of 68% and 1.1% of this is converted into optical pump energy. Twenty-four percent of the optical pump energy lies within the absorption band of BBQ, the dye selected for testing the system. Thus, we effectively convert 0.2% of our charging energy into useful pumpband light in the uv region. In this paper we report on the uv emission observed at 1 Hz operation of the system. We also present preliminary results for theoretical modeling of the plasma acceleration. This research is supported in part by Grant AFOSR-86-0345.

(SIGNATURE, VAS MEMBER)

FOR PAPERS SOLELY BY NON-MEMBERS:

INTRODUCED BY _____ (SIGNATURE, VAS MEMBER)

MAILING ADDRESS (IF DIFFERENT FROM ABOVE) _____

FOURTH INTERNATIONAL LASER SCIENCE CONFERENCE (ILS-IV)

October 2-6, 1988

Marriott Marquis Hotel, Atlanta, Georgia

DO NOT WRITE IN THIS SPACE

Log Number _____

Accepted: Yes____ No____

Session _____

Program Number _____

Organizer _____

Demetrius D. Venable (804) 727-5277

Corresponding Author *Phone Number*

Hampton University Physics

Institution Department

Box 6135

Street Address or Box Number

Hampton, Virginia 23668

City State (Country) Zip

[X] poster preferred [ ] oral preferred [ ] no preference

Which author will most likely present this paper? Demetrius D. Venable

special requirements or comments _____

first choice of subject area Lasers 1.d. second choice Lasers 1.c. (see previous page)

PLEASE LEAVE 8 SPACES BEFORE BEGINNING TITLE

TYPE ABSTRACT ENTIRELY WITHIN A 12.0 CM WIDE x 10.5 CM LONG RECTANGLE IN THIS SPACE (SEE EXAMPLE ON PAGE 2). ONLY MATERIAL WITHIN THIS RECTANGLE WILL BE PRINTED (IF IT DOESN'T FIT, IT WILL BE REDUCED UNTIL IT DOES).

PLEASE MAIL FLAT. DO NOT FOLD FORM, ESPECIALLY THIS AREA.

A One-Hertz Hypocycloidal Pinch Plasma Pump Source for Ultraviolet Dye Lasers.* S. M. LEE, D. D. VENABLE, JA H. LEE, and K. S. HAN, Hampton University, Hampton, VA 23668--We have utilized a repetitively operated hypocycloidal pinch plasma device as a broadband optical pump source for ultraviolet (uv) lasers. This presentation discusses enhancements in the system previously reported[1] to allow 1 Hz operation. The dye selected for testing the system is BBQ which has an absorption peak at a wavelength of 305 nm and a fluorescence peak at a wavelength of 385 nm. We have measured a slope efficiency of 0.01% for pumping BBQ. Dependence of the laser performance on firing rates (up to 1 Hz) and on dye flow rates has been characterized. Our system compares favorably with coaxial flashlamp pumped uv dye lasers with similar input energies and repetition rates and can, however, be scaled to input energies higher than those achievable with flashlamps.

*Supported in part by AFOSR grant AFOSR-86-0345.

1. W. J. Lee, D. D. Venable and Ja H. Lee, Proceedings of the International Conference on Lasers '86, edited by R. W. McMillan, (STS Press, McLean, VA, 1987), pp. 411-415.

Send this form to: Lynn Borders, Iowa Laser Facility, University of Iowa, Iowa City, Iowa 52242-1294; phone: (319) 335-1299; twx: 910-525-1398; Bitnet: BLAWCSPD@UIAMVS.

A ONE-HERTZ HYPOCYCLOIDAL PINCH PLASMA PUMP SOURCE FOR ULTRAVIOLET DYE LASERS

D. D. Venable, S. M. Lee, J. H. Lee and K. S. Han
Hampton University, Hampton, VA 23668

ABSTRACT

We have utilized a repetitively operated hypocycloidal pinch plasma device (HCP) as a broadband optical pump source for ultraviolet (uv) lasers. This presentation discusses enhancements in the system previously reported[1] to allow 1 Hz operation. The dye selected for testing the system is BBQ which has an absorption peak at a wavelength of 305 nm and a fluorescence peak at a wavelength of 385 nm. We have measured a slope efficiency of 0.01% for pumping BBQ. Dependence of the laser performance on firing rates (up to 1 Hz) and on dye flow rates has been characterized. Our system compares favorably with coaxial flashlamp pumped uv dye lasers with similar input energies and repetition rates and can, however, be scaled to input energies higher than those achievable with flashlamps.

INTRODUCTION

Comparisons of various dye laser pump sources typically utilized in the ultraviolet (uv) portion of the spectrum indicate that the hypocycloidal pinch (HCP) device has distinct advantages over other sources.[2] The HCP device has been extensively utilized in our laboratories as a pump source for ultraviolet and blue-green dye lasers. Appropriate references on these works are given in the recent theses by S. M. Lee[3] and by K. S. Nam.[4] In this paper we discuss the operation of an HCP device in a repetitive mode of operation for pumping BBQ dye.

EXPERIMENTAL RESULTS

The new HCP prototype had a net resistance of 178 mΩ and a total inductance of 135 nH. These values were, respectively, 4.5 and 0.68 times higher than those given for the prototype of reference 1. The capacitive storage energy was 1 kJ and 68% of this energy was converted to stored energy within the HCP device. This resulted in a peak current of 64 kA for the system. A complete listing of the electrical characteristics of the prototype is given in Table I. It should be noted that because of the metal construction of the device, higher charging energies can be achieved by replacement of appropriate circuit elements.

The HCP continuum light emission approximated that of a 15,000 K blackbody when operated at the optimum filling gas pressure of 10 Torr of argon. The measurement system was calibrated at wavelengths above 250 nm by comparison to NBS traceable light emission standards. Because of the weak sensitivity of our measuring instruments, we were unable to make quantitative measurements below 250 nm. The time integrated emission within the BBQ absorption band (285-325 nm) was 45 kW/cm^2 which corresponded to a 13% spectral efficiency for the system. The total useful light energy incident on the

lasing medium was 1.2 J.

The pump intensity was monitored for long term operation (greater than 100 shots) and found to fluctuate by less than 8% for the 1 Hz operation mode. Even though the pump light was stable the uv dye laser output showed a strong dependence on the thermal gradients produced in the dye solvent at each firing of the system. To characterize this effect, the beam of a reference He-Ne laser was directed through the HCP laser tube and the defocusing of this probe beam was monitored as the HCP system discharged. The time required for the probe beam to refocus after each firing represented a useful upper limit on the laser repetition rate. Figure 1 shows the laser output energy as a function of the number of shots for various repetition rates. This data show that the laser output energy fluctuates by less than 15% for a given firing rate but decreases from 60 to 8 mJ for near single shot to 1 Hz operation. The data in Fig. 1 were obtained with a dye circulation rate sufficient to refresh the laser tube 15 times per second (a refresh rate of 15 Hz.) Figure 2 shows the laser output energy dependence at 0.5 Hz operation as a function of refresh rate. The smaller laser energies at low refresh rates and high repetition rates result from the heating of the boundary layer of the dye solution by the hot uv irradiance of the HCP pump. Characteristics of the dye laser are given in Table II. The overall system efficiency, defined as the ratio of laser output energy to electrical input energy, of 0.01% compares favorably with other broadband pump systems in this region of the spectrum.

Table I. Electrical circuit parameters.

Power Supply Capacity	40 kV, 200 mA, P_{max} = 8 kW
Operating Rate	1 Hz at V_0 = 30 kV
Stored Capacitor Energy	630 J (1.1 kJ for V_0 = 40 kV)
Damping Factor	7.8 x 10^6 Hz
System Inductance	135 nH
System Resistance	178 mΩ
Average HCP Inductance	80 nH
Average HCP Resistance	150 mΩ
Cycle Period	2.7 μs
Maximum Current	94 kA
Ringing Frequency	370 kHz
Percentage Reversal	12%
Electrode Materials	Molybdenum
Insulator Material	Ceramic

All parameters measured at 10 Torr (Ar).

Table II. Parameters of BBQ dye laser.

Absorption Wavelength (Peak)	307 nm
Untuned Laser Wavelength	386 nm
Laser Energy-Single Shot (for V_o = 30 kV)	60 mJ
Optimum Filling Pressure	10 Torr
Optimum Output Coupler	50%
Extracted Energy Density	50 mJ/cm^3
Maximum Power	260 kW
Pulse Width (FWHM)	0.23 μs
Divergence Angle	2 mrad
Repetition Rate	1 Hz
Laser Energy (at 1 Hz)	8 mJ

SUMMARY

A 1 Hz HCP laser operating at 1 kJ input energy has been fabricated and tested. The time integrated continuum emission of the pump light approximated that of a 15,000 K blackbody at wavelengths above 250 nm. The pump emission was

found to be stable at 1 Hz operation. However thermal effects introduced by heating of the dye solution resulted in a reduction of the laser output as repetition rates increased. The overall efficiency of the system was found to be 0.01% for single shot operation and reduced by 85% for operation at 1 Hz.

This research was supported in part by AFOSR grant AFOSR-86-0345.

REFERENCES

1. W. J. Yi, D. D. Venable and Ja H. Lee, Proceedings of the International Conference on Lasers '86, edited by R. W. McMillan, (STS Press, McLean, VA, 1987), pp. 411-415.
2. W. J. Yi, Ultraviolet Dye Lasers Pumped by Hypocycloidal Pinch Plasmas, M. S. Thesis, Hampton University, Hampton, VA 23668, 1987.
3. S. M. Lee, One Hertz Ultraviolet Source for Laser Excitation, M. S. Thesis, Hampton University, Hampton, VA 23668, 1988.
4. K. S. Nam, Megawatt Blue-Green Dye Laser Excitation by A Hypocycloidal Pinch Plasma, M. S. Thesis, Hampton University, Hampton, VA 23668, 1988.

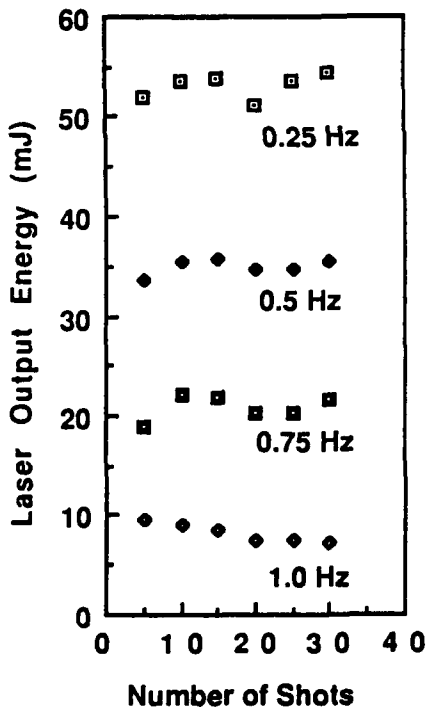

Figure 1. Stability of the laser output at different firing rates. In all cases the refresh rate was 15 Hz.

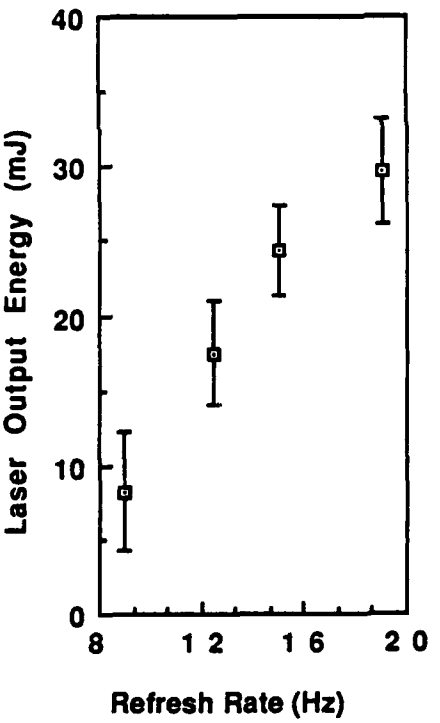

Figure 2. Output laser energy dependence on refresh rate. In all cases the firing rate was 0.5 Hz.

Abstract Submitted
for the 1989 Winter Meeting of the
American Physical Society

January 15-19 1989

Numerical Simulation of the Plasma Motion in a Hypocycloidal Pinch Device. D. D. VENABLE, M. B. WORKMANN AND J. H. LEE, Hampton U.*--A computer model is being developed to describe the electromagnetic acceleration of the plasma produced in the hypocycloidal pinch (HCP) device. We have extensively utilized this device for pumping near uv and blue-green laser dyes.[1-2] The computer model describes the operation of the device in the snow-plow mode and takes into account the unique geometry and electrical parameters of the HCP devices used in our laboratory. Numerical solutions are presented for plasma velocity and appropriate trends are predicted for the risetime of the pump light and total irradiance as a function of pressure of the working gas.

* Supported by AFOSR grant number AFOSR-86-0345

[1]W. J. Yi, D. D. Venable and J. H. Lee, Proceedings of the International Conference on Lasers '86, edited by R. W. McMillan, STS Press, McLean VA, 411-415 (1987).

[2]K. S. Han, S. H. Nam, and J. H. Lee, J. Appl. Phys. 55, 4113 (1984)

Demetrius D. Venable
Hampton University
Hampton, VA 23668